An Aniline-Bridged *Bis*(pyrazolyl)alkane Ligand for Dizinc-Catalysed Ring-Opening Polymerization

Pratyush K. Naik, Zipeng Gu, Robert J. Comito*

Department of Chemistry, The University of Houston, 4800 Calhoun Road, Houston, Texas 77004

Supporting Information

Contents

S1. General Information.

Lactide was obtained from Millipore Sigma. Lactide was recrystallized from toluene then sublimated twice before use. Other commercial reagents were purified prior to use following the guidelines of Perrin and Armarego.[1] All solvents were purified according to the method of Grubbs.[2] Yields refer to pure compounds, unless otherwise indicated. All reactions were performed in an atmosphere of dry, oxygen-free dinitrogen using standard Schlenk techniques or a nitrogen glovebox.

^{1}H-NMR spectra were recorded on a JEOL 400 MHz NMR spectrometer and are internally referenced relative to residual protio solvent signals at δ = 7.26 ppm for $CDCl_3$ and at δ = 7.16 ppm for C_6D_6. Data for ^{1}H-NMR are reported as follows: chemical shift (δ ppm), multiplicity (s = singlet, d = doublet, t = triplet, q = quartet, m = multiplet,), integration, and coupling constant (Hz). ^{13}C-NMR spectra were recorded on a JEOL 400 MHz NMR spectrometer (at 101 MHz) and are referenced relative to δ = 77.00 ppm for $CDCl_3$ and δ = 128 ppm for C_6D_6. Data for ^{13}C-NMR are reported in terms of chemical shift. Homonuclear-decoupled ^{1}H-NMR experiments were performed on a JEOL 400 MHz NMR spectrometer. The irradiation position was set to the lactyl methyl protons ($[C(O)CH(C\boldsymbol{H}_3)O]_n$, δ = 1.57 ppm). The irradiation attenuator was optimized to achieve the best decoupling.

IR spectra were recorded on a ThermoFisher Nicolet iS10 spectrometer with Smart iTR diamond plate and are reported in terms of wavenumber of absorption (cm^{-1}). Differential scanning calorimetry (DSC) was conducted on a TA-DSC 2500 with a crimped aluminum sample pan and reference pan. For the analysis, the instrument was operated between –80 °C and 100 °C at a rate of 10 °C /minute for heating and cooling cycle under nitrogen atmosphere. All thermal data

[1] Perrin, D. D.; Armarego, W. L. F. *Purification of Laboratory Chemicals.* 3rd ed., Pergamon Press, Oxford, 1988.
[2] Pangborn, A. B.; Giardello, M. A.; Grubbs, R. H.; Rosen, R. K.; Timmers, F. J. *Organometallic.* **1996**, *15*, 1518.

reported were taken from the second heat curve. Gel permeation chromatography (GPC) analyses were performed using a Tosoh high performance GPC system HLC-8320 equipped with an auto injector, a dual differential refractive index (RI) detector, and three TSKgel HHR series columns connected in series (7.8×300 mm TSKgel G5000HHR, TSKgel G4000HHR, TSKgel G3000HHR). GPC analysis were carried out in HPLC grade tetrahydrofuran with a flow rate of 1.0 mL/min at 40 °C. Relative molecular weights (M_n and M_w) and molecular weight distributions (Đ) were calculated using conventional column calibration with polystyrene (PS) standards. High Resolution Mass (HRMS) spectra were obtained from University of Texas at Austin Mass Spectrometry Lab. Elemental analysis was performed by Robertson Microlit Laboratories. MALDI-TOF analysis was performed at the University of Houston MALDI TOF Core Facility using the Bruker Daltonics UltrafleXtreme instrument. The poly(*rac*-lactic acid) sample was dissolved in THF (3 mg/mL) with 2,5-Dihydroxybenzoic acid (DHB) as the matrix (2 mg/mL in THF) and sodium trifluoroacetate (NaTFA) (3mg/ml in THF) as the sodium ion source. These solutions were combined in the ratio of 10:1:1 (DHB:PLA:NaTFA) by volume and then spotted into the sample plate for analysis.

S2. Preparation of Ligand 1 ($AD^{Me}H_2$) and Other Precursors

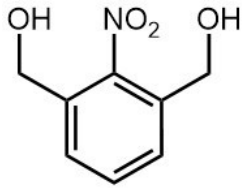

2-nitro-1,3-benzenedimethanol. Prepared according to the reported method.[3] An oven-dried Schlenk flask was charged with 2-nitroisopthalic acid (1.22 g, 5.80 mmol, 1.00 equiv.), anhydrous THF under nitrogen. Borane tetrahydrofuran (29 mL, 1.0 M solution in THF, 29 mmol, 5.0 equiv.) was added to the reaction at 0 °C while stirring. The stirring continued for 48 hours after and then the solvent was removed under vacuum. The residue was then partitioned between ethyl acetate (30 mL) and water (15 mL). The organic layer was rinsed with another portion of water (15 mL), then dried over sodium sulfate, and decanted. The product was obtained as a white solid under vacuum (811 mg, 4.42 mmol, 76% yield). Its ^{1}H-NMR and ^{13}C-NMR were identical to those in the reported procedure. ^{1}H-NMR (400 MHz, DMSO-d6): δ 7.54 (m, 3H), 5.45 (t, 2H), 4.49 (d, 4H). ^{13}C-NMR (101 MHz, DMSO-d6) δ 147.9, 134.9, 131.3, 128.1, 59.8. IR (Diamond ATR) 3200, 2800, 1507, 1359, 1348, 1321, 1283, 1059, 1043, 788, 754, 705, 686, 663, 615 cm^{-1}. HRMS (based on formula $C_8H_9NO_4$) m/z: expected: 183.0532 amu ($[M]^+$), found: 183.0526 amu, difference -3.3 ppm.

[3] Fu, Y.; Xing, Z.; Zhu, C.; Yang, H.; He, W.; Zhu, C.; Cheng, Y. A Novel Calixsalen Macrocycle: Metal Sensing Behavior for Zn^{2+} and Intracellular Imaging Application. *Tetrahedron Lett.* **2012**, *53*, 804-807.

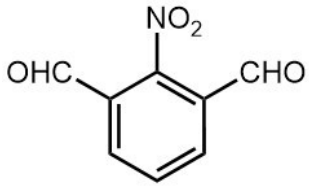

2-nitro-1,3-benzenedialdehyde (**3**). **3** was prepared according to the reported method.[4] A solution of 2,6-*bis*(hydroxymethyl)nitrobenzene (1.03 g, 5.60 mmol, 1.00 equiv.) and pyridinium chlorochromate (PCC, 6.03 g, 28.0 mmol, 5.00 equiv.) and CH_2Cl_2 (150 mL) was stirred at room temperature for 12 hours. The reaction mixture was purified by flash chromatography on silica with 1:1 CH_2Cl_2 to hexane ($R_f = 0.5$). Vacuum drying gave the product as a pale orange solid (687 mg, 3.84 mmol, 68% yield). Its ^{1}H-NMR and ^{13}C-NMR matched those published in the reported method. ^{1}H-NMR (400 MHz, $CDCl_3$): δ 10.07 (s, 2H), 8.25 (d, 2H), 7.89 (t, 1H). ^{13}C-NMR (101 MHz, $CDCl_3$) δ 185.8, 150.8, 135.3, 132.1, 128.0. IR (Diamond ATR) 1700, 1592, 1546, 1513, 1479, 1446, 1394, 1350, 1309, 1231, 1059, 1012, 998, 801, 775, 757, 720, 706, 649, 625 cm^{-1}. HRMS (based on formula $C_8H_5NO_4$) m/z: expected: 179.0219 amu ($[M]^+$), found: 179.0218 amu, difference -0.6 ppm.

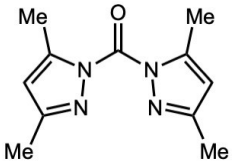

***Bis*(3,5-dimethylpyrazol-1-yl)methanone** (**4**). Methanone **4** was prepared according to the reported method.[4] An oven-dried Schlenk flask was charged with 3,5-dimethylpyrazole (19.4 g, 202 mmol, 6.0 equivalents), triethylamine (30.5 mL, 219 mmol, 6.5 equivalents), and THF (300 mL). The solution was allowed to stir for 30 min and then cooled to 0 °C. Triphosgene (10 g, 34 mmol, 1 equivalent) as a solution in anhydrous THF was added dropwise over 10 min. The resulting pale-yellow and inhomogeneous suspension was allowed to warm to room temperature and stir for 4 hours. The reaction was then filtered, the solids were washed with THF, and the combined filtrate and washings were concentrated in vacuo to yield a pale yellow solid. The crude

[4] Fu, Y.; Xing, Z.; Zhu, C.; Yang, H.; He, W.; Zhu, C.; Cheng, Y. A Novel Calixsalen Macrocycle: Metal Sensing Behavior for Zn^{2+} and Intracellular Imaging Application. *Tetrahedron Lett.* **2012**, *53*, 804-807.

product was recrystallized from dichloromethane/hexanes by first dissolving the crude product in boiling dichloromethane and then slowly adding boiling hexanes until the solution turns turbid, followed by a minimal amount of boiling dichloromethane until the solution just turns clear. After storage at −20 °C overnight, the product was isolated as an white solid (19.12 g, 87.60 mmol, 86% yield). ^{1}H-NMR (400 MHz, $CDCl_3$): δ 6.03 (s, 2H), 2.46 (s, 6H), 2.26 (s, 6H). ^{13}C-NMR (101 MHz, $CDCl_3$): δ 153.1, 148.0, 145.5, 111.5, 14.1, 13.2. Our ^{1}H-NMR and ^{13}C-NMR are consistent with those reported for this compound.[4]

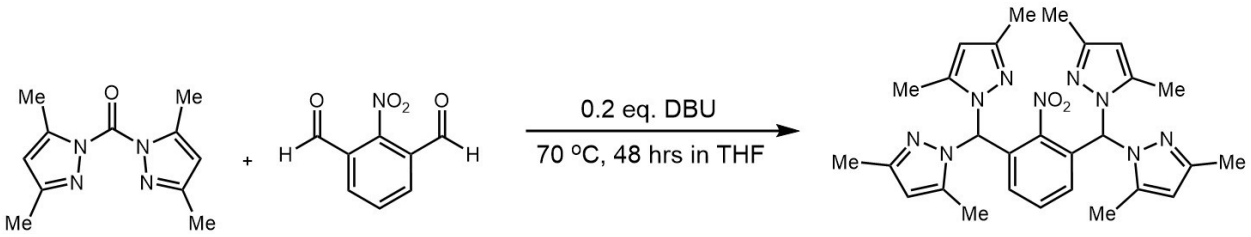

4 **3** **5**

(2,6-*bis*(3,5-dimethylpyrazol-1-ylmethane)nitrophenyl) 5. In a pressure tube with cap and stir bar, a solution of **3** (659 mg, 3.68 mmol, 1 equivalent), **4** (1.61 g, 7.36 mmol, 2 equivalents), 1,8-diazabicyclo[5.4.0]undec-7-ene (DBU) (110 μL, 0.74 mmol, 0.2 equivalents), and tetrahydrofuran was heated to 70 ºC for 48 hours. Volatiles were removed under vacuum, and then, the remaining residue was purified by flash chromatography on silica by increasing eluent polarity starting from 1:9 ethyl acetate/hexane to 1:1 ethyl acetate/hexane (R_f = 0.28). The desired product coelutes with 3,5-dimethypyrazole. This impurity was removed by sublimation under vacuum at 70 ºC, giving the pure product as pale yellow solids (913 mg, 1.73 mmol, 47% yield). ^{1}H-NMR (400 MHz, $CDCl_3$): δ 7.85 (s, 2H), 7.38 (t, 1H), 6.58 (d, 2H), 5.84 (s, 4H), 2.15 (s, 12H), 2.11 (s, 12H). ^{13}C-NMR (101 MHz, $CDCl_3$): δ 148.9, 146.8, 140.8, 131.5, 131.2, 128.7, 107.0, 69.8, 13.8, 11.1. IR (Diamond ATR) 1559, 1536, 1451, 1413, 1379, 1358, 1331, 1304, 1282, 1267, 1254, 1027, 967, 814, 795, 784, 776, 758, 694, 625 cm^{-1}. HRMS (based on formula $C_{28}H_{33}N_9O_2$) m/z: expected: 550.2649 amu ($[M+Na]^+$), found: 550.2654 amu, difference: -0.77 ppm.

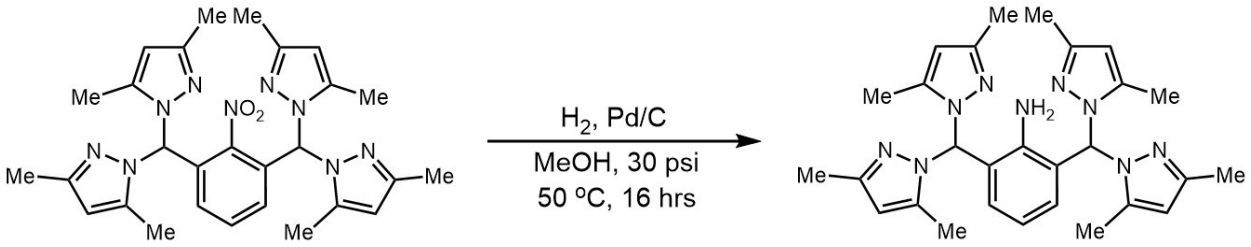

5 $AD^{Me}H_2$ (**1**)

(2,6-*bis*(3,5-dimethylpyrazol-1-ylmethane)aniline) ($AD^{Me}H_2$, **1**). In a dried Fisher-Porter tube under nitrogen, 10.0% palladium on carbon (72.8 mg, 0.68 mmol, 0.82 equivalents) was added to **5** (440 mg, 0.83 mmol, 1 equivalent) in 1 mL of methanol. The tube was pressured with hydrogen gas at 30 psi while the stirring continued at 50 ºC for 16 hours. After the hydrogen was vented, the reaction was diluted with CH_2Cl_2 (15 mL), filtered, and concentrated under vacuum. The crude residue was transferred into a sublimator where 3,5-dimethylpyrazole was removed under vacuum at 70 ºC. The product was recrystallized by dissolving in CH_2Cl_2 and hexane at room temperature and then storing at –40 ºC overnight, giving $AD^{Me}H_2$ (**1**) as pale white solid (220 mg, 0.44 mmol, 53% yield). ^{1}H-NMR (500 MHz, $CDCl_3$) δ 7.38 (s, 2H), 6.61 (t, 1H), 6.38 (d, 2H), 5.85 (s, 4H), 2.19 (s, 12H), 2.11 (s, 12H). ^{13}C-NMR (125 MHz, $CDCl_3$) δ 148.9, 142.4, 141.2, 128.1, 122.0, 117.9, 107.1, 72.3, 13.9, 11.7. IR (Diamond ATR) 3464, 2922, 1641, 1559, 1449, 1416, 1375, 1343, 1302, 1254, 1205, 1166, 1106, 1029, 974, 942, 870, 853, 824, 772, 756, 729, 707, 673, 616, 549, 480, 439 cm^{-1}. HRMS (based on formula $C_{28}H_{35}N_9$) m/z: expected: 520.2908 amu ([M+Na]$^+$), found: 520.2908 amu, difference: 0 ppm.

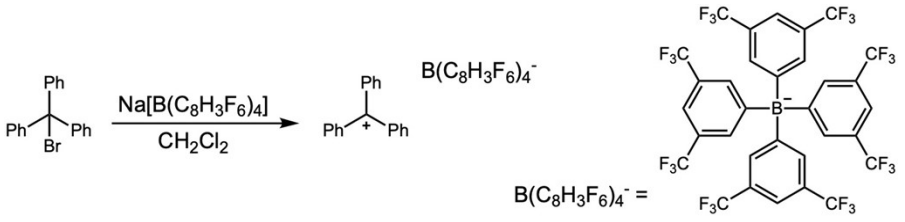

Trityl *tetrakis*(3,5-*bis*(trifluoromethyl)phenyl)borate was prepared according to the reported method.[5] In a glovebox, trityl bromide (1.82 g, 5.64 mmol, 1 equivalent), and sodium tetrakis(3,5-*bis*(trifluoromethyl)phenyl)borate (5.26 g, 5.64 mmol, 1 equivalent), were dissolved in

[5] Scott, Valerie J.; Remle Çelenligil-Çetin; Oleg V. Ozerov. Room-temperature catalytic hydrodefluorination of C (sp3)− F bonds. *J. Am. Chem. Soc.* **2005**, *127*, 2852–2853

dichloromethane (14 mL, each), and then mixed together. After stirring for 4 hours, the reaction mixture was filtered through a glass Buchner funnel. The yellow filtrate was then transferred to a round bottom flask and the solvent was removed under vacuum, providing the product as a flaky yellow solid (5.86 g, 5.30 mmol, 94% yield.). ^{1}H-NMR (400 MHz, CD_2Cl_2) δ 8.12 (t, J = 7.5 Hz, 3H), 7.74 (t, J = 7.7 Hz, 6H), 7.67 (s, 8H), 7.56 (d, *J* = 8.0 Hz, 6H), 7.47 (s, 4H). ^{13}C-NMR (101 MHz, CD_2Cl_2) δ 210.8, 161.8 (dd, J = 50.1 Hz), 143.8, 142.4, 139.8, 134.8, 130.8, 129.0, 125.9 (q), 124 (q), 117.6. ^{19}F-NMR (376 MHz, CD_2Cl_2) δ -62.30. Our ^{1}H-NMR, ^{19}F-NMR, and ^{13}C-NMR are consistent with those reported for this compound.[6]

[6] Wu, F.; Deraedt, C.; Cornaton, Y.; Ruhlmann, L.; Karmazin, L.; Bailly, C.; Kyritsakas, N.; Le Breton, N.; Choua, S.; Djukic, J.P. Fate of Cobaltacycles in Cp* Co-Mediated C–H Bond Functionalization Catalysis: Cobaltacycles May Collapse upon Oxidation via Co (IV) Species. *Organometallics* **2021**, *40*, 2624–2642.

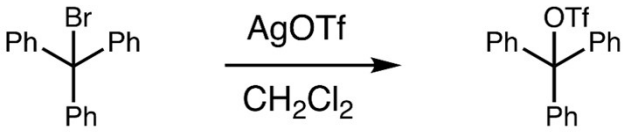

Trityl triflate was prepared according to the reported method.[7] Its ^{1}H-NMR and ^{13}C-NMR were identical to the ones presented there. ^{1}H-NMR (500 MHz, CD_2Cl_2) δ 8.27 (t, J = 6.8 Hz, 3H), 7.89 (t, J = 7.0 Hz, 6H), 7.68 (d, J = 7.0 Hz, 6H). ^{13}C-NMR (126 MHz, CD_2Cl_2) δ 210.9, 143.5, 142.9, 140.0, 130.7. ^{19}F-NMR (470 MHz, CD_2Cl_2) δ -78.78. Our ^{1}H-NMR, ^{19}F-NMR, and ^{13}C-NMR are consistent with those reported for this compound.[7]

[7] Hinz, A.; Labbow, R.; Reiß, F.; Schulz, A.; Sievert, K.; & Villinger, A. Synthesis and Structure of Tritylium Salts. *Struct. Chem.* **2005**, *26*, 1641-1650.

S3. Spectral Data for Ligands 1 ($AD^{Me}H_2$) and Other Precursors

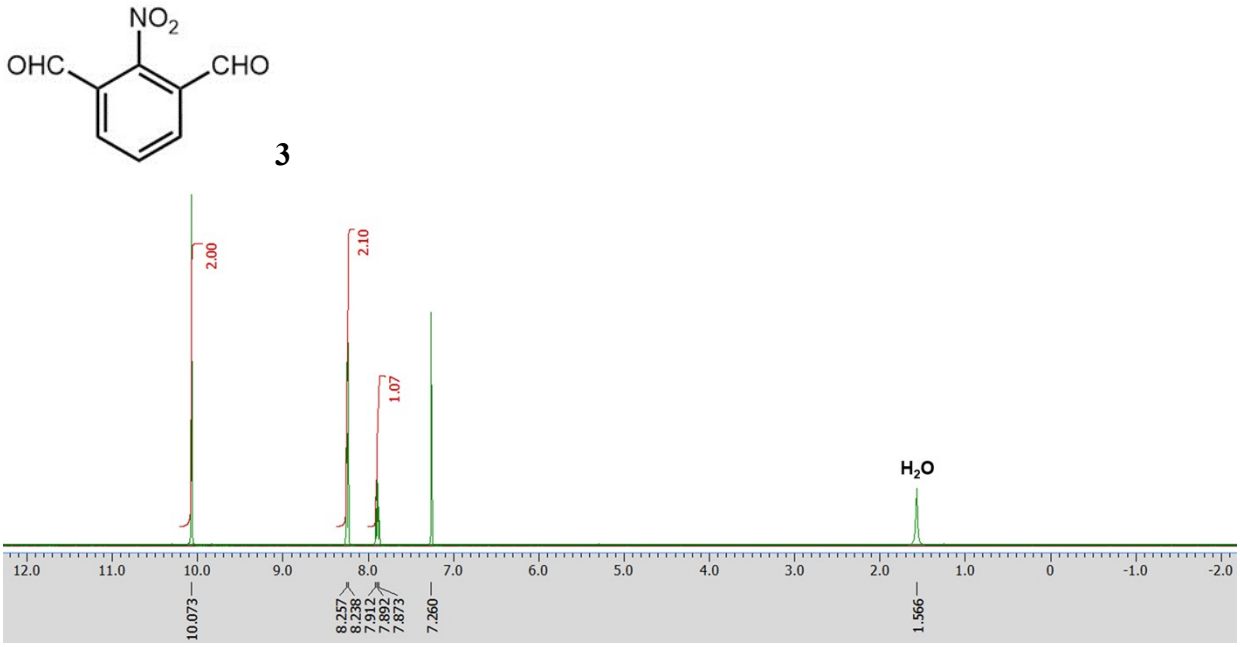

Figure S1. ^{1}H-NMR of **3**, $CDCl_3$, 400 MHz.

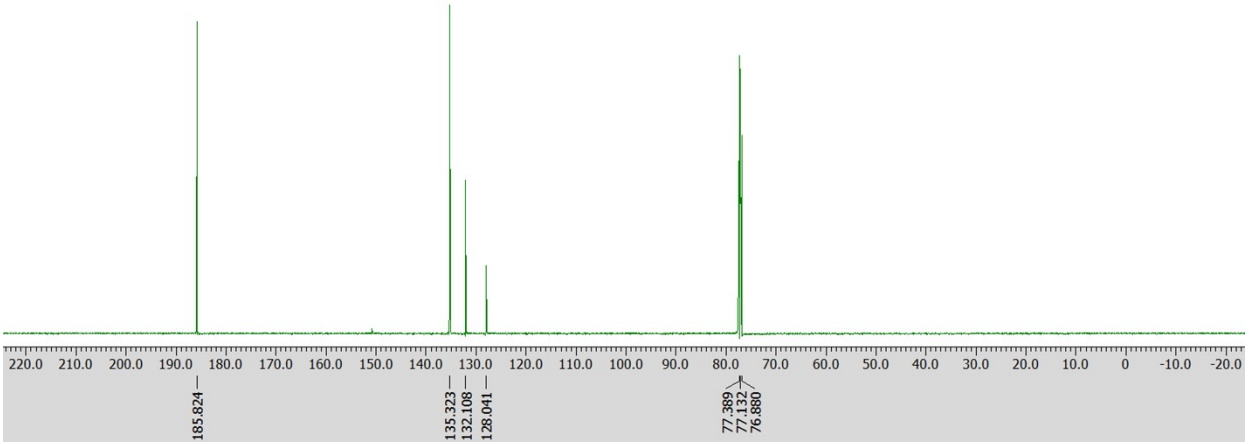

Figure S2. ^{13}C-NMR of **3**, $CDCl_3$, 101 MHz.

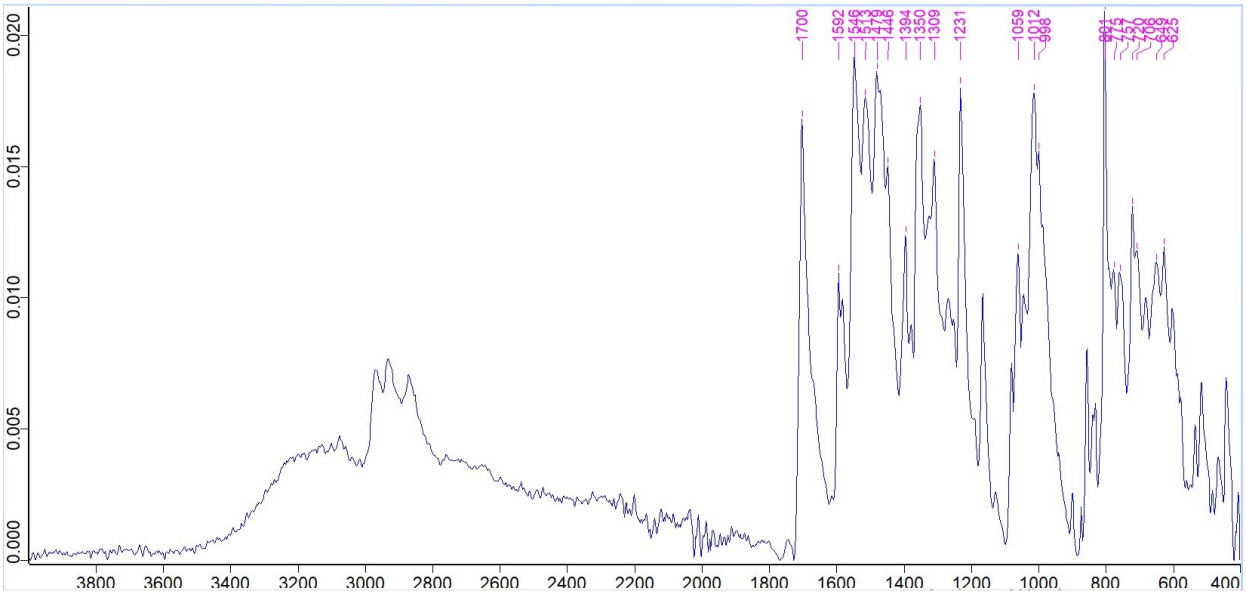

Figure S3. Infrared spectrum of **3**, diamond ATR.

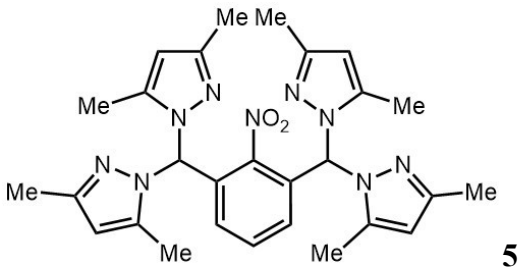

5

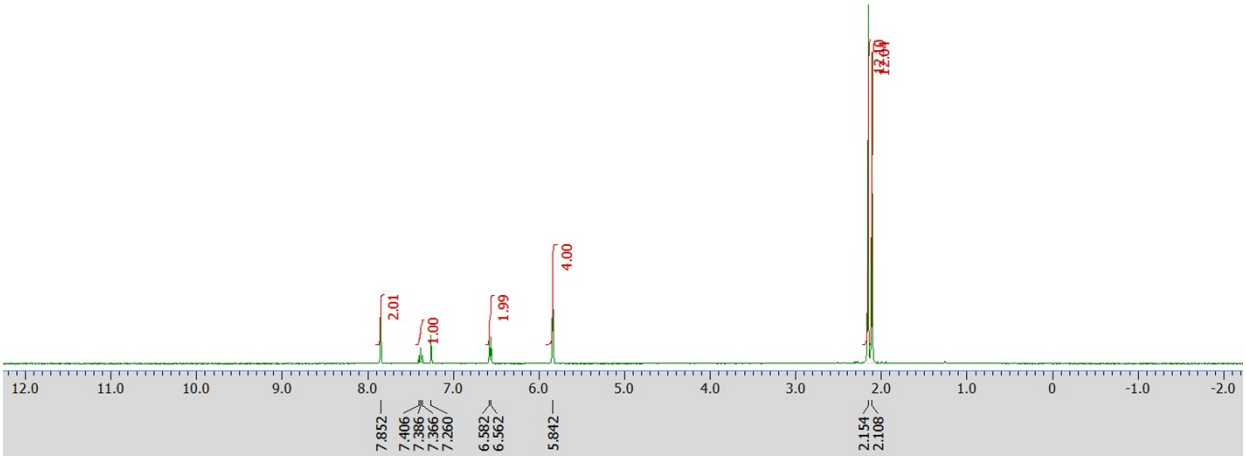

Figure S4. ^{1}H-NMR of **5**, $CDCl_3$, 400 MHz.

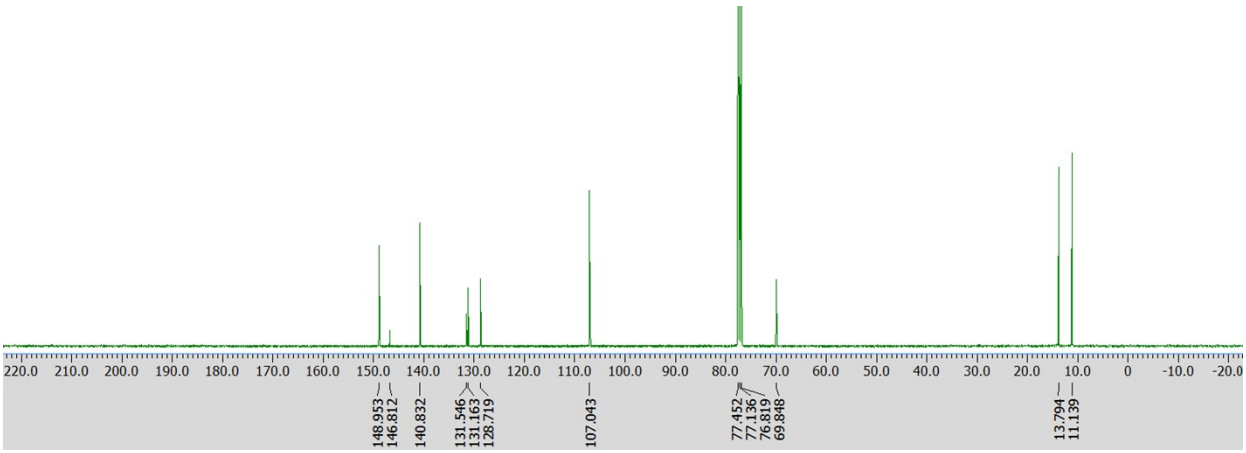

Figure S5. ^{13}C-NMR of **5**, $CDCl_3$, 101 MHz.

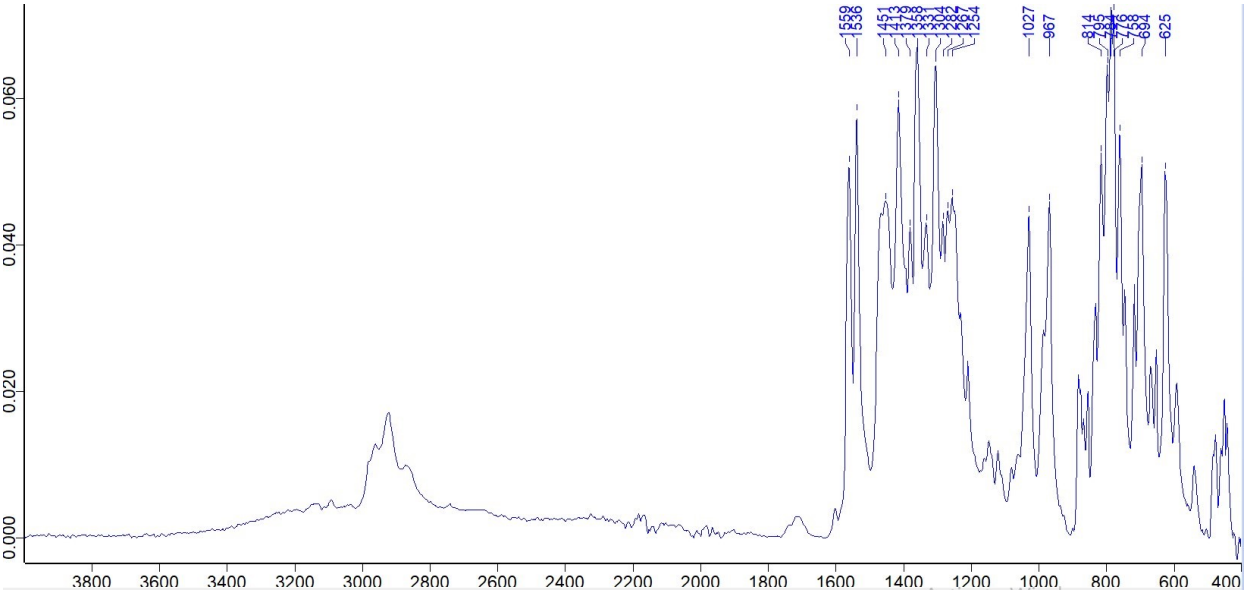

Figure S6. Infrared spectrum of **5**, diamond ATR.

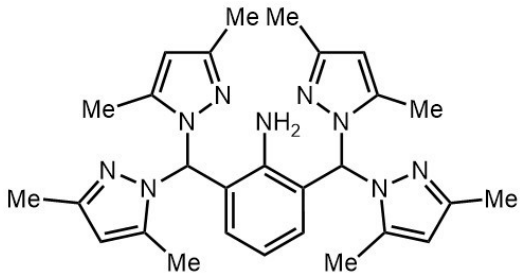

AD^{Me}H$_2$ (1)

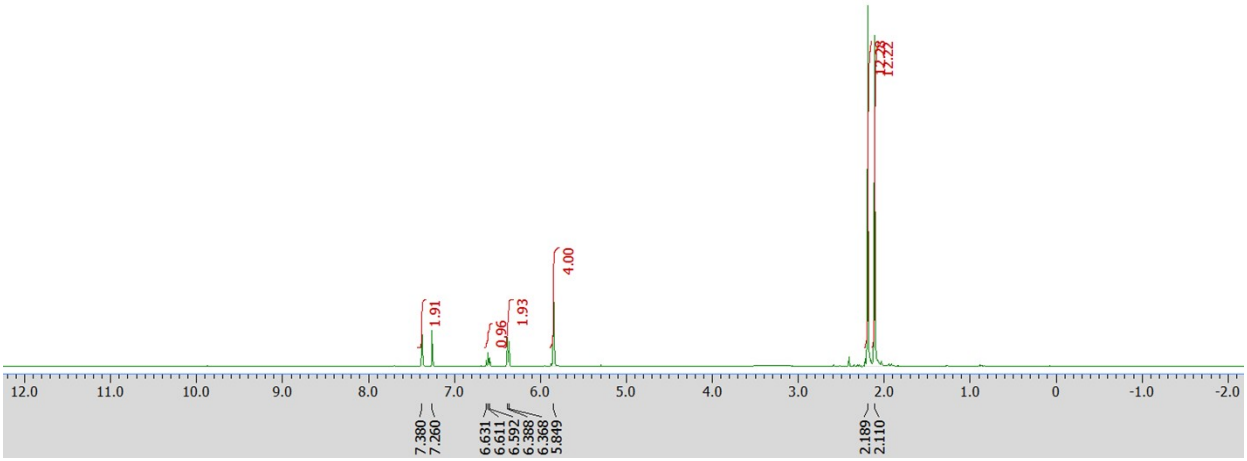

Figure S7. ^{1}H-NMR of **1**, $CDCl_3$, 500 MHz.

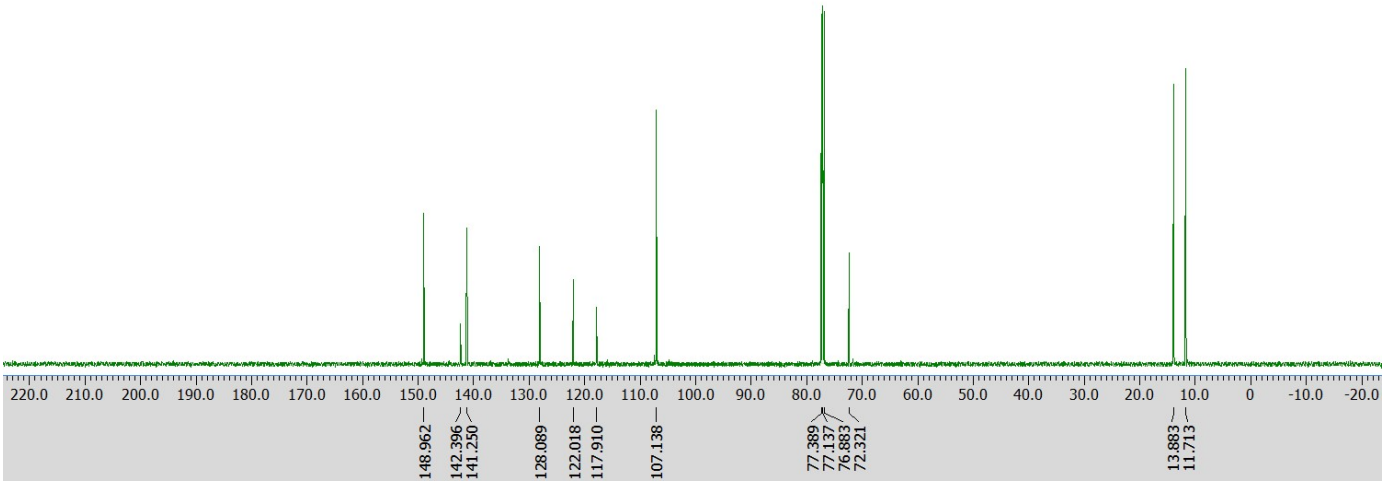

Figure S8. ^{13}C-NMR of **1**, $CDCl_3$, 125 MHz.

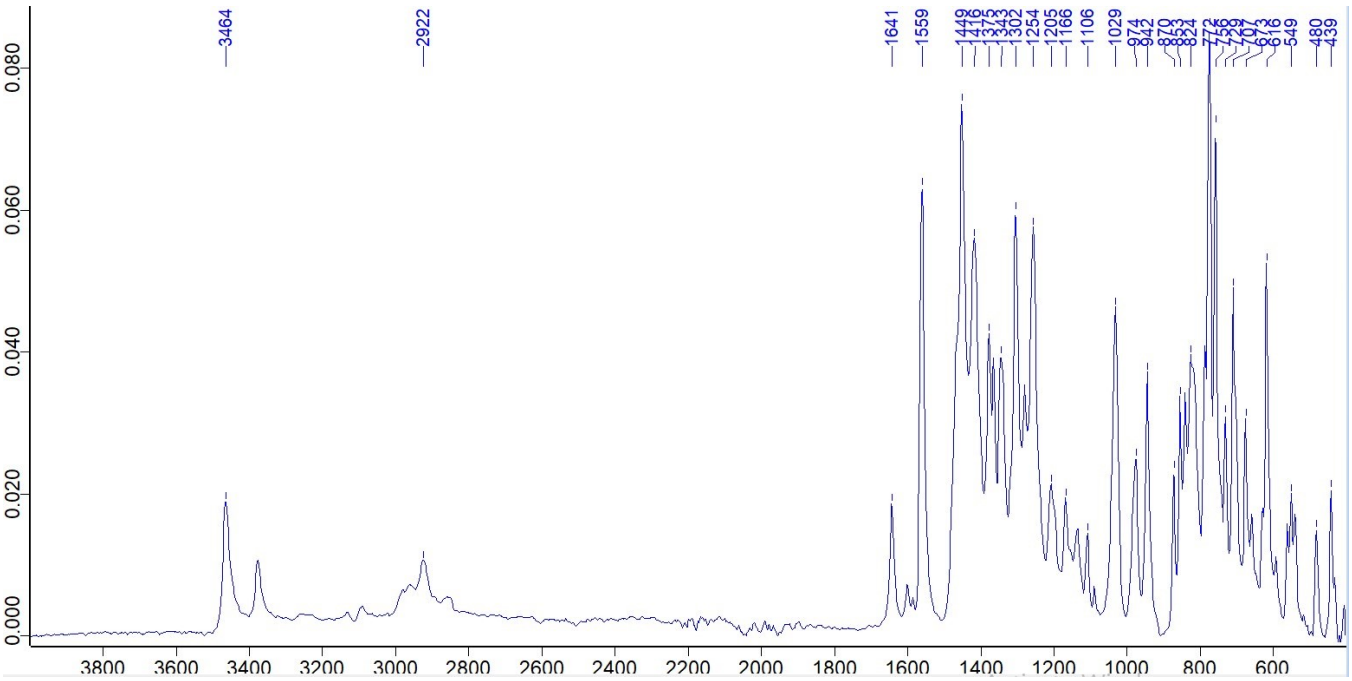

Figure S9. Infrared spectrum of **1**, diamond ATR.

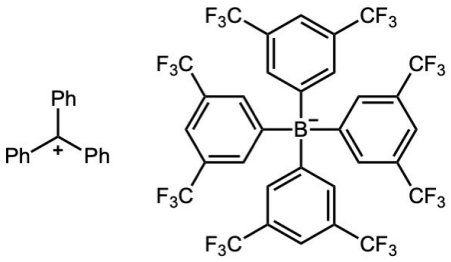

trityl tetrakis(3,5-*bis*(trifluoromethyl)phenyl)borate

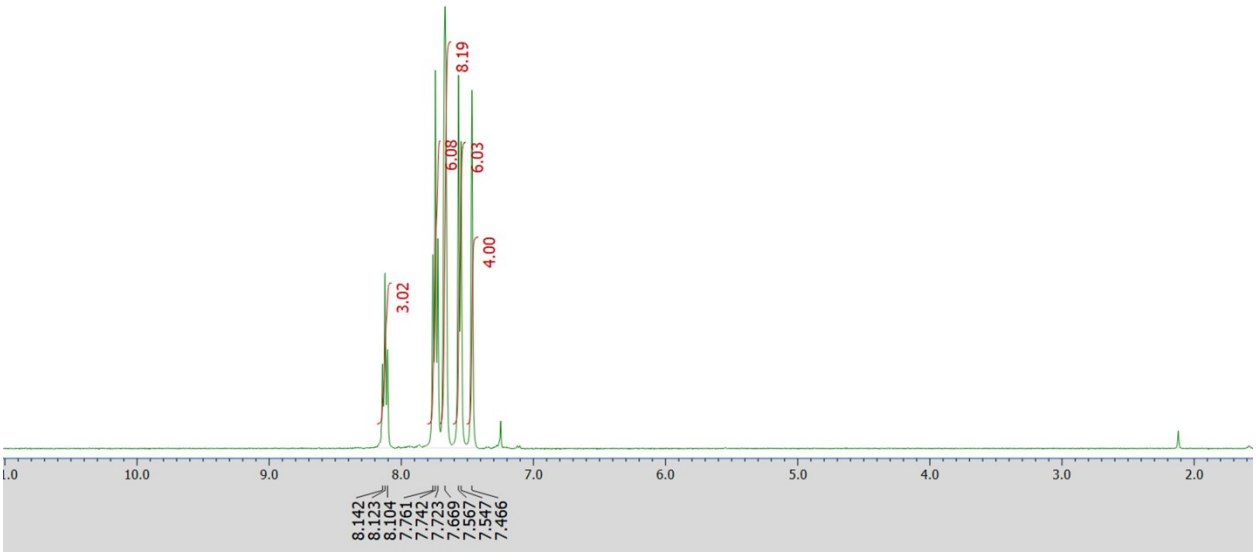

Figure S10. ^{1}H-NMR of trityl *tetrakis*(3,5-*bis*(trifluoromethyl)phenyl)borate, CD_2Cl_2, 400 MHz.

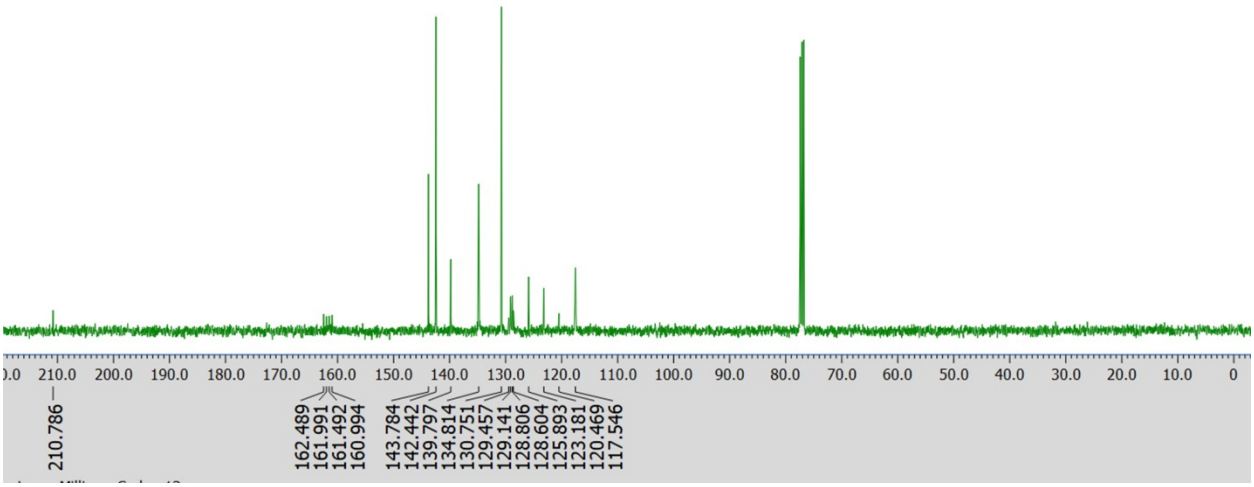

Figure S11. ^{13}C-NMR of trityl tetrakis(3,5-*bis*(trifluoromethyl)phenyl)borate, CD_2Cl_2, 101 MHz.

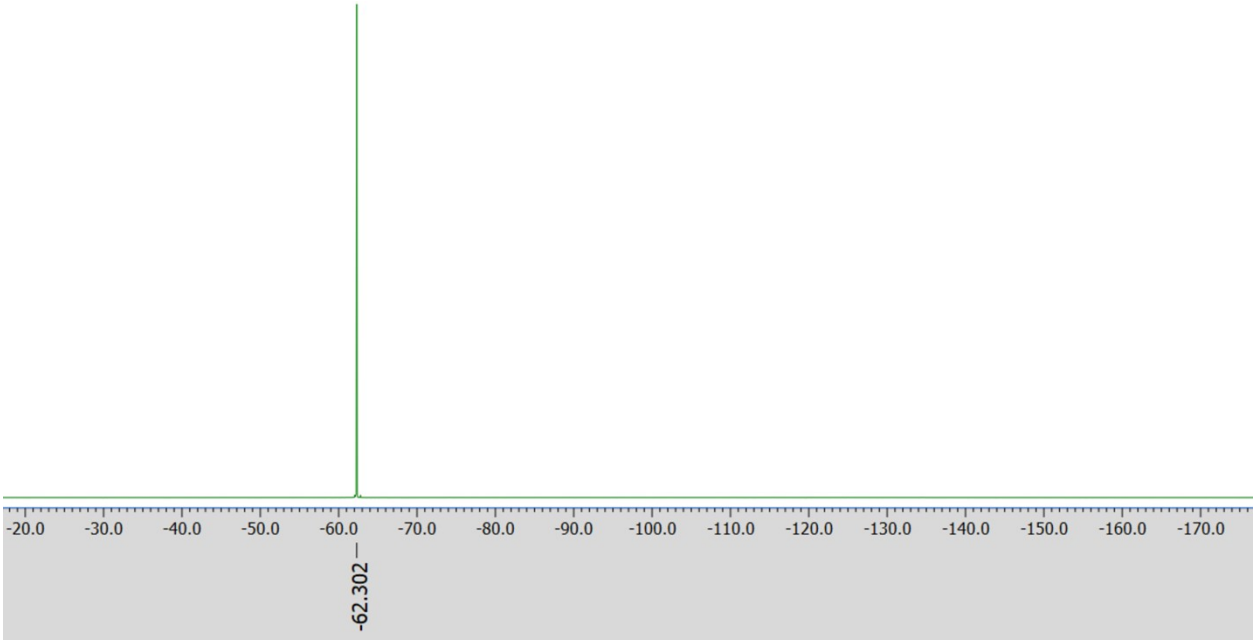

Figure S12. ^{19}F-NMR of trityl tetrakis(3,5-*bis*(trifluoromethyl)phenyl)borate, CD_2Cl_2, 376 MHz.

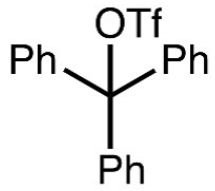

trityl triflate

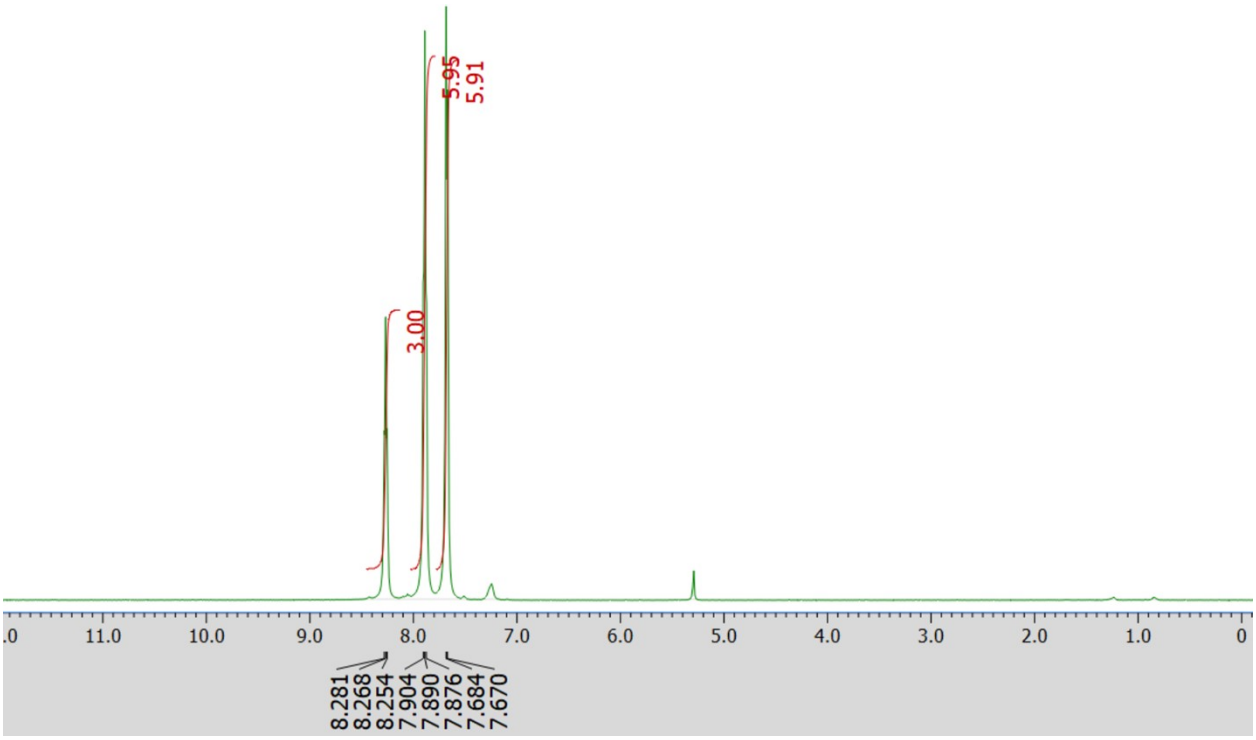

Figure S13. ^{1}H-NMR of trityl triflate, CD_2Cl_2, 500 MHz.

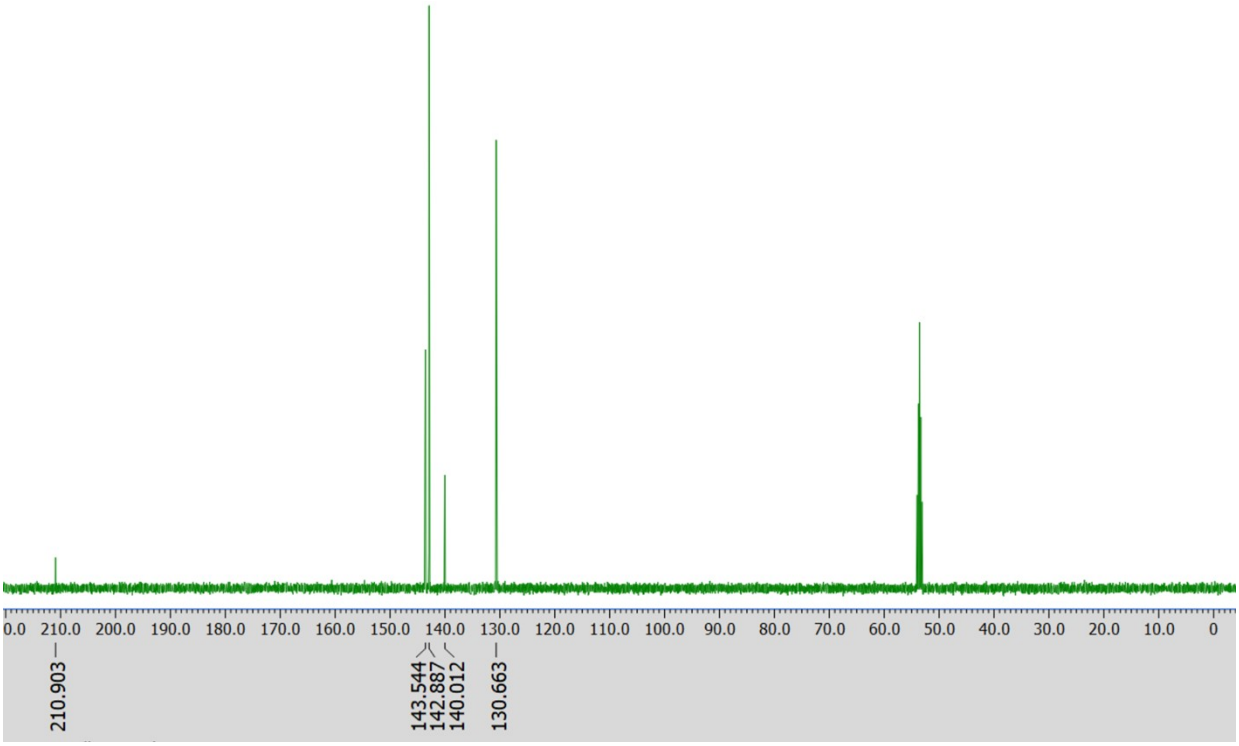

Figure S14. ^{13}C-NMR of trityl triflate, CD_2Cl_2, 126 MHz.

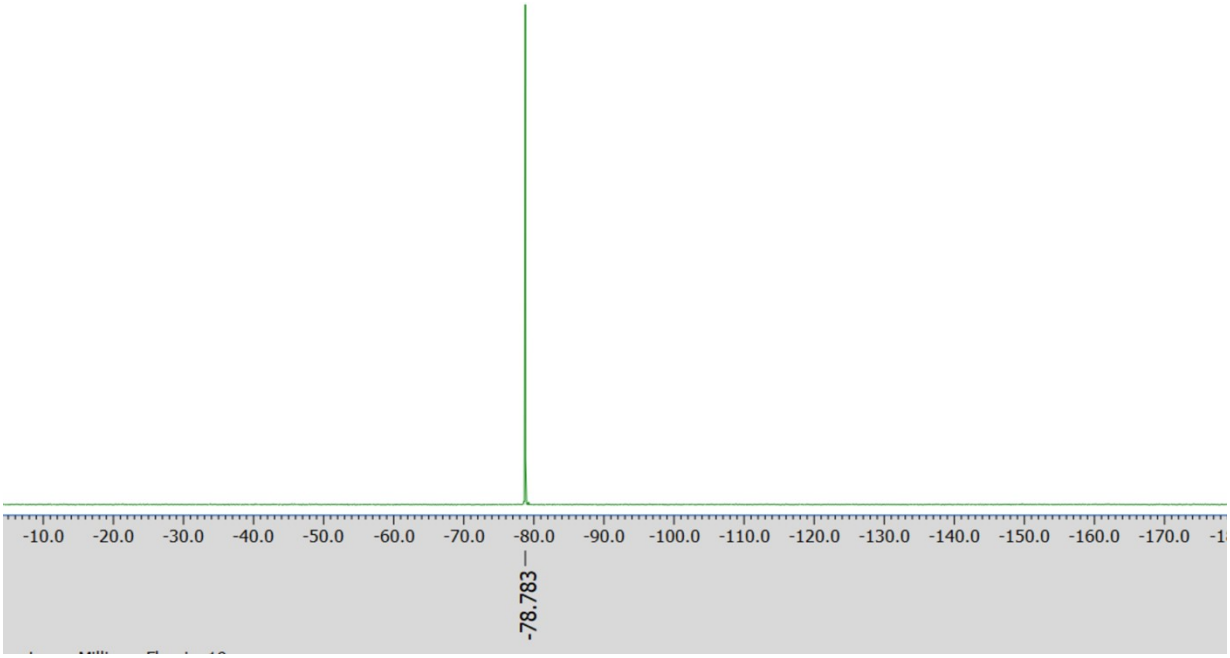

Figure S15. ^{19}F-NMR of trityl triflate, CD_2Cl_2, 470 MHz.

S4. Synthesis of dizinc complexes.

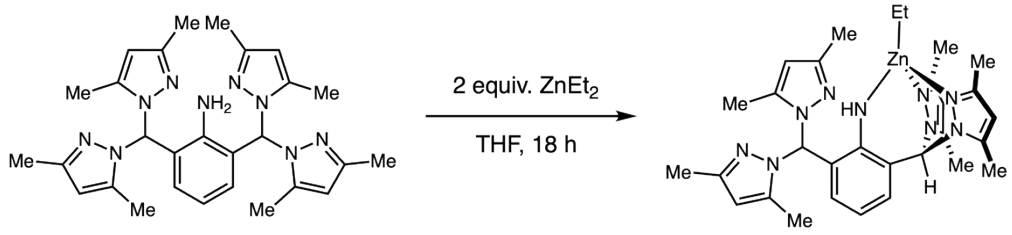

Section S4.1. Synthesis of AD^{Me}HZnEt (**7**). In a nitrogen glovebox, a vial was charged with AD^{Me}H$_2$ (**1**) (25 mg, 0.05 mmol, 1 equivalent), diethylzinc (10.4 µL, 0.10 mmol, 2 equivalents), and THF (3 mL). After stirring for 18 hours, volatiles were removed under vacuum down to a pale yellow solid (29.3 mg, 0.049 mmol, 99% yield). ^{1}H-NMR (400 MHz, $CDCl_3$) δ 7.29 (s, 1H), 6.90-6.88 (m, 2H), 5.98-5.93 (m, 2H), 5.88 (s, 2H), 5.76 (s, 2H), 3.52 (s, 1H), 2.40 (s, 6H), 2.26 (s, 6H), 2.18 (s, 6H), 2.00 (s, 6H), 1.21 (t, J = 8.1 Hz, 3H), 0.14 (q, J = 8.1 Hz, 2H). ^{13}C-NMR (101 MHz, $CDCl_3$) δ 156.4, 149.1, 148.2 141.0, 139.8, 132.5, 129.7, 122.5, 117.1, 107.5, 106.3, 106.3, 74.1, 73.8, 14.0, 13.1, 13.0, 11.7, 11.7, -2.6. IR (Diamond ATR) 3386, 2919, 2840, 1596, 1556, 1385, 1357, 1323, 1279, 1262, 1247, 1209, 1191, 1118, 1100, 1046, 982, 958, 888, 861, 838, 810, 782, 743, 721, 707, 670, 604, 571, 555, 523, 511, 440cm^{-1}. Elemental analysis (based on formula $C_{30}H_{39}N_9Zn$): C (59.79% found, 60.96% expected, 1.17% difference), H (6.64% found, 6.65% expected, 0.01% difference), N (20.72% found, 21.33% expected, 0.61% difference).

The conditions of this synthesis were subsequently modified by using a larger excess of $ZnEt_2$ or by using a different solvent (Table S1). But we never observed a complex with the composition AD^{Me}HZn$_2$Et$_3$ (8) or AD^{Me}Zn$_2$Et$_2$ (**9**).

Table S1. Synthesis of AD^{Me}HZnEt (**12**) from excess $ZnEt_2$.

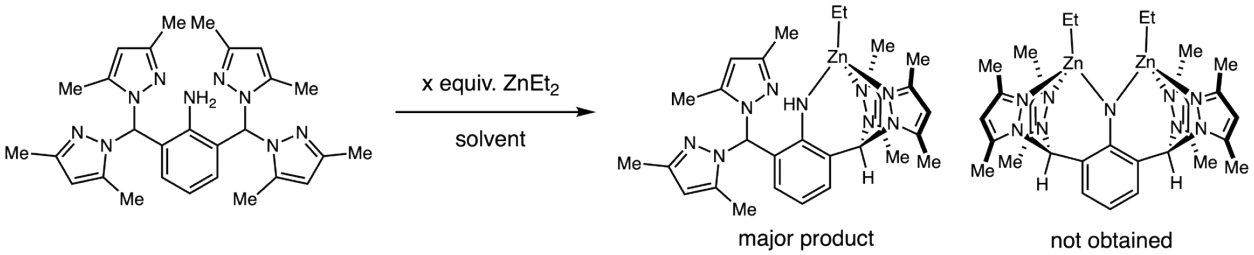

AD^{Me}H$_2$ (**1**) AD^{Me}HZnEt (**7**) AD^{Me}Zn$_2$Et$_2$ (**9**)

$ZnEt_2$ equivalents	**Solvent**	**Isolated Yield**
3 equiv.	THF	≥ 99%
3 equiv.	Et_2O	≥ 99%
2 equiv.	CH_2Cl_2	≥ 99%
2 equiv.	THF	≥ 99%
1 equiv.	toluene	0%
1 equiv.	THF	0%

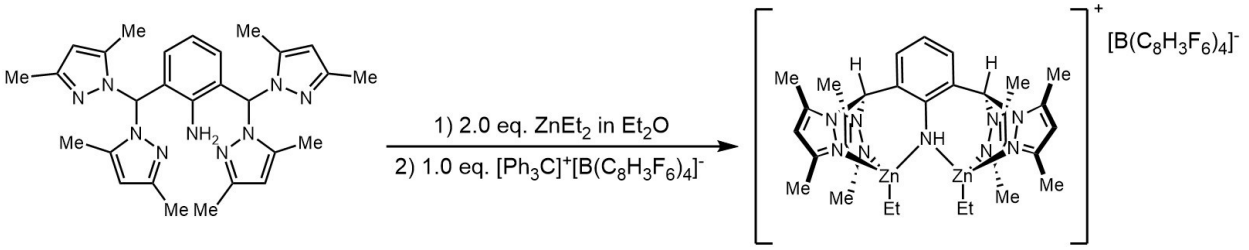

$AD^{Me}H_2$ (**1**) **6**-BArF

6-BArF. ($[AD^{Me}HZn_2Et_2][B(C_8H_3F_6)_4]$). In a nitrogen glovebox, a vial was charged with $AD^{Me}H_2$ (**1**) (25 mg, 0.050 mmol, 1 equivalent), diethylzinc (10.4 µL, 0.10 mmol, 2 equivalents), and diethyl ether (2 mL). After 5 minutes, a solution of trityl *tetrakis*(3,5-*bis*(trifluoromethyl)phenyl)borate[8] ($Ph_3CB(C_8H_3F_6)_4$, 55.5 mg, 0.050 mmol, 1 equivalent) and Et_2O (2 mL) was added. The reaction was judged to be complete after 5 minutes by the disappearance of the red-orange color of the trityl cation. Volatiles were removed under vacuum, leaving a pale yellow solid. Then, the solid was washed three times with totally 15 mL of hexanes, and the desired product was obtained as a white solid (69.7 mg, 0.045 mmol, 90 % yield). ^{1}H-NMR (400 MHz, $CDCl_3$) δ 7.69 (s, 8H), 7.49 (s, 4H), 7.01 (d, J = 7.6 Hz, 2H), 6.92 (s, 2H), 6.60 (t, J = 7.6 Hz, 1H), 5.98 (s, 4H), 2.35 (s, 12H), 2.26 (s, 12H), 1.16 (t, J = 7.9 Hz, 6H), 0.28 (q, 4H). ^{13}C-NMR (101 MHz, $CDCl_3$) δ 152.5, 152.3, 141.9, 134.9, 132.6, 129.8-129.1 (dd), 128.8-128.7 (dd), 125.9, 123.2, 121.3, 117.6 (bs), 107.5, 71.8, 13.2, 12.5, 11.2, -1.9 . ^{19}F-NMR (470 MHz, $CDCl_3$) δ -62.31. IR (Diamond ATR) 2858, 1609, 1560, 1461, 1422, 1388, 1353, 1043, 983, 962,

[8] Specklin, D.; Fliedel, C.; Gourlaouen, C.; Bruyere, J. C.; Avilés, T.; Boudon, C.; Dagorne, S. *N*-Heterocyclic Carbene Based Tri-organyl-Zn–Alkyl Cations: Synthesis, Structures, and Use in CO_2 Functionalization. *Chem. Eur. J.* **2017**, *23*, 5509-5519.

886, 860, 838, 798, 746, 711, 669, 600, 577, 509, 472, 449 cm^{-1}. Elemental analysis (based on formula $C_{64}H_{56}BF_{24}N_9Zn_2$): C (48.77% found, 49.63% expected, 0.86% difference), H (3.74% found, 3.64% expected, -0.10% difference), N (7.97% found, 8.14% expected, 0.17% difference).

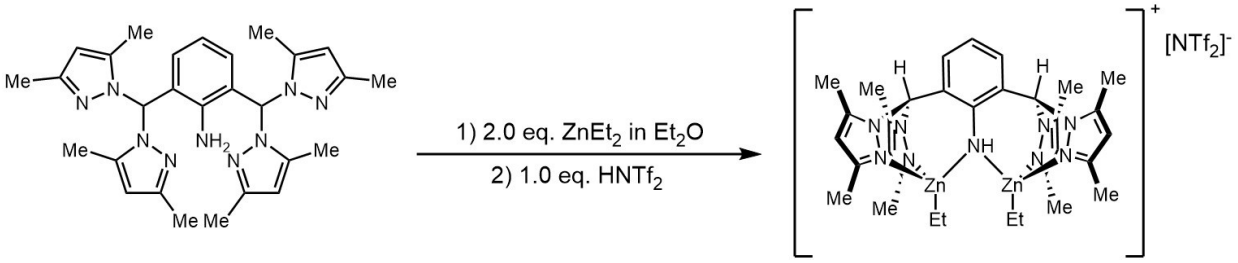

$AD^{Me}H_2$ (**1**) **6**-NTf_2

6-NTf_2. ([$AD^{Me}HZn_2Et_2$][NTf_2]). In a nitrogen glovebox, a vial was charged with $AD^{Me}H_2$ (**1**) (25 mg, 0.05 mmol, 1 equivalent), diethylzinc (10.4 µL, 0.10 mmol, 2 equivalents), and diethyl ether (2 mL). After 5 minutes, a solution of bis(trifluoromethanesulfonyl)imide ($HNTf_2$, 14.1 mg, 0.050 mmol, 1 equivalent) and Et_2O (2 mL) was added. The reaction was judged to be complete after 15 minutes by the appearance of white solid precipitate. Volatiles were removed under vacuum, giving our desired product as a white solid (44.4 mg, 0.046 mmol, 92 % yield). ^{1}H-NMR (400 MHz, $CDCl_3$) δ 7.46 (d, J = 7.8 Hz, 2H), 7.05 (t, J = 7.6 Hz, 1H), 6.13 (s, 4H), 2.62 (s, 12H), 2.42 (s, 12H), 1.30 (t, J = 8.0 Hz, 6H), 0.41 (q, J = 8.1 Hz, 4H). ^{13}C-NMR (101 MHz, $CDCl_3$) δ 151.9, 142.7, 133.4, 129.1, 121.6, 121.4, 107.3, 77.1, 76.8, 71.8, 13.3, 12.6, 11.5, -2.0. ^{19}F-NMR (470 MHz, $CDCl_3$) δ -78.69. IR (Diamond ATR) 1558, 1462, 1349, 1181, 1135, 1050, 985, 884, 858, 786, 751, 738, 702, 615, 569, 513, 470 cm^{-1}. Elemental analysis (based on formula $C_{34}H_{44}F_6N_{10}O_4S_2Zn_2$): C (41.06 % found, 42.29 % expected, 1.23 % difference), H (4.54 % found, 4.59% expected, 0.05 % difference), N (14.09 % found, 14.51 % expected, 0.42 % difference).

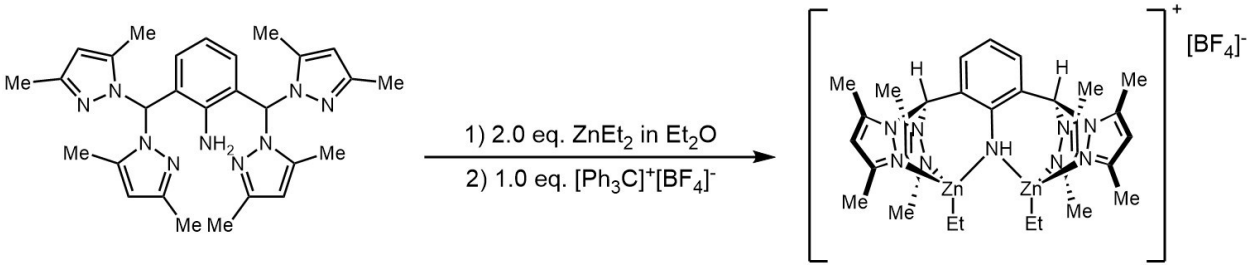

$AD^{Me}H_2$ (**1**) **6**-BF_4

6-BF_4. ([$AD^{Me}HZn_2Et_2$][BF_4]). In a nitrogen glovebox, a vial was charged with $AD^{Me}H_2$ (**1**) (25 mg, 0.050 mmol, 1 equivalent), diethylzinc (10.4 μL, 0.10 mmol, 2 equivalents), and diethyl ether (2 mL). After 5 minutes, a solution of trityl tetrafluoroborate (Ph_3CBF_4, 16.6 mg, 0.050 mmol, 1 equivalent) and Et_2O (2 mL) was added. The reaction was judged to be complete after 5 minutes by the disappearance of the red-orange color of the trityl cation. Volatiles were removed under vacuum, yielding a pale yellow solid. Then, the solid was washed three times with totally 15 mL of hexanes, and the desired product was obtained as a white solid (33.2 mg, 0.043 mmol, 86 % yield). ^{1}H-NMR (400 MHz, $CDCl_3$) δ 7.39 (d, *J* = 7.6 Hz, 2H), 7.20 (s, 2H), 6.87 (t, *J* = 7.6 Hz, 1H), 5.96 (s, 4H), 2.50 (s, 12H), 2.26 (s, 12H), 1.14 (t, *J* = 8.0 Hz, 6H), 0.24 (q, *J* = 8.1 Hz, 4H). ^{13}C-NMR (101 MHz, $CDCl_3$) δ 152.1, 151.8, 143.0, 133.6, 128.9, 121.3, 107.2, 71.8, 13.3, 12.6, 11.5, -2.0 . ^{19}F-NMR (376 MHz, $CDCl_3$) δ -151.72, -151.77. IR (Diamond ATR) 2848, 1594, 1559, 1455, 1422, 1388, 1363, 1319, 1243, 1089, 1050, 974, 953, 883, 851, 778, 762, 738, 700, 604, 574, 524, 502, 474 cm^{-1}. Elemental analysis (based on formula $C_{32}H_{44}BF_4N_9Zn_2$): C (48.96% found, 49.77% expected, 0.81% difference), H (5.33% found, 5.74% expected, 0.41% difference), N (15.30% found, 16.32% expected, 1.02% difference).

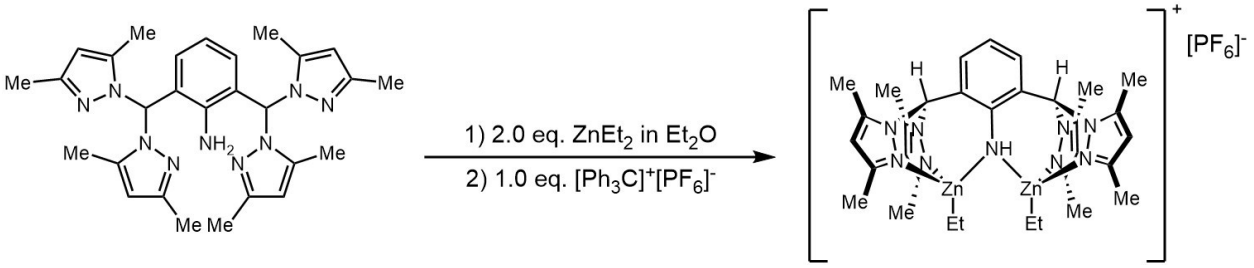

$AD^{Me}H_2$ (**1**) **6**-PF_6

6-PF_6. ([$AD^{Me}HZn_2Et_2$][PF_6]). In a nitrogen glovebox, a vial was charged with $AD^{Me}H_2$ (**1**) (25 mg, 0.050 mmol, 1 equivalent), diethylzinc (10.4 µL, 0.10 mmol, 2 equivalents), and diethyl ether (2 mL). After 5 minutes, a solution of trityl hexafluorophosphate (Ph_3CPF_6, 19.5 mg, 0.0502 mmol, 1 equivalent) and Et_2O (2 mL) was added. The reaction was judged to be complete after 5 minutes by the disappearance of the red-orange color of the trityl cation. Volatiles were removed under vacuum, yielding a pale yellow solid. Then, the solid was washed three times with totally 15 mL of hexanes, and the desired product was obtained as a white solid (36.5 mg, 0.044 mmol, 88 % yield). ^{1}H-NMR (400 MHz, $CDCl_3$) δ 7.38 (d, J = 6.9 Hz, 2H), 7.12 (s, 2H), 6.98-6.95 (t, 1H), 5.98 (s, 4H), 2.48 (s, 12H), 2.26 (s, 12H), 1.18-1.14 (t, 6H), 0.30-0.25 (q, 4H). ^{13}C-NMR (101 MHz, CD_2Cl_2) δ 152.5, 152.1, 142.6, 133.0, 130.6, 127.9, 107.2, 71.9, 13.1, 12.4, 11.2, -2.0. ^{19}F-NMR (376 MHz, CD_2Cl_2) δ -73.30 (d, J = 710.2 Hz). IR (Diamond ATR) 2672, 2348, 2116, 1577, 1554, 1514, 1459, 1352, 1292, 1215, 1184, 957, 939, 782, 762, 726, 703, 658, 601, 569, 535, 512, 490, 437 cm^{-1}. Elemental analysis (based on formula $C_{32}H_{44}F_6N_9PZn_2$): C (47.14% found, 46.28% expected, 0.86% difference), H (5.26% found, 5.34% expected, 0.08% difference), N (13.40% found, 15.18% expected, 1.78% difference).

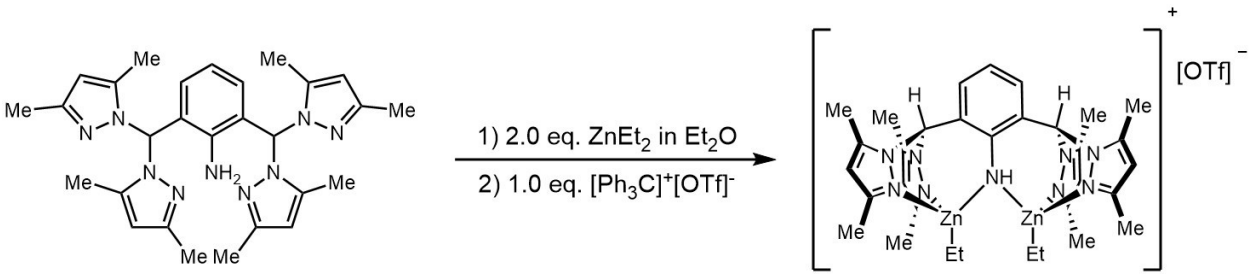

$AD^{Me}H_2$ (**1**) **6**-OTf

6-OTf. ([$AD^{Me}HZn_2Et_2$][OTf]). In a nitrogen glovebox, a vial was charged with $AD^{Me}H_2$ (**1**) (25 mg, 0.050 mmol, 1 equivalent), diethylzinc (10.4 µL, 0.10 mmol, 2 equivalents), and diethyl ether (2 mL). After 5 minutes, a solution of trityl triflate (Ph_3COTf, 19.7 mg, 0.0502 mmol, 1 equivalent) and Et_2O (2 mL) was added. The reaction was judged to be complete after 5 minutes by the disappearance of the red-orange color of the trityl cation. Volatiles were removed under vacuum down to a pale yellow solid. Then, the solid was washed three times with totally 15 mL of hexanes, and the desired product was obtained as a white solid (34.2 mg, 0.041 mmol, 82 % yield). ^{1}H-

NMR (400 MHz, CD_2Cl_2) δ 7.00 (s, 2H), 6.65 (s, 2H), 6.30-6.26 (t, 1H), 5.99 (s, 4H), 2.42 (s, 12H), 2.25 (s, 12H), 1.07-1.04 (t, 6H), 0.11 (dd, J= 15.8, 8.3 Hz, 4H). ^{13}C-NMR (101 MHz, CD_2Cl_2) δ 155.4, 151.2, 142.0, 132.4, 122.2, 122.0, 106.9, 71.1, 13.0, 12.4, 11.3, -2.3. ^{19}F-NMR (376 MHz, CD_2Cl_2) δ -78.76. IR (Diamond ATR) 2852, 1595, 1561, 1457, 1421, 1389, 1364, 1306, 1235, 1209, 1166, 1130, 1045, 1021, 986, 953, 879, 846, 804, 744, 696, 644, 617, 600, 572, 516, 478 cm^{-1}. Elemental analysis (based on formula $C_{33}H_{44}F_3N_9O_3SZn_2$): C (46.02% found, 47.49% expected, 1.47% difference), H (5.22% found, 5.31% expected, 0.09% difference), N (14.39% found, 15.10% expected, 0.71% difference).

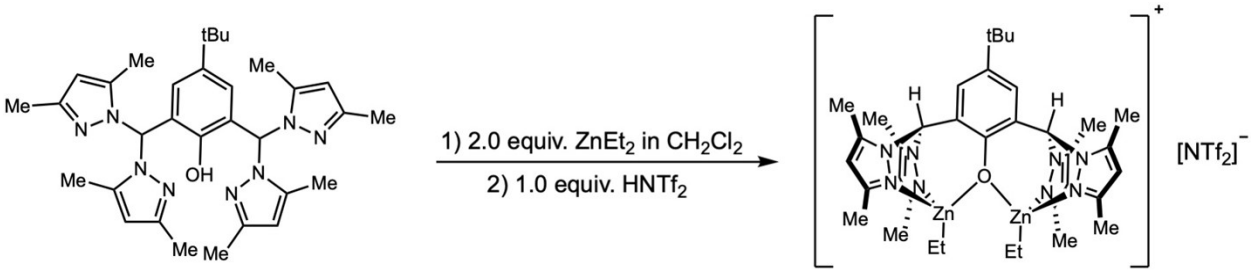

$PD^{Me}H$ $[PD^{Me}Zn_2Et_2][NTf_2]$ (**11**)

$[PD^{Me}Zn_2Et_2][NTf_2]$ (**11**). In a nitrogen glovebox, a vial was charged with $PD^{Me}H$ (27.0 mg, 0.049 mmol, 1 equivalent), diethylzinc (10 μL, 0.98 mmol, 2 equivalents), and CH_2Cl_2 (2 mL). After 5 minutes, a solution of trifluoromethanesulfonimide ($HNTf_2$, 13.7 mg, 0.049 mmol, 1 equivalent) and CH_2Cl_2 (2 mL) was added. The reaction was judged to be complete after 15 minutes by the appearance of white solid precipitate. Volatiles were removed under vacuum, giving our desired product as a white solid (45.10 mg, 0.044 mmol, 90 % yield). ^{1}H-NMR (400 MHz, CD_2Cl_2) δ 7.09 (s, 2H), 6.92 (s, 2H), 6.01 (s, 4H), 2.42 (s, 12H), 2.28 (s, 12H), 1.23 (s, 9H), 1.18 (t, J = 8.1 Hz, 6H), 0.35 (q, J = 8.1 Hz, 4H). ^{13}C-NMR (101 MHz, CD_2Cl_2) δ 158.2, 152.0, 142.2, 140.6, 129.7, 125.6, 107.1, 71.6, 33.7, 30.9, 13.2, 12.0, 11.3, -1.7. ^{19}F-NMR (376 MHz, $CD2Cl_2$) δ -79.4. IR (Diamond ATR) 2931, 2897, 2859, 1558, 1483, 1465, 1423, 1383, 1344, 1324, 1223, 1186, 1137, 1054, 986, 954, 917, 892, 855, 836, 813, 786, 760, 737, 709, 679, 657, 632, 608, 569, 511, 469, 441, 411 cm^{-1}. Elemental analysis (based on formula $C_{38}H_{51}F_6N_9O_5S_2Zn_2$): C (42.70% found, 44.63% expected, 1.93% difference), H (4.44% found, 5.03% expected, 0.59% difference), N (11.62% found, 12.33% expected, 0.71% difference).

$PD^{H}H$ (**2**-H) $[PD^{H}Zn_2Et_2][NTf_2]$ (**12**)

$[PD^{H}Zn_2Et_2][NTf_2]$ (**12**). In a nitrogen glovebox, a vial was charged with $PD^{H}H$ (**2**-H) (88 mg, 0.2 mmol, 1 equivalent), diethylzinc (42 µL, 0.4 mmol, 2 equivalent), and dichloromethane (3 mL). After 1 minute, a solution of *bis*(trifluoromethanesulfonyl)imide ($HNTf_2$ 56 mg, 0.2 mmol, 1 equivalents) and CH_2Cl_2 (2 mL) was added, resulting in the evolution of gas. After five minutes, no bubbles were observed and the reaction was deemed to be complete. Volatiles were removed under vacuum down to a white solid (177 mg, 0.195 mmol, 98% yield). ^{1}H-NMR (400 MHz, CD_2Cl_2) δ 8.03 (d, J = 2.5 Hz, 4H), 7.71 (d, J = 2.0 Hz, 4H), 7.59 (s, 2H), 7.40 (s, 2H), 6.42 (t, J = 2.3 Hz, 4H), 1.25 (t, J = 8.0 Hz, 6H), 1.19 (s, 9H), 0.42 (q, J = 8.2 Hz, 4H). ^{13}C-NMR (101 MHz, CD_2Cl_2) δ 157.4, 142.1, 141.1, 133.1, 131.4, 125.1, 107.1, 78.0, 33.9, 30.8, 12.7, -2.3. The spectrum matches with the existing literature report.[9]

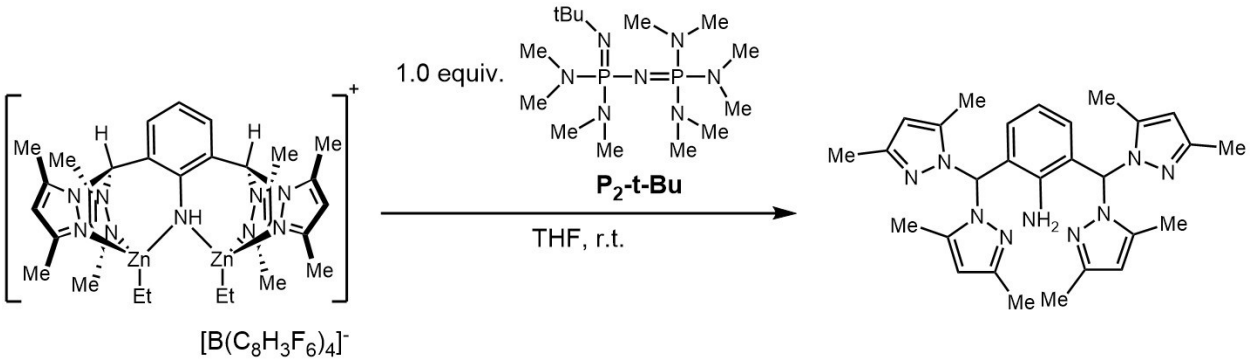

$[AD^{Me}HZn_2Et_2][BArF]$ (**6**-BArF) $AD^{Me}H_2$ (**1**)

Section S4.2. Deprotonation of $[AD^{Me}HZn_2Et_2][B(C_8H_3F_6)_4]$ (**6**-BArF). In a nitrogen glovebox, $[AD^{Me}HZn_2Et_2][B(C_8H_3F_6)_4]$ (**6**-BArF) (15.50 mg. 0.01 mmol, 1 equivalents) was weighed out in

[9]Gu, Z.; Comito, R. J. Binucleating *Bis*(Pyrazolyl)Alkane Ligands and Their Cationic Dizinc Complexes: Modular, Bimetallic Catalysts for Ring-Opening Polymerization. *Organometallics* **2022**, *41*, 1911–1916.

a dry vial. THF (2 mL) which was degassed and dried prior use was added into the vial to dissolve the solid giving a clear solution. To the clear solution, P_2-t-Bu 2.0 M in THF solution (5.0 µL, 0.01 mmol, 1 equivalents) was added using a micropipette. Upon addition the solution turned cloudy due to precipitate formation. The vial was left stirring for overnight under nitrogen atmosphere. Later, the volatiles were removed under vacuum to give a white powdery solid. The solid was partially soluble in CD_2Cl_2, which was then taken for NMR analysis. The ^{1}H NMR analysis of the crude reaction mixture completely matched with our proligand $AD^{Me}H_2$ (**1**), **5** along with residual P_2-t-Bu. ^{1}H-NMR (400 MHz, CD_2Cl_2) δ 7.70 (s, 8H), 7.54 (s, 4H), 7.30 (s, 2H), 6.60 (t, J = 7.8 Hz, 1H), 6.43 (d, J = 7.8 Hz, 2H), 5.85 (s, 4H), 2.15 (s, 12H), 2.08 (s, 12H).

Deprotonation of $[AD^{Me}HZn_2Et_2][B(C_8H_3F_6)_4]$ using lithium bases like LiHMDS, PhLi and n-BuLi in THF and Et_2O did not give the desired product but instead produced a complex mixture of products. Also, deprotonation using TBD (1,5,7-Triazabicyclo[4.4.0]dec-5-ene) gave us the proligand $AD^{Me}H_2$, (**1**).

S5. Spectral data of metal complexes.

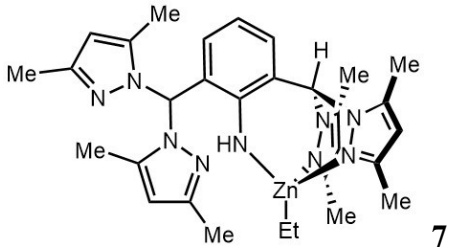

7

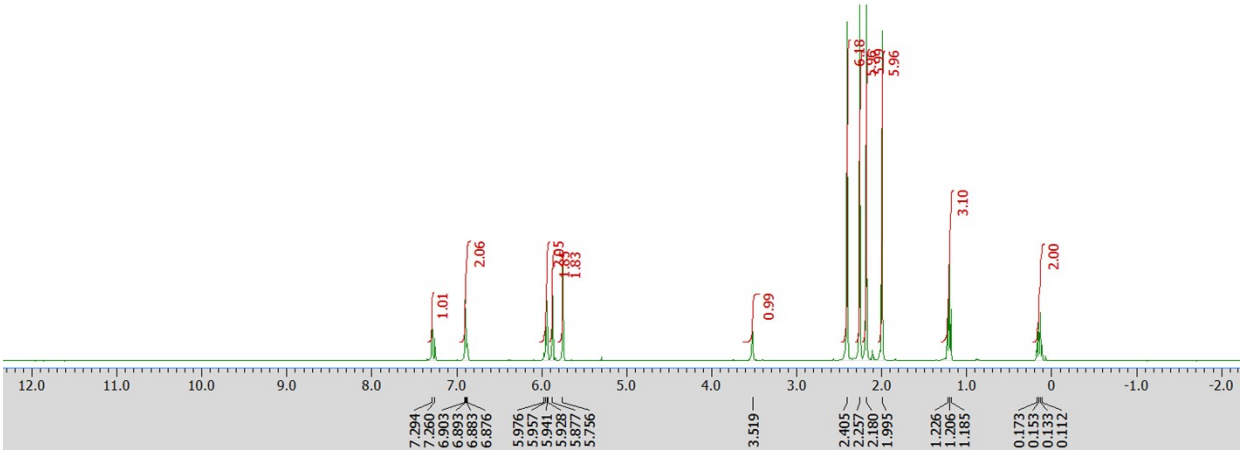

Figure S16. ^{1}H-NMR of **7**, $CDCl_3$, 400 MHz.

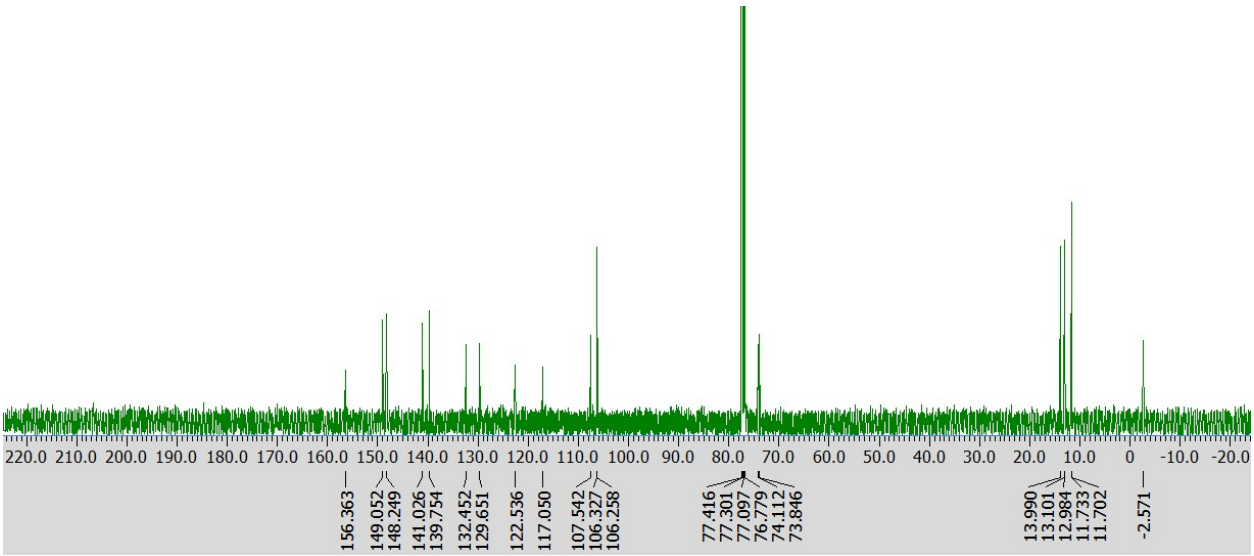

Figure S17. ^{13}C-NMR of **7**, $CDCl_3$, 101 MHz.

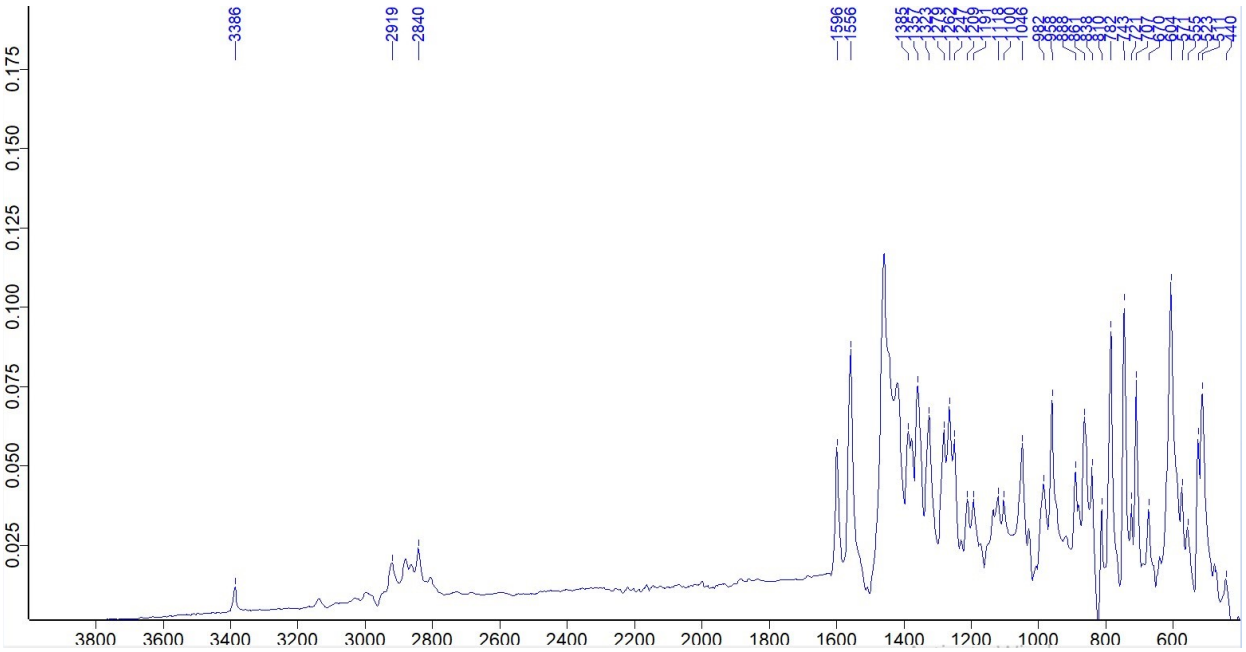

Figure S18. Infrared spectrum of **7**, diamond ATR.

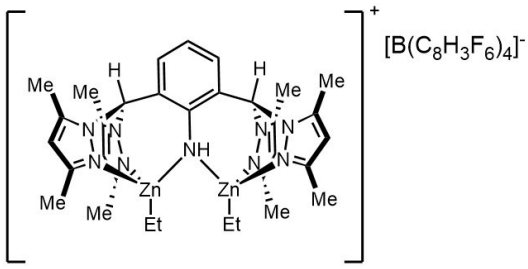

6-BArF

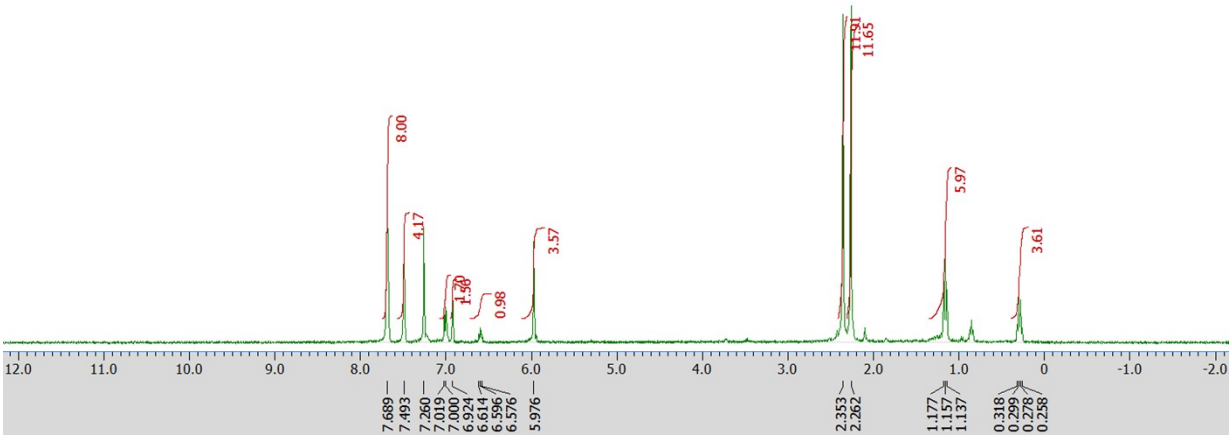

Figure S19. ^{1}H-NMR of **6**-BArF, $CDCl_3$, 400 MHz.

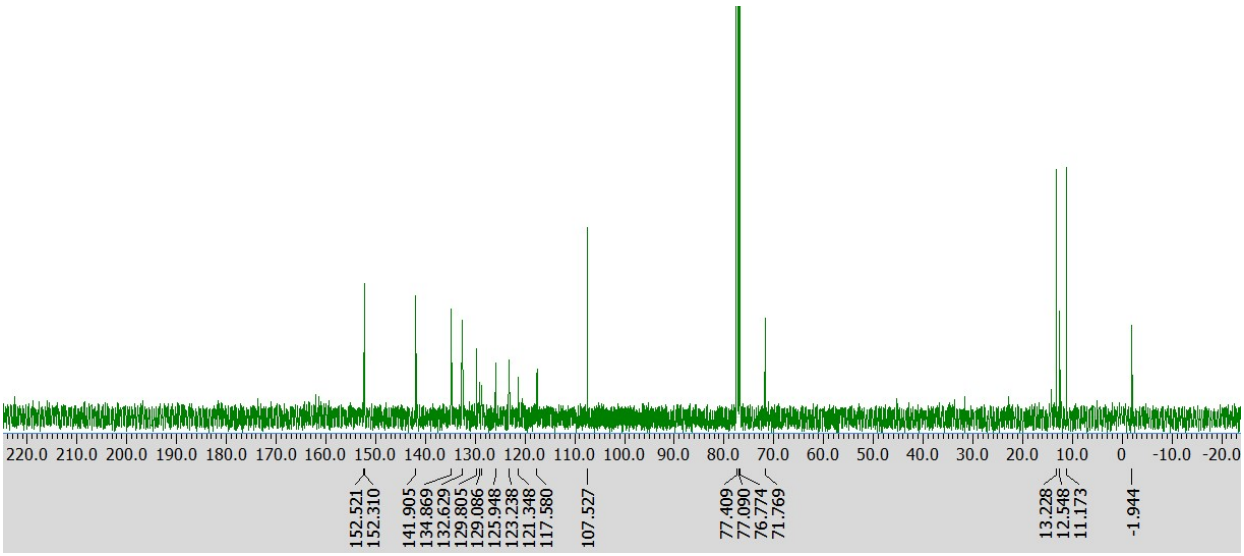

Figure S20. ^{13}C-NMR of **6**-BArF, $CDCl_3$, 101 MHz.

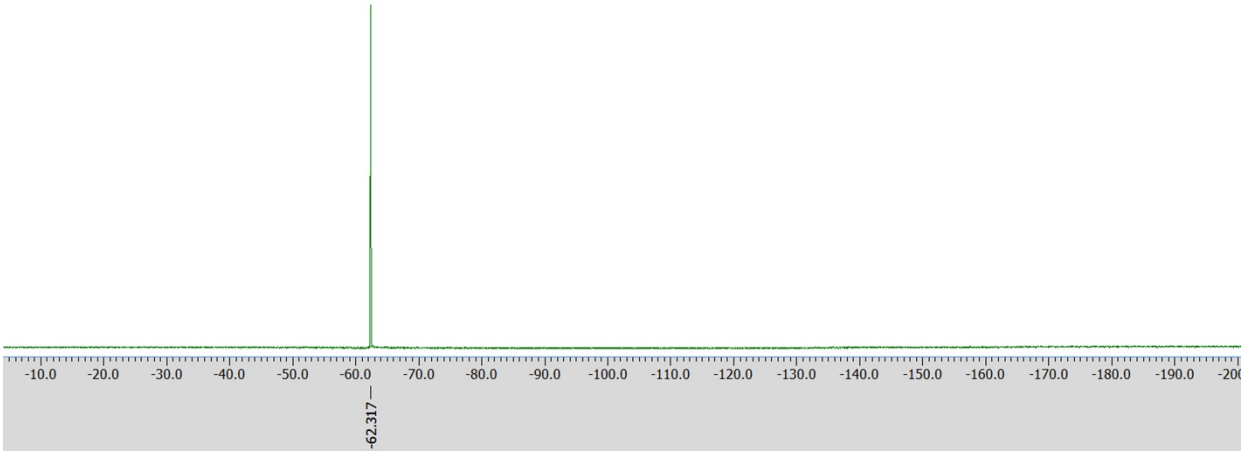

Figure S21. ^{19}F-NMR of **6**-BArF, $CDCl_3$, 470 MHz.

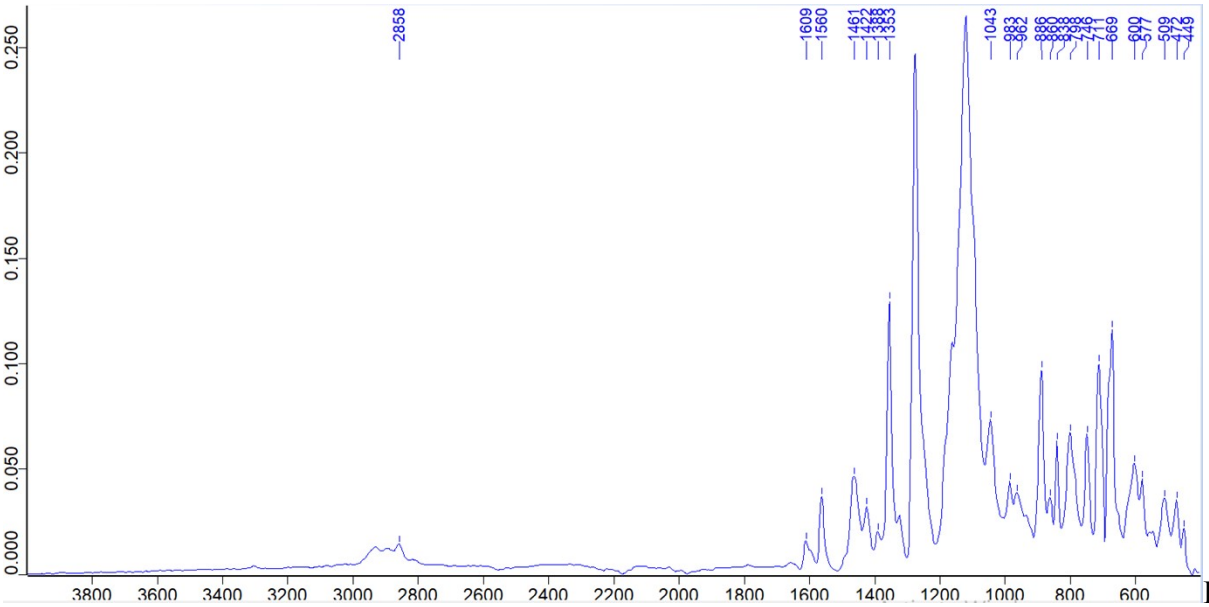

Figure S22. Infrared spectrum of **6**-BArF, diamond ATR.

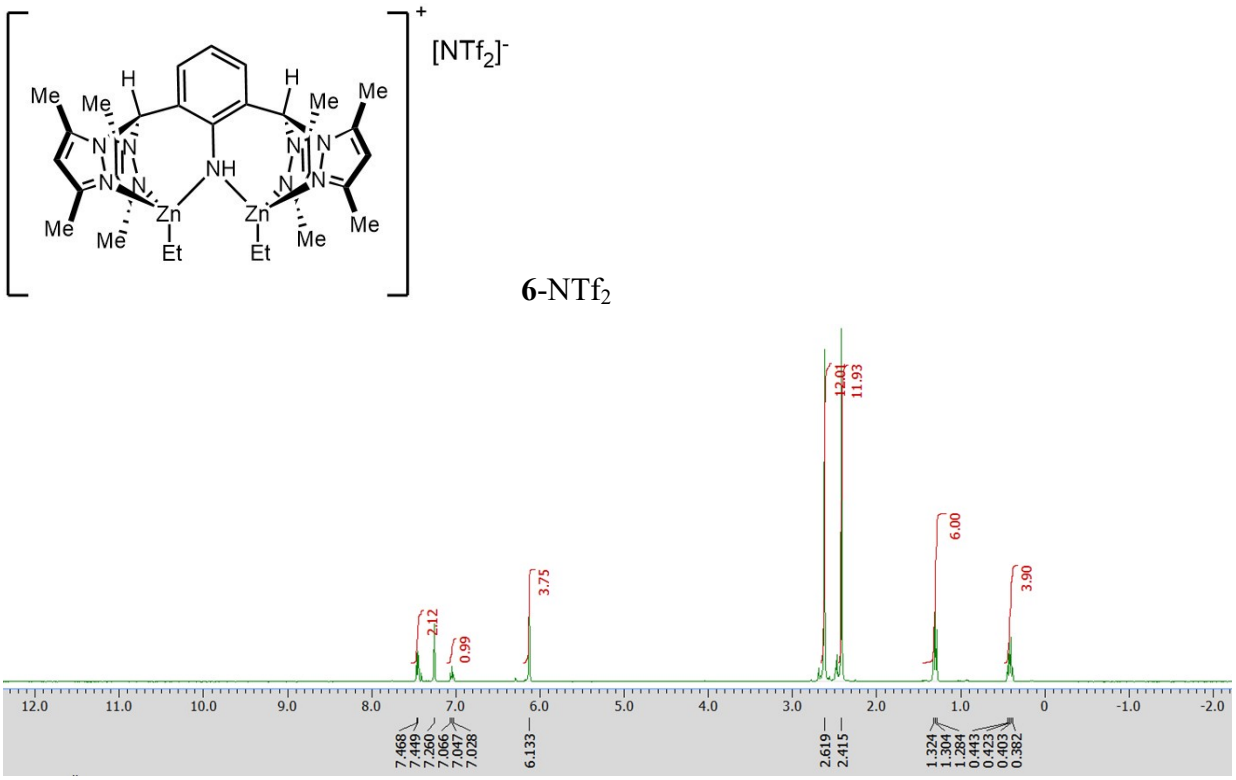

Figure S23. ^{1}H-NMR of **6**-NTf_2, $CDCl_3$, 400 MHz.

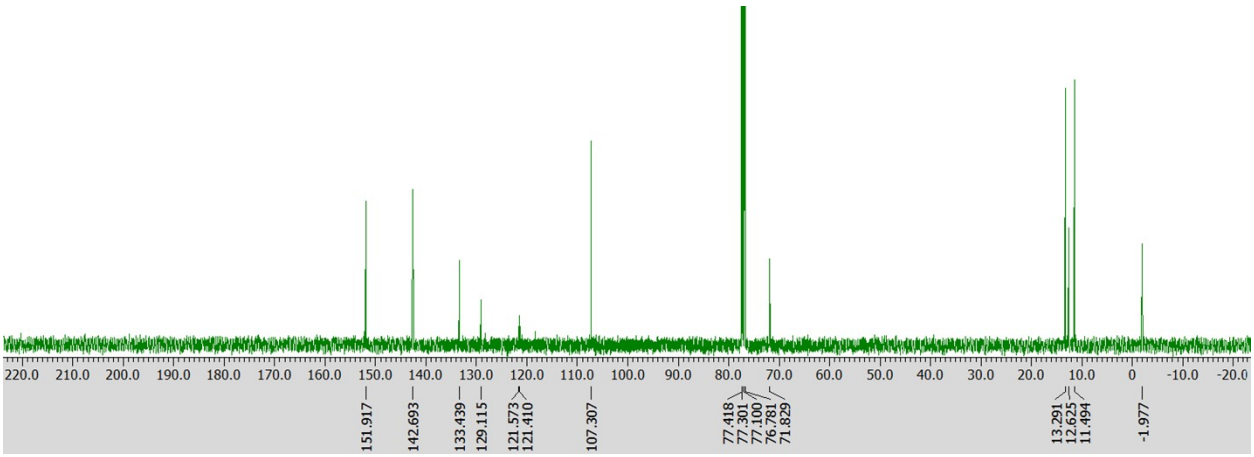

Figure S24. ^{13}C-NMR of **6**-NTf_2, $CDCl_3$, 101 MHz.

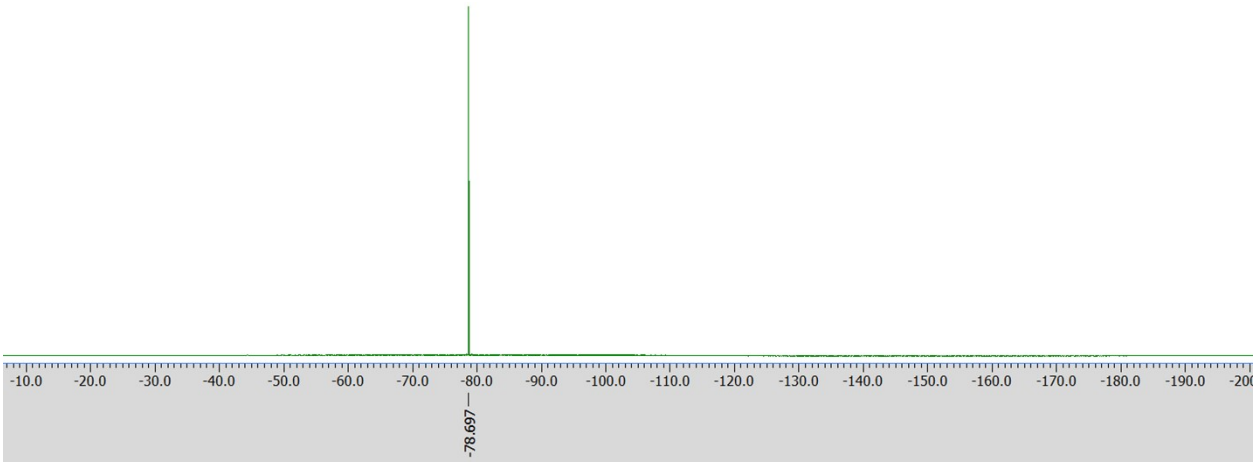

Figure S25. ^{19}F-NMR of **6**-NTf_2, $CDCl_3$, 376 MHz.

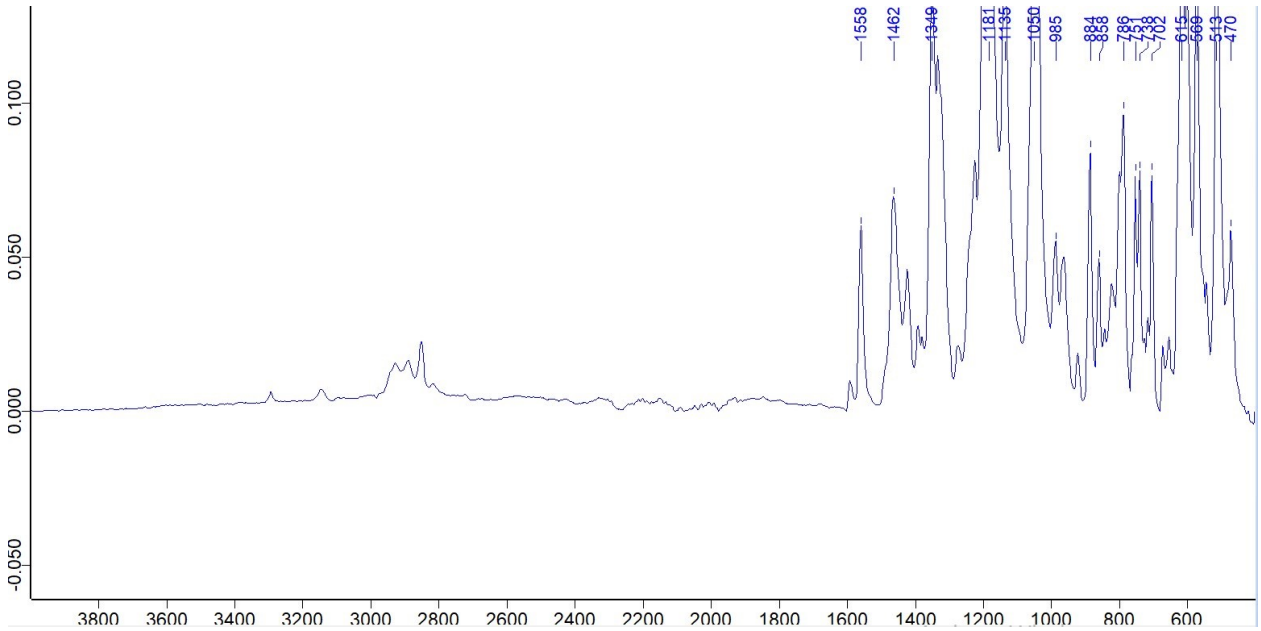

Figure S26. Infrared spectrum of **6**-NTf_2, diamond ATR.

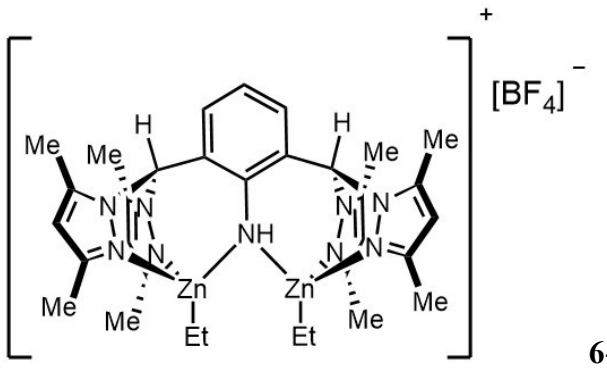

6-BF_4

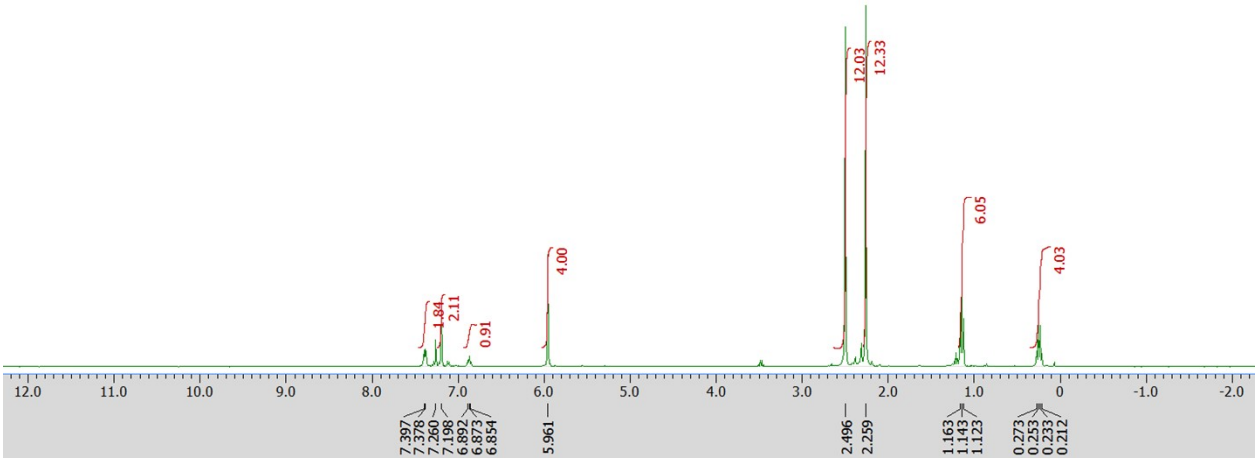

Figure S27. ^{1}H-NMR of **6**-BF_4, $CDCl_3$, 400 MHz.

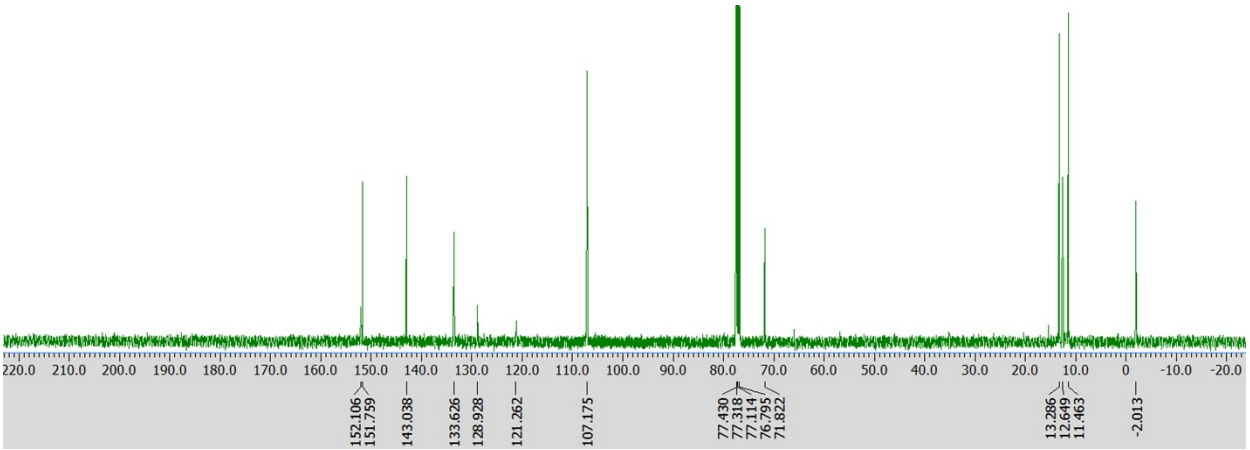

Figure S28. ^{13}C-NMR of **6**-BF_4, $CDCl_3$, 101 MHz.

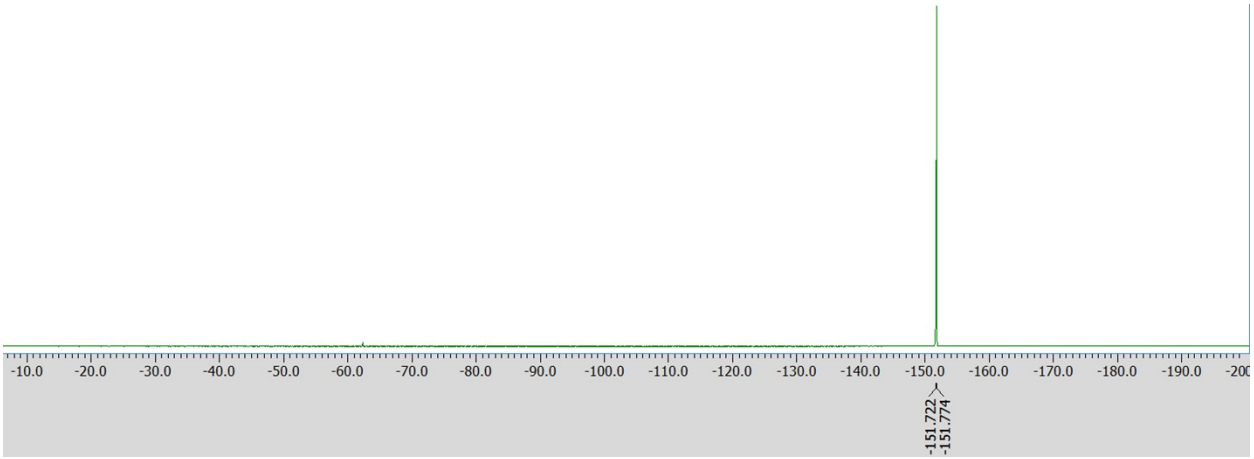

Figure S29. ^{19}F-NMR of **6**-BF_4, $CDCl_3$, 376 MHz.

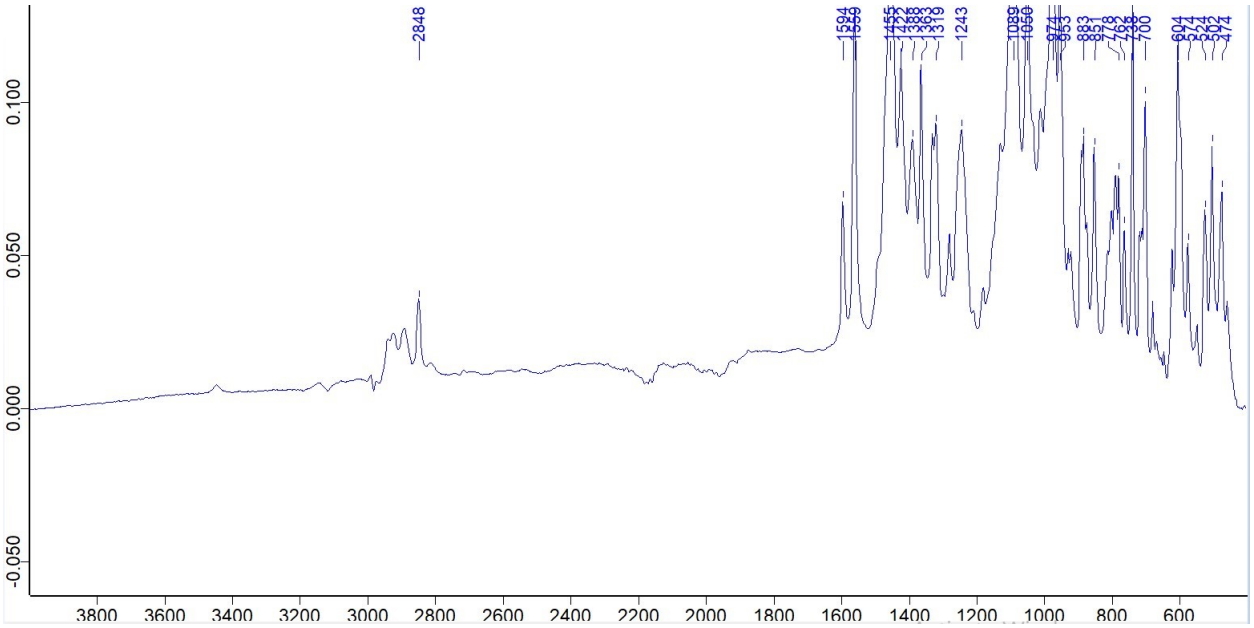

Figure S30. Infrared spectrum of **6**-BF_4, diamond ATR.

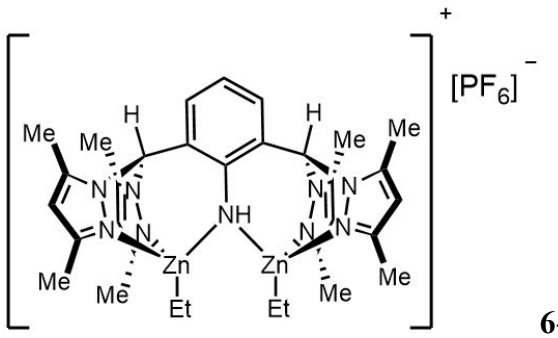

6-PF_6

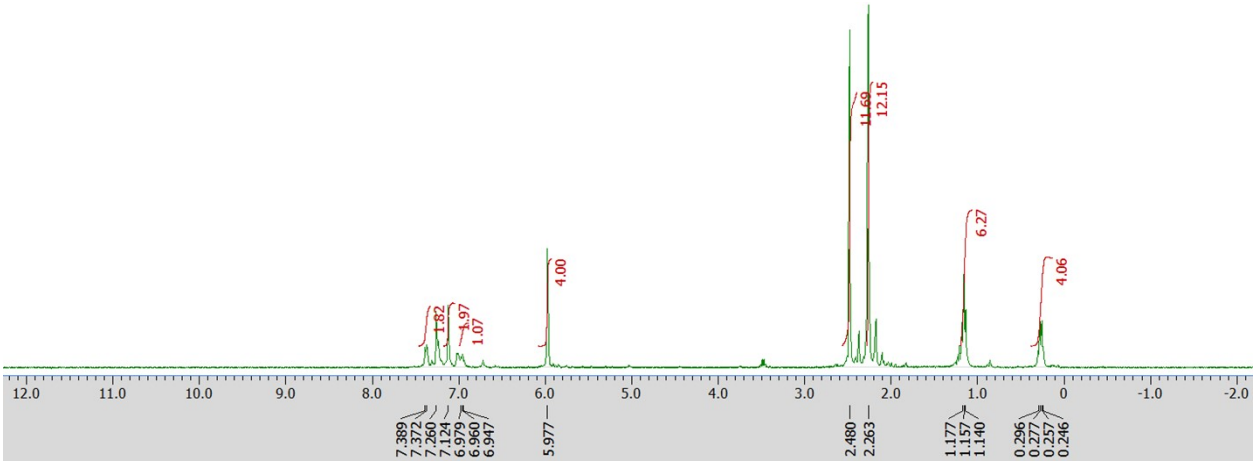

Figure S31. ^{1}H-NMR of **6**-PF_6, $CDCl_3$, 400 MHz.

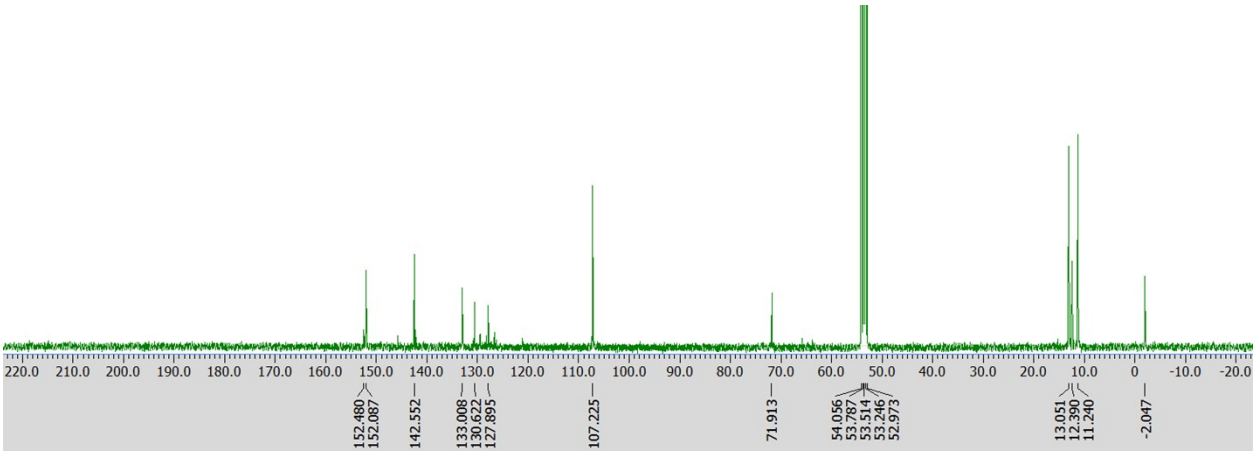

Figure S32. ^{13}C-NMR of **6**-PF_6, CD_2Cl_2, 101 MHz.

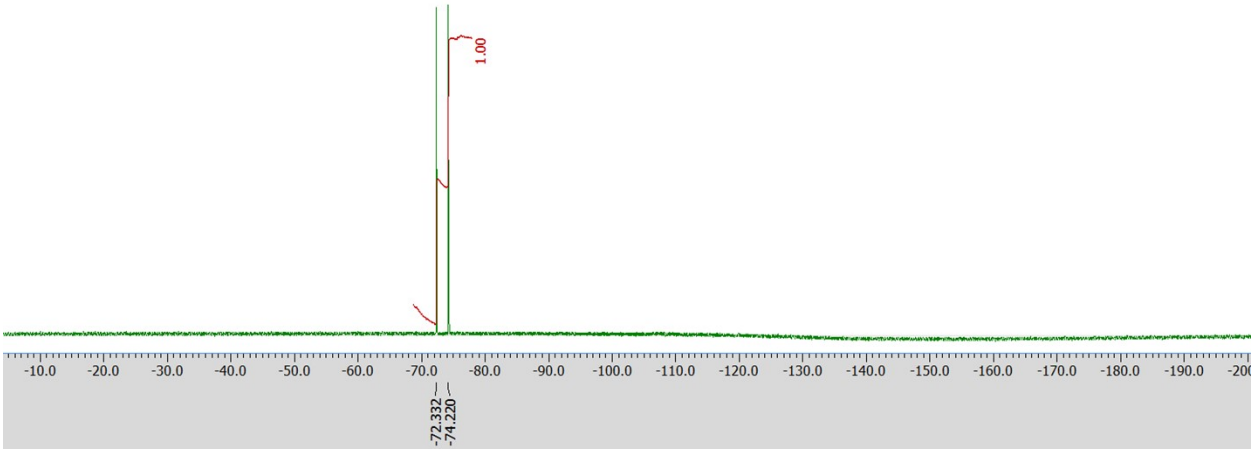

Figure S33. ^{19}F-NMR of **6**-PF_6, $CDCl_3$, 376 MHz.

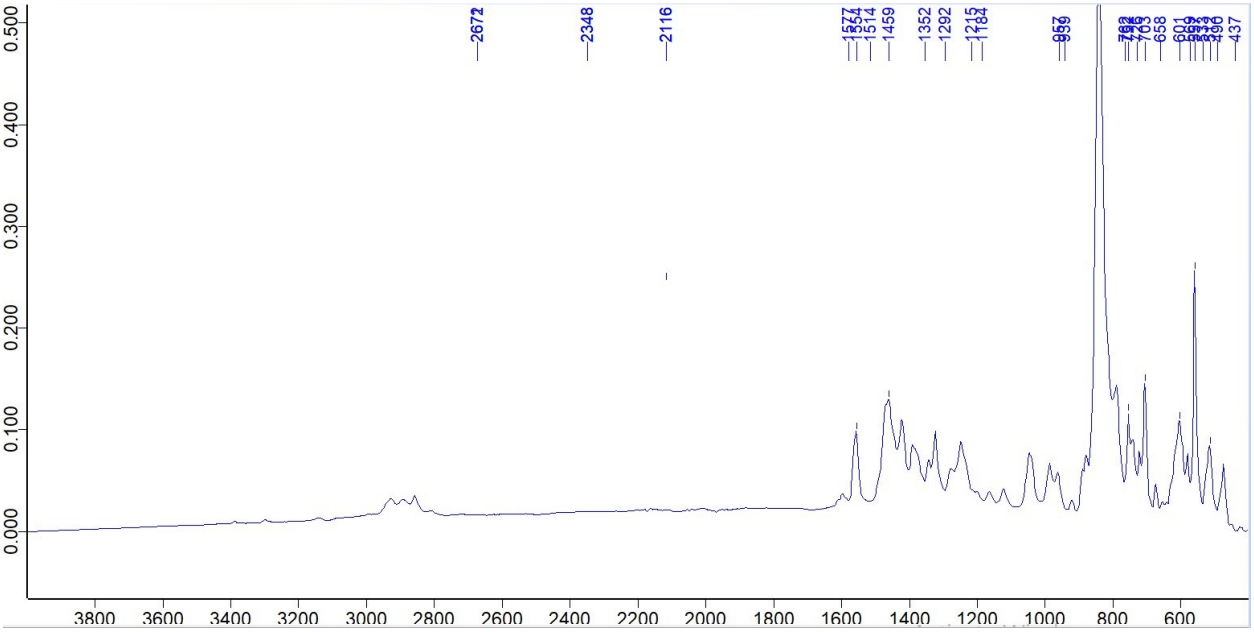

Figure S34. Infrared spectrum of **6**-PF_6, diamond ATR.

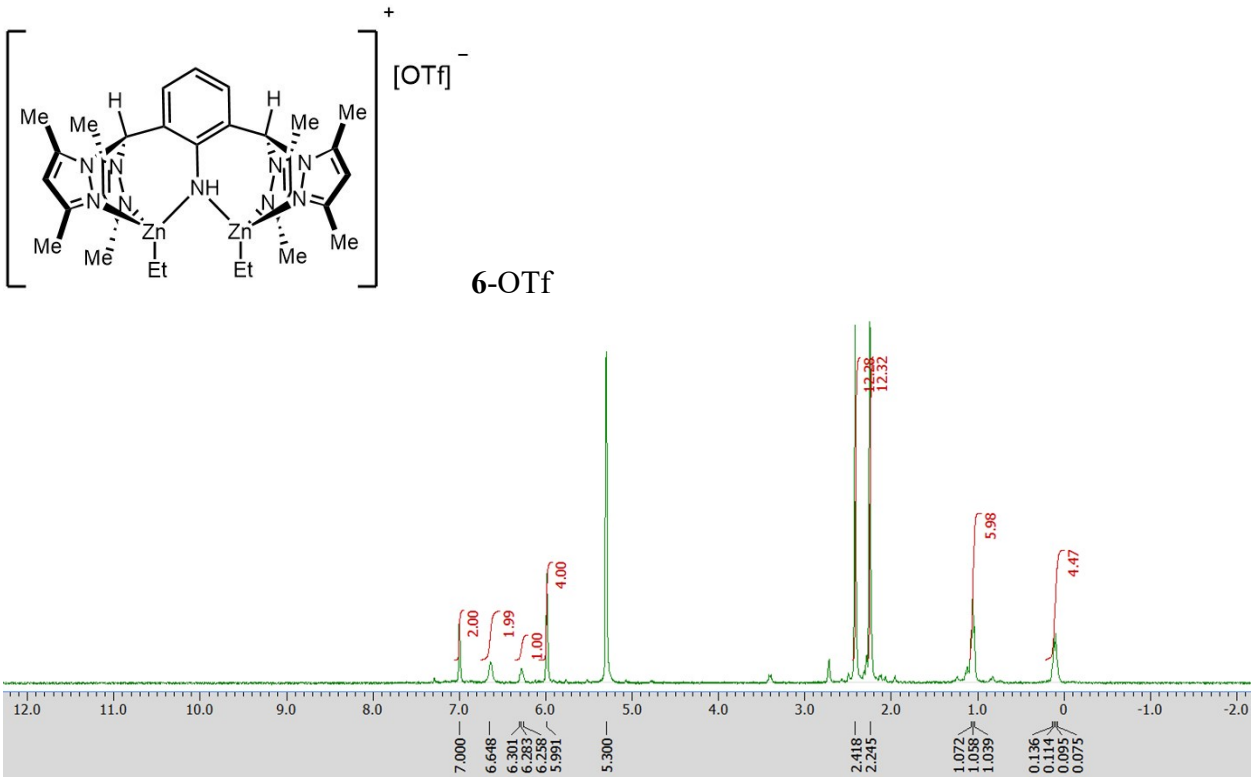

Figure S35. ^{1}H-NMR of **6**-OTf, CD_2Cl_2, 400 MHz.

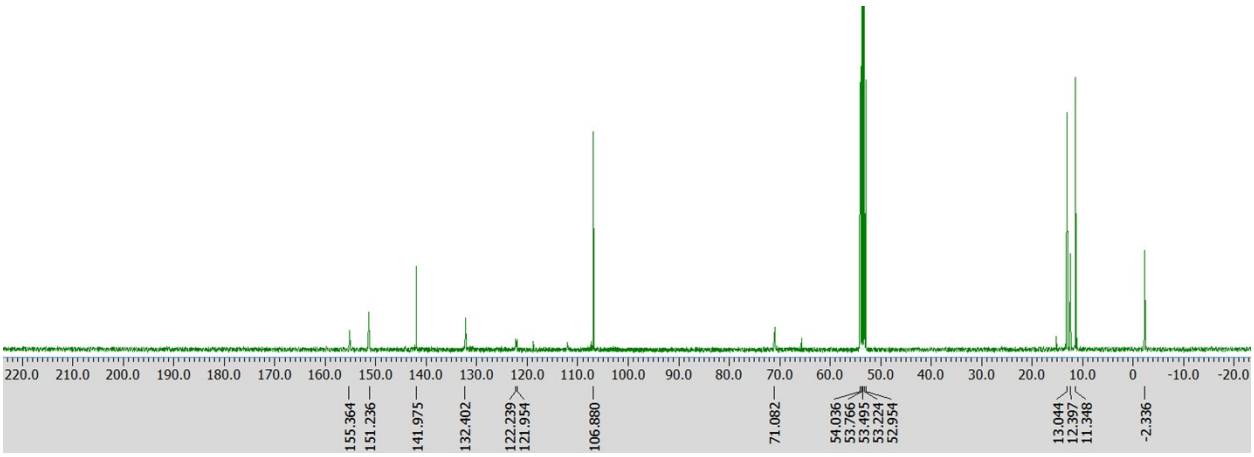

Figure S36. ^{13}C-NMR of **6**-OTf, CD_2Cl_2, 101 MHz.

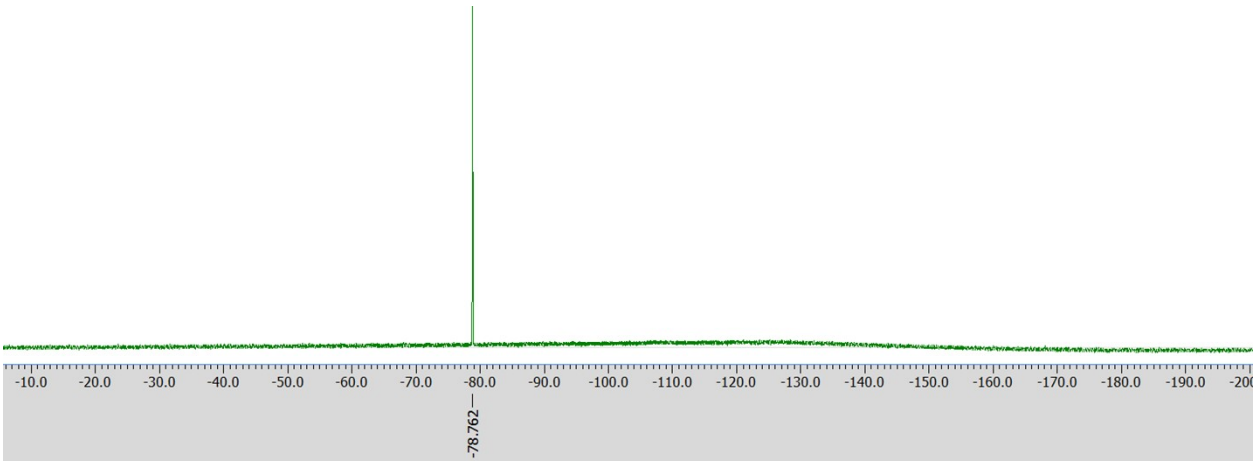

Figure S37. ^{19}F-NMR of **6**-OTf, CD_2Cl_2, 376 MHz.

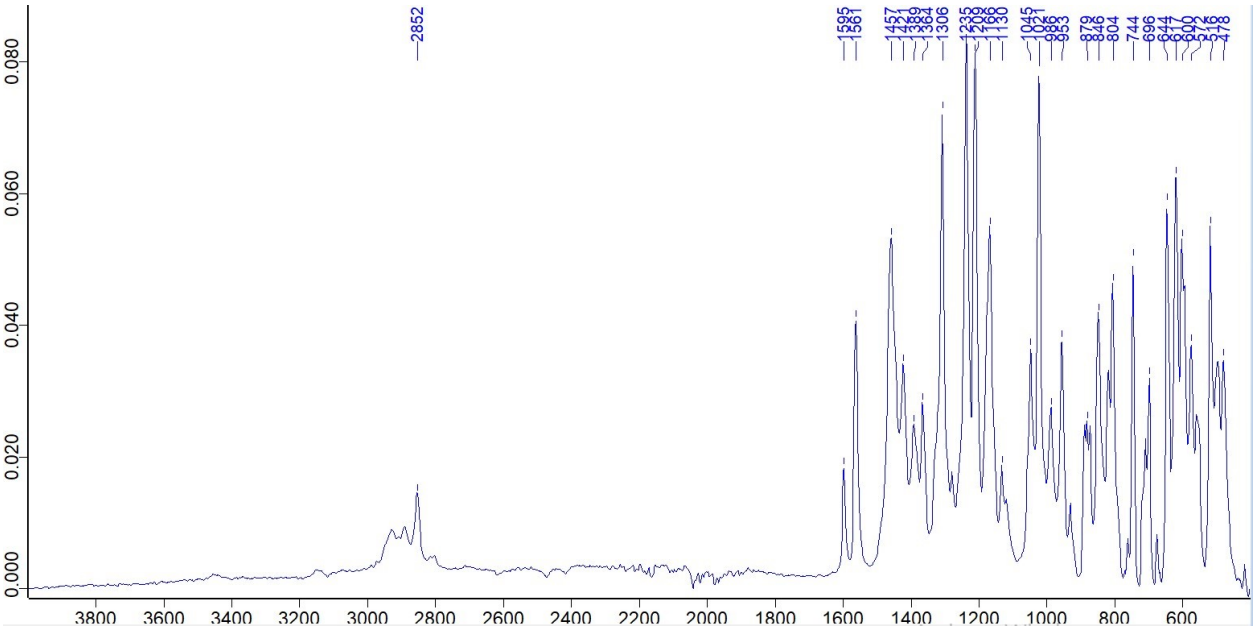

Figure S38. Infrared spectrum of **6**-OTf, diamond ATR.

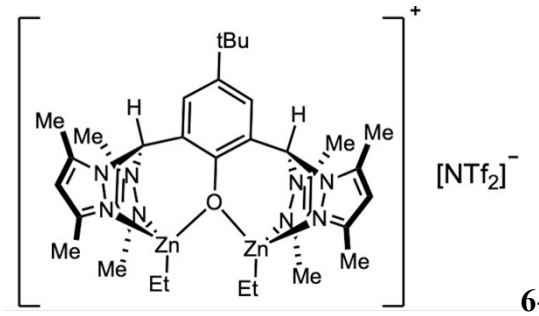

6-NTf_2

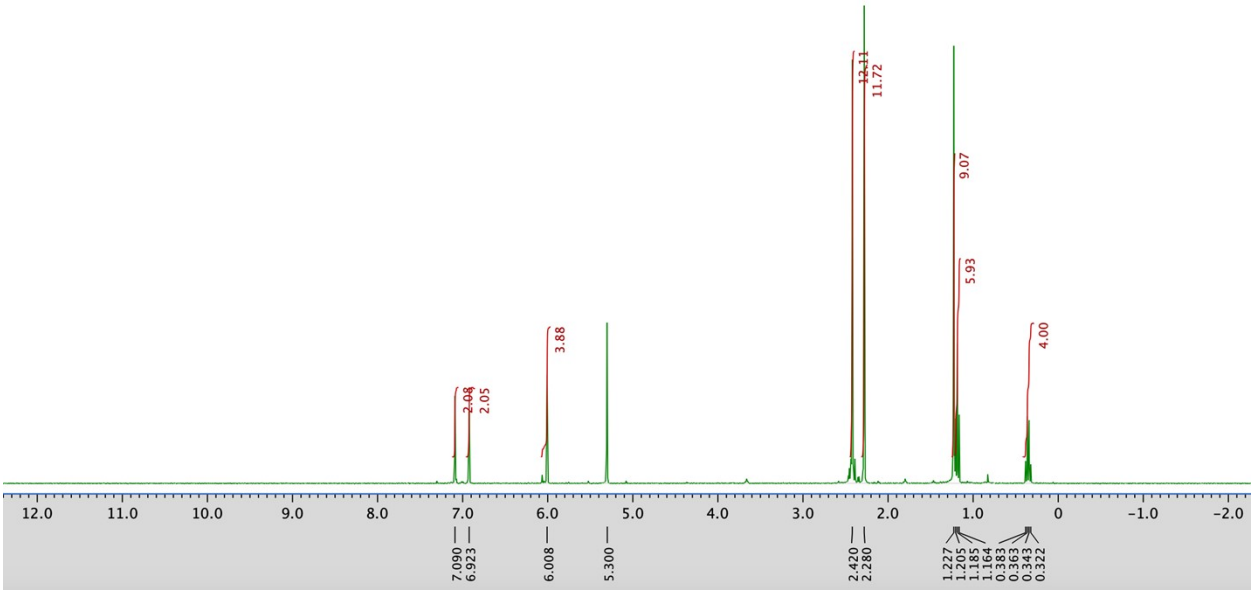

Figure S39. ^{1}H-NMR of **6**-NTf_2, CD_2Cl_2, 400 MHz.

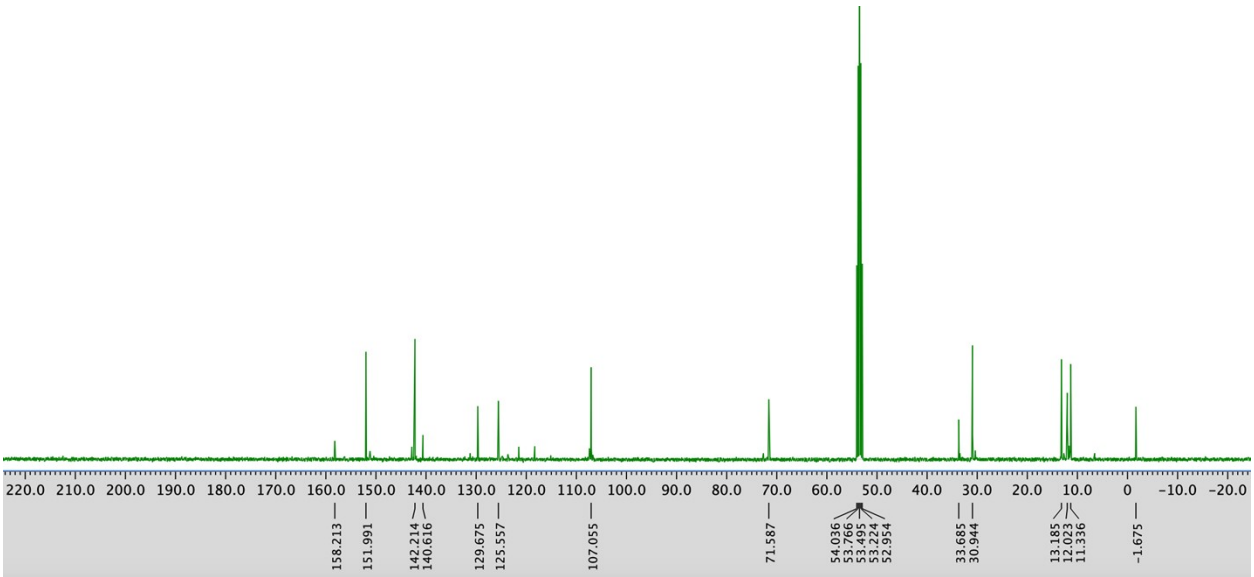

Figure S40. ^{13}C-NMR of **6**-NTf_2, CD_2Cl_2, 101 MHz.

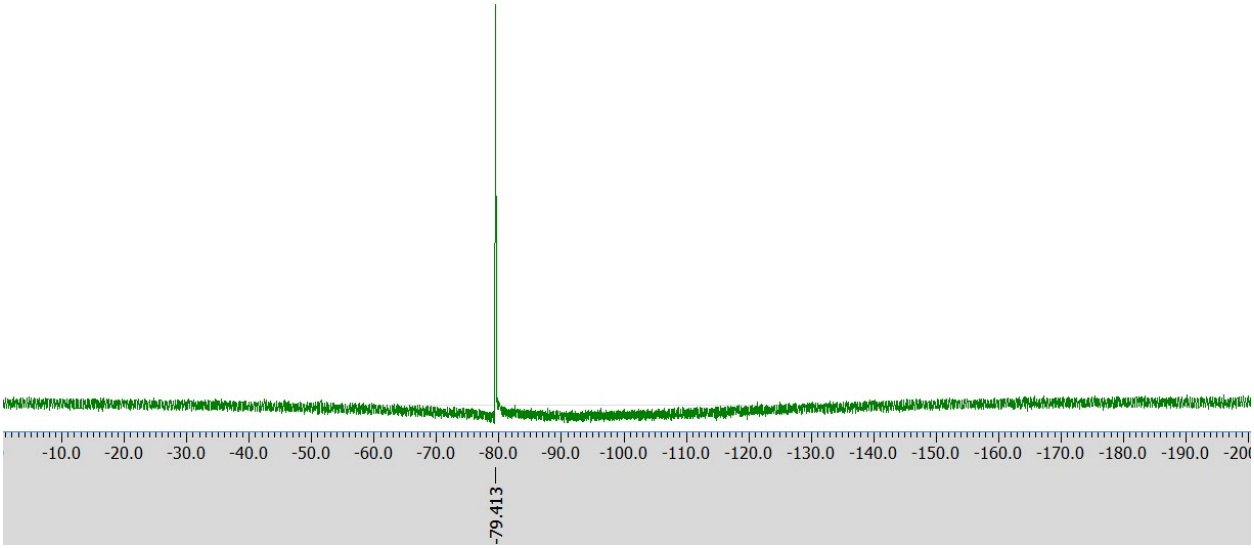

Figure S41. ^{19}F-NMR of **6**-NTf_2, CD_2Cl_2, 376 MHz.

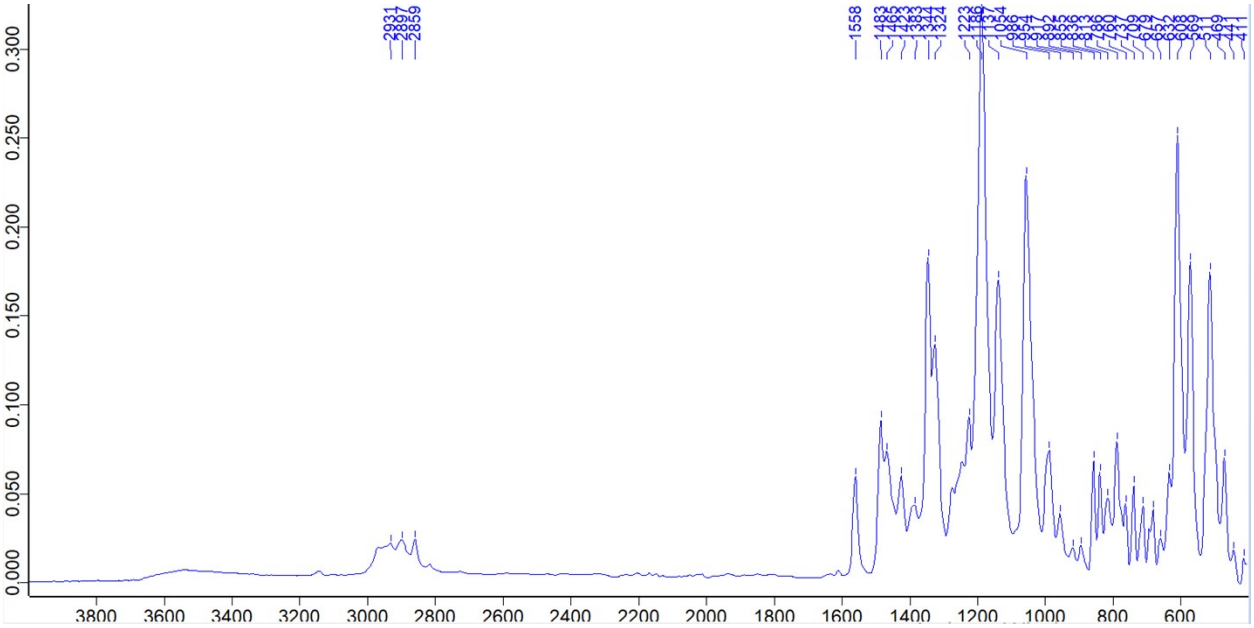

Figure S42. Infrared spectrum of **6**-NTf_2, diamond ATR.

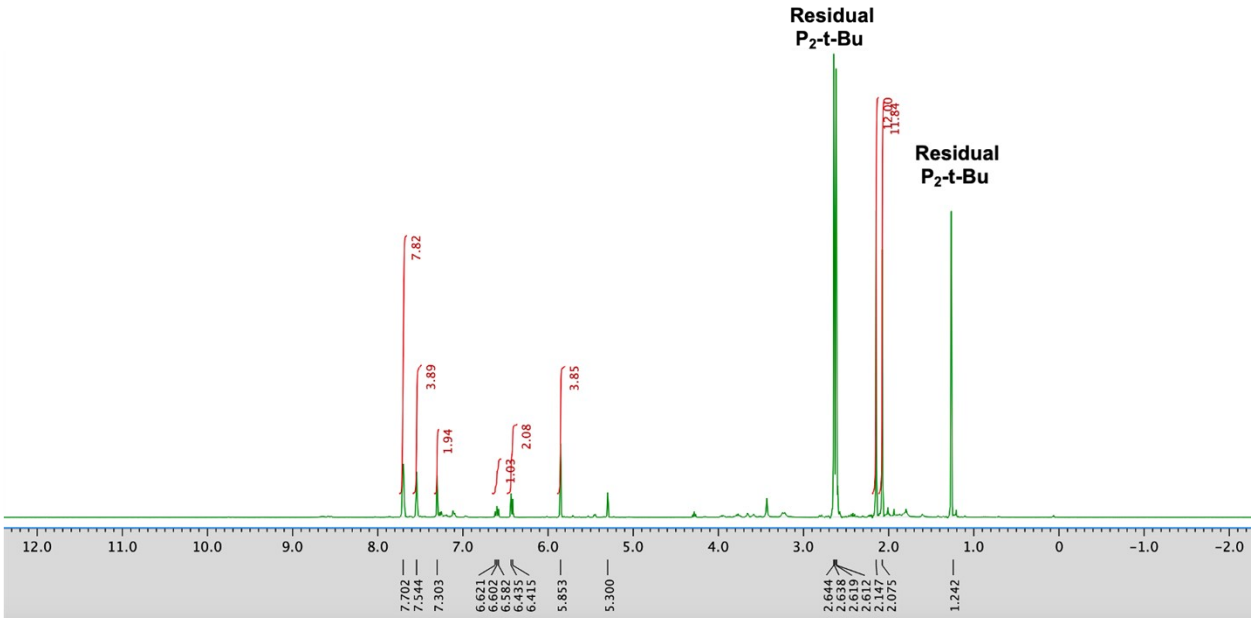

Figure S43. Crude ^{1}H-NMR of the reaction between 1-Ethyl-2,2,4,4,4-pentakis(dimethylamino)-2λ^{5},4λ^{5}-catenadi(phosphazene) and [AD^{Me}HZn$_2$Et$_2$][B(C$_8$H$_3$F$_6$)$_4$], CD_2Cl_2, 400 MHz),

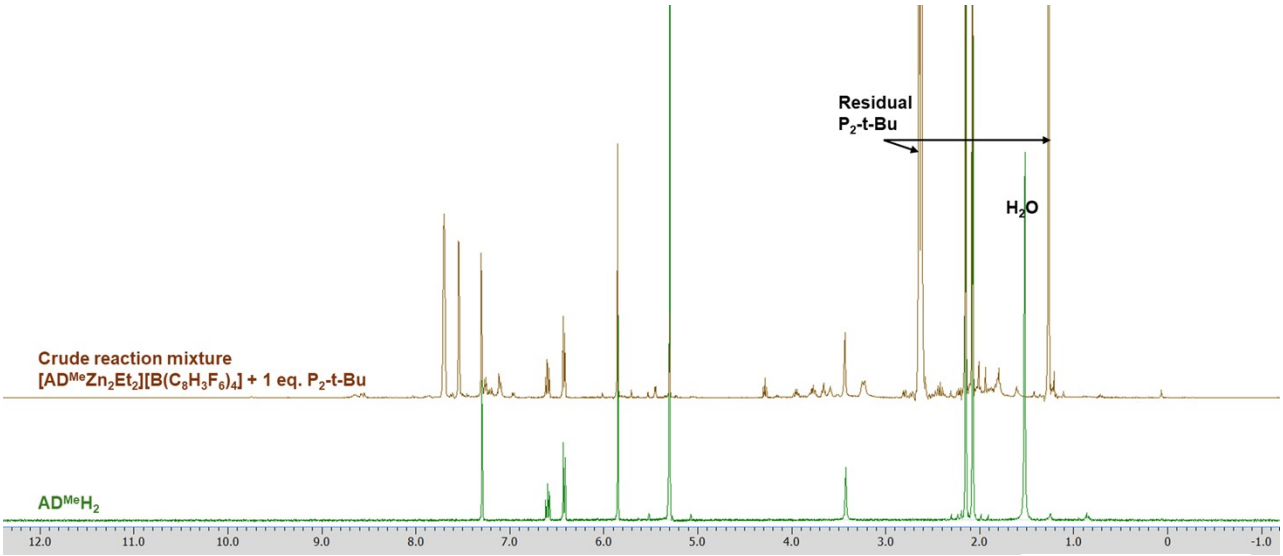

Figure S44. Stacked ^{1}H-NMR of the reaction between 1-Ethyl-2,2,4,4,4-pentakis(dimethylamino)-2λ^{5},4λ^{5}-catenadi(phosphazene) and [AD^{Me}HZn$_2$Et$_2$][B(C$_8$H$_3$F$_6$)$_4$] and AD^{Me}H$_2$ **5**, CD_2Cl_2, 400 MHz),

S6. X-ray diffraction analysis of 6-BArF.

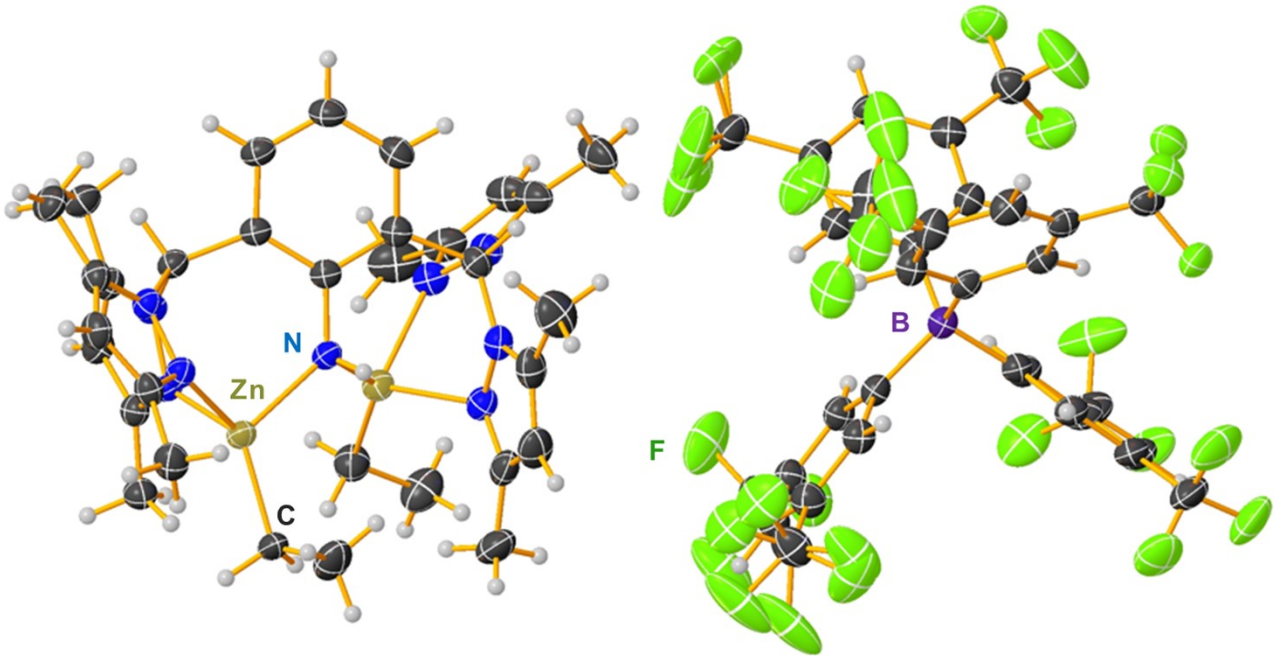

Figure S45. X-ray structure of $AD^{Me}HZn_2Et_2B(C_8H_3F_6)_4$. Thermal ellipsoids are 50% equiprobability envelopes.

Table S2. Crystal data and structure refinement for $[AD^{Me}HZn_2Et_2][B(C_8H_3F_6)_4]$ **6**-BArF.

Identification code	PN2-022__XW399_sq
Empirical formula	$C_{65}H_{58}BCl_2F_{24}N_9Zn_2$
Formula weight	1633.65
Temperature/K	123(2)
Crystal system	triclinic
Space group	P-1
a/Å	13.2518(3)
b/Å	13.6360(3)
c/Å	21.3029(4)
α/°	77.1250(10)
β/°	76.3660(10)
γ/°	85.9300(10)
Volume/Å^3	3646.25(14)
Z	2

ρ_{calc}g/cm^3	1.488
μ/mm^{-1}	2.440
F(000)	1652.0
Crystal size/mm^3	0.19 × 0.16 × 0.02
Radiation	CuKα (λ = 1.54178)
2Θ range for data collection/°	6.65 to 132.064
Index ranges	$-15 \leq h \leq 15$, $-16 \leq k \leq 16$, $-25 \leq l \leq 25$
Reflections collected	59186
Independent reflections	12262 [R_{int} = 0.0241, R_{sigma} = 0.0182]
Data/restraints/parameters	12262/598/986
Goodness-of-fit on F^2	1.027
Final R indexes [I>=2σ (I)]	R_1 = 0.0371, wR_2 = 0.0970
Final R indexes [all data]	R_1 = 0.0388, wR_2 = 0.0984
Largest diff. peak/hole / e Å^{-3}	0.72/-0.66

Table S3. Fractional Atomic Coordinates (×10^4) and Equivalent Isotropic Displacement Parameters (Å^2×10^3) for [AD^{Me}HZn$_2$Et$_2$][B(C$_8$H$_3$F$_6$)$_4$] **6**-BArF. U_{eq} is defined as 1/3 of of the trace of the orthogonalised U_{IJ} tensor.

Atom	***x***	***y***	***z***	**U(eq)**
Zn1	10579.2(2)	4566.5(2)	1517.3(2)	27.85(8)
Zn2	11212.4(2)	4998.5(2)	2860.1(2)	30.51(8)
Cl1	7272.0(6)	4573.7(5)	2411.8(4)	58.07(17)
Cl2	7155.5(7)	2427.8(6)	2531.8(5)	81.5(3)
F1	404.3(11)	-708.2(11)	9015.3(7)	49.5(3)
F2	1861.5(12)	-1311.1(10)	9222.6(7)	49.2(4)
F3	8858.2(13)	-132(2)	5119.0(11)	89.0(7)
F4	8699.3(12)	340.7(14)	6018.8(8)	61.2(4)
F10	1447.4(11)	233.7(10)	9234.7(7)	44.1(3)
F11	4735.5(13)	4292.9(11)	8265.6(8)	56.2(4)
F13	8093.0(14)	-665.7(13)	8962.8(9)	65.5(5)
F14	5335.0(16)	-3547.4(11)	8525.3(9)	68.8(5)
F16	8237.3(14)	1346.2(15)	5227.7(10)	83.6(6)
F17	3800.1(16)	3020.4(17)	8764.2(9)	86.9(7)
F18	5437.3(17)	2913.7(14)	8649.8(9)	73.6(5)
F21	7386.2(16)	790.7(13)	8689.0(12)	82.4(7)
F22	8438.7(13)	151.7(14)	7958.3(11)	72.8(5)
F23	4158.6(14)	-2877.1(13)	9164.4(11)	85.1(7)
F24	5624.2(17)	-3310.7(12)	9421.2(9)	74.0(5)
N1	9386.6(14)	5095.1(13)	1032.0(8)	29.4(4)

Table S3. Fractional Atomic Coordinates ($\times 10^4$) and Equivalent Isotropic Displacement Parameters ($Å^2 \times 10^3$) for $[AD^{Me}HZn_2Et_2][B(C_8H_3F_6)_4]$ **6**-BArF. U_{eq} is defined as 1/3 of of the trace of the orthogonalised U_{IJ} tensor.

Atom	*x*	*y*	*z*	U(eq)
N2	9214.3(13)	6111.9(13)	900.1(8)	27.9(4)
N3	10006.0(14)	5033.5(13)	2381.6(8)	27.0(3)
N4	10625.6(14)	5979.6(14)	3508.6(9)	34.1(4)
N5	9720.6(14)	5700.6(14)	3965.2(9)	32.1(4)
N6	10734.6(13)	6769.6(12)	1074.3(8)	27.5(4)
N7	11333.3(13)	5910.8(13)	1074.0(8)	28.2(4)
N8	10297.3(14)	3858.8(13)	3611.0(9)	32.5(4)
N9	9273.1(14)	4129.6(14)	3800.4(8)	31.9(4)
C2	7666(2)	-84(2)	8498.4(16)	54.1(7)
C3	1410.4(17)	-500.9(16)	8906.8(11)	35.5(5)
C4	4687(2)	3300.7(19)	8339.5(13)	43.5(6)
C5	6503(3)	3583(3)	2434(3)	85.7(12)
C6	5181(2)	-2893.7(19)	8920.4(14)	49.0(6)
C7	5125(2)	4032.4(18)	5890.4(12)	43.4(5)
F1C	4750(3)	4956.8(18)	5970.0(12)	65.4(9)
F2C	4651(4)	3769(3)	5486.0(17)	93.2(14)
F3C	6106(3)	4193(4)	5593(2)	77.5(13)
F4C	5201(16)	3591(12)	5371(7)	93.2(14)
F5C	6028(11)	4481(16)	5655(9)	76(5)
F6C	4383(10)	4673(9)	5821(6)	65.4(9)
C8	8579.7(16)	6388.6(17)	471.4(10)	31.5(4)
C9	8347.7(18)	5515.9(18)	322.4(10)	35.4(5)
C10	8858.4(17)	4732.1(16)	674.8(10)	31.2(4)
C11	9582.8(19)	6168.9(19)	4481.8(12)	40.3(5)
C12	10438(2)	6740(2)	4361.8(14)	48.6(6)
C13	11067.7(19)	6612.2(18)	3754.5(13)	42.8(6)
C14	9601.3(16)	6753.1(15)	1251.9(10)	27.7(4)
C15	12310.6(16)	6212.5(16)	836.0(10)	29.2(4)
C16	12335.1(17)	7266.4(16)	675.9(11)	32.7(5)
C17	11327.0(17)	7600.7(15)	825.2(10)	30.1(4)
C18	8282.2(19)	7455.3(18)	225.9(12)	40.1(5)
C19	8869(2)	3631.9(17)	691.3(12)	39.5(5)
C20	11189.4(18)	3178.5(15)	1575.4(10)	33.5(5)
C21	10430(3)	2358.2(19)	1977.0(14)	53.2(7)
C22	9263.5(15)	5809.9(15)	2496.7(10)	26.0(4)

Table S3. Fractional Atomic Coordinates ($\times 10^4$) and Equivalent Isotropic Displacement Parameters ($Å^2 \times 10^3$) for $[AD^{Me}HZn_2Et_2][B(C_8H_3F_6)_4]$ **6**-BArF. U_{eq} is defined as 1/3 of of the trace of the orthogonalised U_{IJ} tensor.

Atom	*x*	*y*	*z*	U(eq)
C23	9066.5(15)	6596.3(15)	1984.6(10)	26.3(4)
C24	8283.1(16)	7309.5(16)	2122.2(11)	31.5(4)
C25	7676.9(17)	7266.0(17)	2750.2(11)	35.4(5)
C26	7892.4(16)	6526.0(17)	3261.3(11)	33.3(5)
C27	8687.9(16)	5820.3(16)	3146.9(10)	28.4(4)
C28	12722.8(18)	4776(2)	2594.8(12)	41.8(5)
C29	13238(2)	4359(2)	3174.4(15)	52.7(7)
C30	10302.7(19)	2865.9(17)	3650.7(11)	37.5(5)
C31	9290(2)	2514.0(18)	3863.0(12)	46.4(6)
C32	8644(2)	3327.5(18)	3956.3(11)	40.8(5)
C33	8951.0(17)	5182.4(16)	3778.7(10)	31.0(4)
C34	8638(2)	6028(2)	5037.3(13)	52.0(7)
C35	12076(2)	7087(2)	3380.4(17)	58.8(7)
C36	13186.0(17)	5463.7(17)	763.6(11)	34.7(5)
C37	10861.3(18)	8638.0(16)	755.6(12)	36.9(5)
C38	11297(2)	2297.5(19)	3480.1(14)	49.0(6)
C39	7500(2)	3407(2)	4188.3(15)	57.0(7)
C40	3572.1(16)	155.9(14)	7376.6(10)	27.9(4)
C41	2987.1(17)	331.5(17)	6894.7(11)	34.0(5)
C42	1915.2(19)	245.3(19)	7055.6(12)	40.8(5)
C43	1368.8(18)	-36.1(17)	7708.4(12)	37.9(5)
C44	1931.9(16)	-204.1(15)	8192.9(11)	30.7(4)
C45	3003.7(16)	-95.3(15)	8030.8(10)	28.8(4)
C46	5472.6(16)	-0.8(15)	6530.9(10)	29.8(4)
C47	5162.8(17)	-727.4(17)	6247.9(11)	33.7(5)
C48	5822.1(19)	-1078.9(18)	5728.5(11)	38.0(5)
C49	6828.8(18)	-735.5(18)	5476.9(11)	38.3(5)
C50	7154.0(17)	-24.1(17)	5754.7(11)	35.4(5)
C51	6489.8(17)	334.8(16)	6261.7(10)	33.0(5)
C52A	1247(9)	629(9)	6565(6)	56.0(14)
F1A	345(4)	1085(6)	6764(2)	93.6(12)
F2A	925(6)	-174(4)	6405(3)	73.4(8)
F3A	1690(30)	1255(17)	6009(14)	70.8(14)
C52B	1393(5)	357(6)	6484(4)	56.0(14)
F4A	1787(3)	-244(2)	6057.6(15)	73.4(8)

Table S3. Fractional Atomic Coordinates ($\times 10^4$) and Equivalent Isotropic Displacement Parameters ($Å^2 \times 10^3$) for $[AD^{Me}HZn_2Et_2][B(C_8H_3F_6)_4]$ **6**-BArF. U_{eq} is defined as 1/3 of of the trace of the orthogonalised U_{IJ} tensor.

Atom	*x*	*y*	*z*	U(eq)
F5A	1575(16)	1264(10)	6097(8)	70.8(14)
F6A	412(2)	117(4)	6678.4(17)	93.6(12)
C53	4918.7(15)	1553.0(15)	7153.0(10)	27.9(4)
C54	4794.8(16)	1938.6(16)	7723.6(10)	29.9(4)
C55	4796.5(16)	2962.8(17)	7705.0(11)	32.7(5)
C56	4901.6(17)	3656.7(16)	7110.7(11)	34.7(5)
C57	5009.7(17)	3297.9(16)	6537.0(11)	33.6(5)
C58	5025.3(16)	2268.0(16)	6558.1(10)	30.8(4)
C59	5380.8(16)	-318.6(15)	7774.6(10)	29.1(4)
C60	6248.0(17)	29.5(16)	7917.4(11)	32.9(5)
C61	6773.2(18)	-550.1(18)	8369.5(12)	38.4(5)
C62	6445.4(19)	-1505.6(18)	8705.1(12)	41.2(5)
C63	5590.0(18)	-1871.4(17)	8569.4(11)	37.0(5)
C64	5078.3(17)	-1297.7(16)	8108.2(11)	32.2(4)
C65	5446(2)	-1847(2)	5440.9(13)	49.7(6)
F1B	4836(11)	-2497(11)	5883(7)	79(4)
F2B	6233(7)	-2522(9)	5297(6)	105.7(16)
F3B	5120(8)	-1479(7)	4947(5)	73.5(10)
F4B	6110(3)	-2073(4)	4915(2)	105.7(16)
F5B	4555(3)	-1527(2)	5213.3(19)	73.5(10)
F6B	5133(5)	-2663(4)	5866(3)	83.5(19)
C66	8238(2)	375(2)	5522.7(12)	47.0(6)
B1	4823.3(18)	344.0(18)	7202.7(11)	28.8(5)

Table S4. Anisotropic Displacement Parameters ($Å^2 \times 10^3$) for $[AD^{Me}HZn_2Et_2][B(C_8H_3F_6)_4]$ **6**-BArF. The Anisotropic displacement factor exponent takes the form: $-2\pi^2[h^2a^{*2}U_{11}+2hka^*b^*U_{12}+\ldots]$.

Atom	U_{11}	U_{22}	U_{33}	U_{23}	U_{13}	U_{12}
Zn1	33.17(15)	23.19(14)	28.31(14)	-5.95(10)	-9.37(11)	1.77(11)
Zn2	28.72(15)	31.32(15)	33.15(15)	-6.52(11)	-10.84(11)	0.40(11)
Cl1	54.8(4)	46.0(3)	78.7(5)	-18.4(3)	-18.2(3)	-9.1(3)
Cl2	79.9(6)	44.2(4)	116.4(7)	-26.8(4)	-3.3(5)	-7.9(4)
F1	34.7(7)	54.9(9)	53.0(8)	-7.6(7)	1.7(6)	-13.0(6)
F2	56.1(9)	37.0(7)	41.2(7)	5.3(6)	-0.6(6)	9.0(6)

Table S4. Anisotropic Displacement Parameters ($Å^2 \times 10^3$) for $[AD^{Me}HZn_2Et_2][B(C_8H_3F_6)_4]$ **6**-BArF. The Anisotropic displacement factor exponent takes the form: $-2\pi^2[h^2a^{*2}U_{11}+2hka^*b^*U_{12}+\ldots]$.

Atom	U_{11}	U_{22}	U_{33}	U_{23}	U_{13}	U_{12}
F3	39.4(9)	149(2)	89.7(14)	-72.0(14)	14.2(9)	-23.0(11)
F4	43.3(8)	82.5(12)	60.8(10)	-10.8(8)	-17.0(7)	-18.6(8)
F10	49.7(8)	39.4(7)	41.3(7)	-11.8(6)	-2.8(6)	-3.1(6)
F11	73.9(11)	41.6(8)	62.6(10)	-26.3(7)	-20.0(8)	0.7(7)
F13	66.5(10)	57.9(10)	90.1(12)	-14.4(9)	-58.0(10)	11.6(8)
F14	93.7(13)	32.7(8)	81.6(12)	-8.0(8)	-26.2(10)	-3.7(8)
F16	60.8(11)	78.6(13)	89.7(14)	34.2(11)	-14.3(10)	-33.1(10)
F17	85.1(13)	112.0(16)	64.6(11)	-53.7(11)	28.1(10)	-50.0(12)
F18	107.8(15)	68.2(11)	69.0(11)	-34.7(9)	-56.2(11)	25.8(10)
F21	84.6(13)	55.8(10)	144.8(19)	-49.0(11)	-81.4(13)	23.7(9)
F22	46.7(9)	72.8(12)	101.1(14)	-2.1(10)	-33.6(10)	-12.1(9)
F23	55.7(10)	51.3(10)	109.2(15)	30.8(10)	10.9(10)	4.9(8)
F24	107.4(15)	43.1(9)	68.5(11)	13.8(8)	-40.3(10)	4.9(9)
N1	34.9(9)	25.7(9)	29.1(9)	-5.5(7)	-10.4(7)	-1.7(7)
N2	30.8(9)	26.7(8)	27.9(8)	-4.9(7)	-10.8(7)	-0.7(7)
N3	30.4(9)	22.7(8)	29.0(9)	-4.7(7)	-9.9(7)	0.5(7)
N4	33.5(10)	34.0(10)	40.0(10)	-11.4(8)	-14.6(8)	-2.0(8)
N5	33.3(9)	37.0(10)	31.0(9)	-12.1(7)	-12.9(7)	0.2(8)
N6	28.9(9)	24.1(8)	30.3(9)	-4.4(7)	-10.0(7)	1.2(7)
N7	29.7(9)	26.0(8)	30.0(9)	-5.9(7)	-10.0(7)	3.6(7)
N8	35.3(10)	31.6(9)	31.7(9)	-4.1(7)	-12.5(7)	-0.7(8)
N9	35.6(10)	32.7(9)	27.3(9)	-3.5(7)	-8.3(7)	-5.4(8)
C2	50.0(16)	45.5(15)	79(2)	-14.6(14)	-40.3(15)	10.1(13)
C3	34.4(12)	26.3(10)	43.1(12)	-6.2(9)	-4.7(9)	-1.3(9)
C4	47.4(14)	39.6(13)	46.6(14)	-14.8(11)	-10.3(11)	-4.4(11)
C5	58(2)	59(2)	159(4)	-42(2)	-44(2)	-1.4(16)
C6	51.1(15)	35.7(13)	53.1(15)	2.4(11)	-12.7(12)	11.1(11)
C7	50.4(14)	31.5(12)	44.4(13)	0.4(10)	-10.6(11)	-1.3(10)
F1C	101(2)	31.1(11)	53.1(13)	3.5(9)	-10.2(12)	11.2(12)
F2C	169(4)	60.3(16)	65.5(16)	24.5(11)	-78(2)	-48(2)
F3C	62.9(16)	85(3)	52.8(18)	19.7(16)	14.8(15)	5.4(15)
F4C	169(4)	60.3(16)	65.5(16)	24.5(11)	-78(2)	-48(2)
F5C	97(7)	87(11)	50(7)	26(6)	-47(7)	-74(8)
F6C	101(2)	31.1(11)	53.1(13)	3.5(9)	-10.2(12)	11.2(12)
C8	30.8(11)	38.6(12)	26.0(10)	-4.5(9)	-10.8(8)	0.5(9)

Table S4. Anisotropic Displacement Parameters ($Å^2 \times 10^3$) for $[AD^{Me}HZn_2Et_2][B(C_8H_3F_6)_4]$ **6**-BArF. The Anisotropic displacement factor exponent takes the form: $-2\pi^2[h^2a^{*2}U_{11}+2hka^*b^*U_{12}+\ldots]$.

Atom	U_{11}	U_{22}	U_{33}	U_{23}	U_{13}	U_{12}
C9	37.2(12)	44.5(13)	28.6(11)	-8.2(9)	-13.9(9)	-4.2(10)
C10	33.4(11)	35.7(11)	25.9(10)	-8.0(8)	-6.4(8)	-5.9(9)
C11	45.8(13)	45.7(13)	39.2(12)	-20.0(10)	-22.3(10)	12.0(11)
C12	52.3(15)	50.6(15)	59.0(16)	-30.3(13)	-28.7(13)	7.2(13)
C13	42.2(13)	36.1(12)	60.0(15)	-16.8(11)	-25.6(12)	2.9(10)
C14	29.7(10)	24.6(10)	31.2(10)	-5.6(8)	-12.1(8)	1.4(8)
C15	30.8(11)	31.9(11)	26.5(10)	-5.8(8)	-9.8(8)	-1.1(9)
C16	32.4(11)	30.5(11)	35.7(11)	-4.7(9)	-10.1(9)	-4.6(9)
C17	36.0(11)	25.5(10)	30.7(10)	-4.5(8)	-11.9(9)	-3.4(9)
C18	43.2(13)	41.3(13)	37.8(12)	-4.0(10)	-19.1(10)	5.9(10)
C19	48.5(14)	36.9(12)	37.5(12)	-11.8(10)	-12.6(10)	-7.4(10)
C20	45.1(12)	24.8(10)	30.0(11)	-5.9(8)	-9.9(9)	7.8(9)
C21	80(2)	30.4(12)	50.4(15)	-4.0(11)	-21.5(14)	-3.6(13)
C22	25.3(10)	25.9(10)	30.8(10)	-9.4(8)	-10.5(8)	-2.1(8)
C23	25.8(10)	25.9(10)	31.1(10)	-9.0(8)	-11.0(8)	-0.6(8)
C24	32.4(11)	27.5(10)	39.1(12)	-10.0(9)	-15.6(9)	3.7(9)
C25	31.4(11)	37.2(12)	42.9(12)	-16.9(10)	-13.6(9)	8.3(9)
C26	28.3(10)	40.9(12)	34.9(11)	-16.0(9)	-8.0(9)	0.0(9)
C27	27.6(10)	30.7(10)	30.5(10)	-9.4(8)	-10.7(8)	-2.5(8)
C28	33.7(12)	48.1(14)	41.8(13)	-6.0(10)	-9.3(10)	1.4(10)
C29	37.0(13)	55.3(16)	65.2(17)	0.5(13)	-22.2(12)	-3.2(12)
C30	52.6(14)	30.7(11)	29.7(11)	-1.8(9)	-14.6(10)	-0.8(10)
C31	62.4(16)	32.4(12)	41.8(13)	-2.4(10)	-8.0(12)	-13.9(12)
C32	48.7(14)	41.5(13)	30.3(11)	-3.5(9)	-5.2(10)	-15.1(11)
C33	31.0(11)	35.4(11)	28.4(10)	-9.9(9)	-7.4(8)	-1.7(9)
C34	54.5(16)	71.5(18)	38.7(13)	-27.1(13)	-17.4(11)	13.4(14)
C35	46.0(15)	49.4(16)	91(2)	-24.9(15)	-23.3(15)	-8.2(13)
C36	31.3(11)	35.9(11)	36.8(11)	-8.0(9)	-8.1(9)	2.7(9)
C37	39.9(12)	27.6(11)	44.8(13)	-5.8(9)	-14.2(10)	-0.9(9)
C38	63.1(17)	32.5(12)	53.6(15)	-6.2(11)	-23.0(13)	8.5(12)
C39	47.8(15)	61.0(17)	57.6(17)	-10.6(14)	0.7(13)	-20.1(13)
C40	31.4(11)	20.4(9)	33.1(10)	-3.8(8)	-10.7(8)	-2.7(8)
C41	35.9(12)	34.4(11)	32.3(11)	-3.4(9)	-10.0(9)	-7.8(9)
C42	37.7(12)	45.4(13)	41.7(13)	-1.6(10)	-18.3(10)	-9.6(10)
C43	29.7(11)	36.3(12)	47.9(13)	-3.3(10)	-13.1(10)	-5.5(9)

Table S4. Anisotropic Displacement Parameters ($Å^2 \times 10^3$) for $[AD^{Me}HZn_2Et_2][B(C_8H_3F_6)_4]$ **6**-BArF. The Anisotropic displacement factor exponent takes the form: $-2\pi^2[h^2a^{*2}U_{11}+2hka^*b^*U_{12}+\ldots]$.

Atom	U_{11}	U_{22}	U_{33}	U_{23}	U_{13}	U_{12}
C44	31.2(11)	22.0(10)	37.5(11)	-3.8(8)	-6.8(9)	-2.1(8)
C45	30.2(10)	23.4(10)	34.3(11)	-5.2(8)	-11.4(8)	0.0(8)
C46	32.4(11)	26.6(10)	30.1(10)	-2.1(8)	-9.8(8)	-2.0(8)
C47	32.3(11)	34.1(11)	35.1(11)	-6.3(9)	-7.9(9)	-6.2(9)
C48	42.1(13)	38.3(12)	36.9(12)	-11.5(10)	-11.0(10)	-4.5(10)
C49	39.2(12)	41.2(12)	33.1(11)	-8.5(10)	-4.9(9)	0.4(10)
C50	33.5(11)	37.7(12)	33.0(11)	-3.2(9)	-6.3(9)	-4.9(10)
C51	35.1(11)	30.9(11)	32.8(11)	-3.6(9)	-9.2(9)	-5.5(9)
C52A	46(2)	77(4)	50(2)	-3(2)	-25.4(18)	-22(2)
F1A	35.9(11)	195(4)	51.9(14)	-18(2)	-18.4(10)	-13(2)
F2A	103(2)	76.6(16)	59.0(17)	-17.5(13)	-44.5(15)	-21.8(18)
F3A	80(4)	80.4(12)	56(4)	1.1(19)	-40(2)	5.0(17)
C52B	46(2)	77(4)	50(2)	-3(2)	-25.4(18)	-22(2)
F4A	103(2)	76.6(16)	59.0(17)	-17.5(13)	-44.5(15)	-21.8(18)
F5A	80(4)	80.4(12)	56(4)	1.1(19)	-40(2)	5.0(17)
F6A	35.9(11)	195(4)	51.9(14)	-18(2)	-18.4(10)	-13(2)
C53	23.6(10)	28.6(10)	32.3(10)	-4.8(8)	-8.9(8)	-2.2(8)
C54	27.4(10)	30.9(11)	31.9(11)	-3.6(8)	-9.9(8)	-3.0(8)
C55	27.3(10)	33.7(11)	39.6(12)	-10.7(9)	-9.4(9)	-2.2(9)
C56	31.9(11)	27.1(10)	45.5(13)	-7.8(9)	-8.6(9)	-2.3(9)
C57	30.9(11)	29.7(11)	38.3(12)	-1.1(9)	-9.8(9)	-2.6(9)
C58	29.7(10)	31.2(11)	32.1(11)	-5.4(9)	-9.0(8)	-2.0(9)
C59	29.4(10)	28.1(10)	29.9(10)	-6.2(8)	-7.0(8)	1.3(8)
C60	31.9(11)	30.4(11)	37.4(11)	-6.1(9)	-11.3(9)	1.0(9)
C61	35.7(12)	38.6(12)	46.2(13)	-12.7(10)	-18.8(10)	7.5(10)
C62	45.1(13)	37.0(12)	43.8(13)	-6.8(10)	-20.8(11)	13.8(11)
C63	39.6(12)	29.3(11)	39.9(12)	-5.2(9)	-9.2(10)	8.6(10)
C64	29.9(11)	30.0(11)	37.0(11)	-7.1(9)	-9.2(9)	2.0(9)
C65	53.8(15)	52.0(15)	49.1(14)	-23.6(12)	-8.6(12)	-8.3(12)
F1B	74(6)	86(8)	84(7)	-55(5)	16(5)	-48(6)
F2B	82.1(17)	147(4)	104(3)	-103(3)	32(2)	-49(2)
F3B	87(2)	69.8(13)	86(2)	-22.8(16)	-54(2)	-14.0(19)
F4B	82.1(17)	147(4)	104(3)	-103(3)	32(2)	-49(2)
F5B	87(2)	69.8(13)	86(2)	-22.8(16)	-54(2)	-14.0(19)
F6B	141(5)	37.3(16)	91(3)	-7(2)	-64(3)	-19(2)

Table S4. Anisotropic Displacement Parameters ($Å^2 \times 10^3$) for $[AD^{Me}HZn_2Et_2][B(C_8H_3F_6)_4]$ **6**-BArF. The Anisotropic displacement factor exponent takes the form: $-2\pi^2[h^2a^{*2}U_{11}+2hka^*b^*U_{12}+\ldots]$.

Atom	U_{11}	U_{22}	U_{33}	U_{23}	U_{13}	U_{12}
C66	39.6(13)	57.9(16)	39.8(13)	-6.7(12)	-2.7(10)	-9.5(12)
B1	29.3(12)	28.0(12)	29.7(12)	-4.1(9)	-8.9(9)	-3.7(9)

Table S5. Bond Lengths for $[AD^{Me}HZn_2Et_2][B(C_8H_3F_6)_4]$ **6**-BArF.

Atom	Atom	Length/Å	Atom	Atom	Length/Å
Zn1	N1	2.0886(17)	C15	C16	1.402(3)
Zn1	N3	2.0413(17)	C15	C36	1.493(3)
Zn1	N7	2.0722(18)	C16	C17	1.368(3)
Zn1	C20	1.994(2)	C17	C37	1.493(3)
Zn2	N3	2.0816(17)	C20	C21	1.524(4)
Zn2	N4	2.1149(18)	C22	C23	1.408(3)
Zn2	N8	2.1656(18)	C22	C27	1.418(3)
Zn2	C28	1.968(2)	C23	C24	1.396(3)
Cl1	C5	1.735(3)	C24	C25	1.380(3)
Cl2	C5	1.737(4)	C25	C26	1.379(3)
F1	C3	1.338(3)	C26	C27	1.391(3)
F2	C3	1.340(3)	C27	C33	1.532(3)
F3	C66	1.320(3)	C28	C29	1.531(3)
F4	C66	1.331(3)	C30	C31	1.394(4)
F10	C3	1.352(3)	C30	C38	1.491(4)
F11	C4	1.331(3)	C31	C32	1.374(4)
F13	C2	1.334(3)	C32	C39	1.484(4)
F14	C6	1.331(3)	C40	C41	1.397(3)
F16	C66	1.334(3)	C40	C45	1.399(3)
F17	C4	1.324(3)	C40	B1	1.637(3)
F18	C4	1.336(3)	C41	C42	1.388(3)
F21	C2	1.344(3)	C42	C43	1.390(3)
F22	C2	1.342(4)	C42	C52A	1.510(11)
F23	C6	1.333(3)	C42	C52B	1.512(7)
F24	C6	1.336(3)	C43	C44	1.381(3)
N1	N2	1.366(2)	C44	C45	1.391(3)
N1	C10	1.335(3)	C46	C47	1.398(3)
N2	C8	1.359(3)	C46	C51	1.400(3)
N2	C14	1.458(3)	C46	B1	1.635(3)

Table S5. Bond Lengths for [AD^{Me}HZn$_2$Et$_2$][B(C$_8$H$_3$F$_6$)$_4$] **6**-BArF.

Atom	Atom	Length/Å	Atom	Atom	Length/Å
N3	C22	1.415(3)	C47	C48	1.392(3)
N4	N5	1.371(3)	C48	C49	1.388(3)
N4	C13	1.334(3)	C48	C65	1.492(3)
N5	C11	1.362(3)	C49	C50	1.383(3)
N5	C33	1.454(3)	C50	C51	1.381(3)
N6	N7	1.367(2)	C50	C66	1.504(3)
N6	C14	1.460(3)	C52A	F1A	1.330(11)
N6	C17	1.358(3)	C52A	F2A	1.341(11)
N7	C15	1.333(3)	C52A	F3A	1.330(13)
N8	N9	1.371(3)	C52B	F4A	1.347(7)
N8	C30	1.337(3)	C52B	F5A	1.327(9)
N9	C32	1.356(3)	C52B	F6A	1.310(7)
N9	C33	1.462(3)	C53	C54	1.400(3)
C2	C61	1.489(4)	C53	C58	1.400(3)
C3	C44	1.491(3)	C53	B1	1.640(3)
C4	C55	1.495(3)	C54	C55	1.388(3)
C6	C63	1.499(3)	C55	C56	1.385(3)
C7	F1C	1.353(3)	C56	C57	1.388(3)
C7	F2C	1.301(4)	C57	C58	1.394(3)
C7	F3C	1.315(4)	C59	C60	1.395(3)
C7	F4C	1.355(12)	C59	C64	1.403(3)
C7	F5C	1.320(11)	C59	B1	1.639(3)
C7	F6C	1.281(9)	C60	C61	1.391(3)
C7	C57	1.494(3)	C61	C62	1.384(4)
C8	C9	1.370(3)	C62	C63	1.384(4)
C8	C18	1.490(3)	C63	C64	1.390(3)
C9	C10	1.394(3)	C65	F1B	1.302(10)
C10	C19	1.492(3)	C65	F2B	1.366(9)
C11	C12	1.363(4)	C65	F3B	1.221(7)
C11	C34	1.497(4)	C65	F4B	1.332(4)
C12	C13	1.404(4)	C65	F5B	1.386(4)
C13	C35	1.494(4)	C65	F6B	1.292(5)
C14	C23	1.528(3)			

Table S6. Bond Angles for [AD^{Me}HZn$_2$Et$_2$][B(C$_8$H$_3$F$_6$)$_4$] **6**-BArF.

Atom	Atom	Atom	Angle/°	Atom	Atom	Atom	Angle/°
N3	Zn1	N1	99.53(7)	C24	C23	C14	113.35(18)
N3	Zn1	N7	92.21(7)	C24	C23	C22	119.89(19)
N7	Zn1	N1	88.70(7)	C25	C24	C23	122.0(2)
C20	Zn1	N1	123.58(8)	C26	C25	C24	118.65(19)
C20	Zn1	N3	117.55(8)	C25	C26	C27	121.0(2)
C20	Zn1	N7	127.39(8)	C22	C27	C33	124.86(18)
N3	Zn2	N4	101.52(7)	C26	C27	C22	120.87(19)
N3	Zn2	N8	84.08(7)	C26	C27	C33	113.82(18)
N4	Zn2	N8	85.56(7)	C29	C28	Zn2	114.00(17)
C28	Zn2	N3	133.15(9)	N8	C30	C31	109.9(2)
C28	Zn2	N4	119.38(9)	N8	C30	C38	120.8(2)
C28	Zn2	N8	118.76(9)	C31	C30	C38	129.2(2)
N2	N1	Zn1	116.65(13)	C32	C31	C30	107.2(2)
C10	N1	Zn1	135.88(15)	N9	C32	C31	105.7(2)
C10	N1	N2	105.60(16)	N9	C32	C39	122.9(2)
N1	N2	C14	120.92(16)	C31	C32	C39	131.4(2)
C8	N2	N1	111.55(17)	N5	C33	N9	109.56(17)
C8	N2	C14	127.21(17)	N5	C33	C27	108.89(17)
Zn1	N3	Zn2	108.43(8)	N9	C33	C27	119.35(17)
C22	N3	Zn1	127.77(13)	C41	C40	C45	115.55(19)
C22	N3	Zn2	113.11(12)	C41	C40	B1	122.88(18)
N5	N4	Zn2	116.16(13)	C45	C40	B1	121.27(18)
C13	N4	Zn2	133.63(16)	C42	C41	C40	122.1(2)
C13	N4	N5	105.28(19)	C41	C42	C43	121.4(2)
N4	N5	C33	118.53(16)	C41	C42	C52A	122.9(5)
C11	N5	N4	111.66(19)	C41	C42	C52B	116.4(3)
C11	N5	C33	127.90(19)	C43	C42	C52A	114.7(5)
N7	N6	C14	122.39(16)	C43	C42	C52B	121.8(3)
C17	N6	N7	111.04(16)	C44	C43	C42	117.4(2)
C17	N6	C14	126.21(17)	C43	C44	C3	121.1(2)
N6	N7	Zn1	116.49(12)	C43	C44	C45	121.0(2)
C15	N7	Zn1	137.10(14)	C45	C44	C3	117.82(19)
C15	N7	N6	105.88(16)	C44	C45	C40	122.46(19)
N9	N8	Zn2	113.86(13)	C47	C46	C51	115.4(2)
C30	N8	Zn2	128.76(15)	C47	C46	B1	125.41(19)
C30	N8	N9	105.38(18)	C51	C46	B1	118.48(18)
N8	N9	C33	121.28(17)	C48	C47	C46	121.9(2)
C32	N9	N8	111.77(19)	C47	C48	C65	119.5(2)

Table S6. Bond Angles for $[AD^{Me}HZn_2Et_2][B(C_8H_3F_6)_4]$ **6**-BArF.

C32	N9	C33	126.8(2)	C49	C48	C47	121.2(2)
F13	C2	F21	107.1(2)	C49	C48	C65	119.2(2)
F13	C2	F22	106.2(2)	C50	C49	C48	117.8(2)
F13	C2	C61	113.7(2)	C49	C50	C66	121.5(2)
F21	C2	C61	111.5(2)	C51	C50	C49	120.7(2)
F22	C2	F21	104.9(3)	C51	C50	C66	117.9(2)
F22	C2	C61	112.8(2)	C50	C51	C46	123.0(2)
F1	C3	F2	106.69(18)	F1A	C52A	C42	118.7(9)
F1	C3	F10	105.79(17)	F1A	C52A	F2A	101.0(9)
F1	C3	C44	113.86(19)	F1A	C52A	F3A	103.5(15)
F2	C3	F10	105.51(19)	F2A	C52A	C42	107.4(8)
F2	C3	C44	112.47(18)	F3A	C52A	C42	116(2)
F10	C3	C44	111.91(18)	F3A	C52A	F2A	108.3(17)
F11	C4	F18	105.3(2)	F4A	C52B	C42	114.9(5)
F11	C4	C55	113.9(2)	F5A	C52B	C42	109.5(13)
F17	C4	F11	106.7(2)	F5A	C52B	F4A	101.6(9)
F17	C4	F18	105.9(2)	F6A	C52B	C42	112.4(6)
F17	C4	C55	112.4(2)	F6A	C52B	F4A	103.2(5)
F18	C4	C55	112.0(2)	F6A	C52B	F5A	114.8(11)
Cl1	C5	Cl2	112.78(19)	C54	C53	C58	115.77(19)
F14	C6	F23	105.1(3)	C54	C53	B1	120.84(18)
F14	C6	F24	105.9(2)	C58	C53	B1	123.11(18)
F14	C6	C63	112.8(2)	C55	C54	C53	122.5(2)
F23	C6	F24	107.2(2)	C54	C55	C4	118.6(2)
F23	C6	C63	112.4(2)	C56	C55	C4	120.7(2)
F24	C6	C63	112.8(2)	C56	C55	C54	120.7(2)
F1C	C7	C57	111.8(2)	C55	C56	C57	118.1(2)
F2C	C7	F1C	106.8(3)	C56	C57	C7	119.0(2)
F2C	C7	F3C	108.9(3)	C56	C57	C58	120.9(2)
F2C	C7	C57	113.4(2)	C58	C57	C7	120.1(2)
F3C	C7	F1C	103.4(3)	C57	C58	C53	122.0(2)
F3C	C7	C57	111.9(3)	C60	C59	C64	115.82(19)
F4C	C7	C57	113.4(8)	C60	C59	B1	121.46(19)
F5C	C7	F4C	94.7(10)	C64	C59	B1	122.50(19)
F5C	C7	C57	116.3(8)	C61	C60	C59	122.3(2)
F6C	C7	F4C	101.8(9)	C60	C61	C2	117.4(2)
F6C	C7	F5C	110.1(10)	C62	C61	C2	121.7(2)

Table S6. Bond Angles for [AD^{Me}HZn$_2$Et$_2$][B(C$_8$H$_3$F$_6$)$_4$] **6**-BArF.

F6C	C7	C57	117.4(5)	C62	C61	C60	120.9(2)
N2	C8	C9	105.80(19)	C61	C62	C63	118.0(2)
N2	C8	C18	123.2(2)	C62	C63	C6	121.0(2)
C9	C8	C18	131.0(2)	C62	C63	C64	121.0(2)
C8	C9	C10	107.15(19)	C64	C63	C6	118.0(2)
N1	C10	C9	109.90(19)	C63	C64	C59	122.0(2)
N1	C10	C19	120.87(19)	F1B	C65	C48	112.7(9)
C9	C10	C19	129.2(2)	F1B	C65	F2B	95.6(8)
N5	C11	C12	106.0(2)	F2B	C65	C48	109.2(4)
N5	C11	C34	122.7(2)	F3B	C65	C48	112.9(5)
C12	C11	C34	131.4(2)	F3B	C65	F1B	115.0(9)
C11	C12	C13	107.1(2)	F3B	C65	F2B	110.0(6)
N4	C13	C12	110.0(2)	F4B	C65	C48	114.5(3)
N4	C13	C35	120.5(2)	F4B	C65	F5B	103.8(3)
C12	C13	C35	129.5(2)	F5B	C65	C48	112.2(2)
N2	C14	N6	110.64(16)	F6B	C65	C48	113.9(4)
N2	C14	C23	113.81(17)	F6B	C65	F4B	109.9(4)
N6	C14	C23	117.83(16)	F6B	C65	F5B	101.3(4)
N7	C15	C16	109.95(18)	F3	C66	F4	105.9(2)
N7	C15	C36	120.70(19)	F3	C66	F16	109.1(2)
C16	C15	C36	129.4(2)	F3	C66	C50	113.0(2)
C17	C16	C15	106.51(19)	F4	C66	F16	104.4(2)
N6	C17	C16	106.60(18)	F4	C66	C50	112.6(2)
N6	C17	C37	121.90(19)	F16	C66	C50	111.3(2)
C16	C17	C37	131.5(2)	C40	B1	C53	104.52(16)
C21	C20	Zn1	113.72(17)	C40	B1	C59	112.00(17)
N3	C22	C27	120.19(18)	C46	B1	C40	114.72(17)
C23	C22	N3	122.46(18)	C46	B1	C53	111.83(17)
C23	C22	C27	117.35(18)	C46	B1	C59	103.05(16)
C22	C23	C14	126.71(17)	C59	B1	C53	110.93(17)

Table S7. Hydrogen Atom Coordinates (Å×10^4) and Isotropic Displacement Parameters (Å^2×10^3) for [AD^{Me}HZn$_2$Et$_2$][B(C$_8$H$_3$F$_6$)$_4$] **6**-BArF.

Atom	***x***	***y***	***z***	**U(eq)**
H1	9730(20)	4510(20)	2625(13)	40

Table S7. Hydrogen Atom Coordinates (Å×10^4) and Isotropic Displacement Parameters (Å^2×10^3) for [AD^{Me}HZn$_2$Et$_2$][B(C$_8$H$_3$F$_6$)$_4$] **6**-BArF.

Atom	*x*	*y*	*z*	U(eq)
H5A	6256.76	3705.54	2018.64	103
H5B	5885.19	3559.03	2804.24	103
H9	7919.28	5456.28	33.11	43
H12	10581.46	7148.2	4637.14	58
H14	9381.85	7448.82	1056.39	33
H16	12934.01	7669.31	498.58	39
H18A	8900.19	7824.38	-42.43	60
H18B	7978.42	7765.56	602.8	60
H18C	7772.38	7477.26	-43.92	60
H19A	8682.48	3525.67	293.24	59
H19B	8367.18	3298.02	1083.82	59
H19C	9565.94	3349.18	707.77	59
H20A	11441.68	3057.53	1122.67	40
H20B	11796.26	3130.85	1777.66	40
H21A	9900.97	2307.21	1733.51	80
H21B	10095.16	2526.5	2402.6	80
H21C	10806.59	1713.38	2053.12	80
H24	8163.89	7840.76	1772.82	38
H25	7122.29	7736.32	2828.91	42
H26	7492.01	6497.59	3697.98	40
H28A	12860.53	4301.24	2292.81	50
H28B	13047.26	5422.22	2345.9	50
H29A	13981.76	4246.02	3005.05	79
H29B	12919.24	3721.5	3426.55	79
H29C	13143.65	4843.16	3462.47	79
H31	9085.54	1837.79	3930.57	56
H33	8304.8	5174.95	4134.57	37
H34A	8034.27	6344.29	4874.46	78
H34B	8742.12	6340.99	5388.6	78
H34C	8517.66	5308	5212.44	78
H35A	12361.62	6779.42	3000.02	88
H35B	12566.52	6983.96	3670.25	88
H35C	11962.48	7810.03	3225.53	88
H36A	13540.26	5549.14	296.43	52
H36B	12913.68	4781.72	927.27	52
H36C	13678.6	5568.79	1019.77	52

Table S7. Hydrogen Atom Coordinates (Å×10^4) and Isotropic Displacement Parameters (Å^2×10^3) for [AD^{Me}HZn$_2$Et$_2$][B(C$_8$H$_3$F$_6$)$_4$] **6**-BArF.

Atom	*x*	*y*	*z*	U(eq)
H37A	11409.74	9130.45	547.49	55
H37B	10516.08	8756.09	1193.43	55
H37C	10352.38	8708.32	480.24	55
H38A	11154.83	1665.88	3372.85	74
H38B	11626.98	2149.88	3857.71	74
H38C	11761.75	2703.22	3097.68	74
H39A	7221.71	3932.92	3874.82	85
H39B	7332.1	3579.63	4624.47	85
H39C	7189.35	2762.18	4218.87	85
H41	3334.23	515.78	6442.4	41
H43	636.69	-110.07	7816.99	45
H45	3363.19	-195.51	8377.43	35
H47	4483.28	-988.71	6414.71	40
H49	7279.79	-981.1	5125.38	46
H51	6734.03	832.2	6435.86	40
H54	4706.09	1481.81	8139.62	36
H56	4899.86	4358.23	7096.1	42
H58	5110.84	2044.37	6156.72	37
H60	6488.31	684.98	7698.41	39
H62	6796.82	-1898.36	9018.94	49
H64	4506.37	-1577.4	8016.35	39

Table S8. Atomic Occupancy for [AD^{Me}HZn$_2$Et$_2$][B(C$_8$H$_3$F$_6$)$_4$] **6**-BArF**.**

Atom	*Occupancy*	Atom	*Occupancy*	Atom	*Occupancy*
F1C	0.819(7)	F2C	0.819(7)	F3C	0.819(7)
F4C	0.181(7)	F5C	0.181(7)	F6C	0.181(7)
C52A	0.382(2)	F1A	0.382(2)	F2A	0.382(2)
F3A	0.382(2)	C52B	0.618(2)	F4A	0.618(2)
F5A	0.618(2)	F6A	0.618(2)	F1B	0.287(5)
F2B	0.287(5)	F3B	0.287(5)	F4B	0.713(5)
F5B	0.713(5)	F6B	0.713(5)		

S7. Polymerization.

S7.1 Catalyst Optimization.

General procedure. *rac*-lactide (144 mg, 1 mmol, 100 equivalents with respect to zinc) was dissolved in the CH_2Cl_2 (1.0 mL). If no alcohol cocatalyst was used, 1.0 mL solution of metal complex (0.005 mmol, 1 equivalent) in CH_2Cl_2 was then added to the monomer solution. If an alcohol cocatalyst was used, then a 1 mL solution of complex, cocatalyst, and CH_2Cl_2 was premixed and stirred for 24 hours before being added to the monomer solution. Note that the small volumes of cocatalysts were measured by preparing a stock solution of cocatalyst in CH_2Cl_2. At various time points, aliquots (about 0.3 mL) of the crude reaction mixture were quenched with a solution of benzoic acid in CH_2Cl_2 (0.1 M), concentrated under vacuum, and dissolved in $CDCl_3$ for crude NMR analysis. Fractional conversion was calculated based on the ratio of residual monomer to polymer. See Figure S46 for the identification of ^{1}H-NMR peaks. Where indicated, ^{1}H-NMR, GPC, and DSC analysis was performed on a purified polymer sample obtained by precipitation in cold methanol followed by filtration and drying.

Table S9, entry 1. By the general procedure with $AD^{Me}H_2$ (**1**, 2.5 mg, 0.005 mmol, 1 equivalents), Et_2Zn (1 μL, 0.01 mmol, 2 equiv.) *rac*-lactide (144 mg, 1 mmol, 200 equivalents), and CH_2Cl_2 (2 mL).

Table S9, entry 2. By the general procedure with diethylzinc (1.03 μL, 0.01 mmol, 1 equivalents), ethyl alcohol (0.58 μL, 0.01 mmol, 1 equivalents), *rac*-lactide (144 mg, 1 mmol, 100 equivalents), and CH_2Cl_2 (2 mL).

Table S9, entry 3. By the general procedure with diethylzinc (1.03 μL, 0.01 mmol, 1 equivalents), ethyl alcohol (1.17 μL, 0.01 mmol, 1 equivalents), *rac*-lactide (144 mg, 1 mmol, 100 equivalents), and CH_2Cl_2 (2 mL).

Table S9, entry 4. By the general procedure with $AD^{Me}HZnEt$ (**7**) (5.9 mg, 0.01 mmol, 1 equivalents), ethyl alcohol (0.58 μL, 0.01 mmol, 1 equivalents), *rac*-lactide (144 mg, 1 mmol, 100 equivalents), and CH_2Cl_2 (2 mL).

Table S9, entry 5. By the general procedure with $[AD^{Me}HZn_2Et_2][BArF]$ (**6**-ArF, 7.7 mg, 0.005 mmol, 1 equivalents), ethyl alcohol (0.58 μL, 0.01 mmol, 2 equivalents), *rac*-lactide (144 mg, 1 mmol, 200 equivalents), and CH_2Cl_2 (2 mL).

Table S9, entry 6. By the general procedure with $[AD^{Me}HZn_2Et_2][NTf_2]$ (**6**-NTf_2, 4.8 mg, 0.005 mmol, 1 equivalents), ethyl alcohol (0.58 μL, 0.01 mmol, 2 equivalents), *rac*-lactide (144 mg, 1 mmol, 200 equivalents), and CH_2Cl_2 (2 mL).

Table S9, entry 7. By the general procedure with $[AD^{Me}HZn_2Et_2][BF_4]$ (**6**-BF_4, 3.9 mg, 0.005 mmol, 1 equivalents), ethyl alcohol (0.58 μL, 0.01 mmol, 2 equivalents), *rac*-lactide (144 mg, 1 mmol, 200 equivalents), and CH_2Cl_2 (2 mL).

Table S9, entry 8. By the general procedure with [AD^{Me}HZn$_2$Et$_2$][PF$_6$] (**6**-PF$_6$, 4.2 mg, 0.005 mmol, 1 equivalents), ethyl alcohol (0.58 μL, 0.01 mmol, 2 equivalents), *rac*-lactide (144 mg, 1 mmol, 200 equivalents), and CH_2Cl_2 (2 mL).

Table S9, entry 9. By the general procedure with [AD^{Me}HZn$_2$Et$_2$][OTf] (**6**-OTf, 4.2 mg, 0.005 mmol, 1 equivalents), ethyl alcohol (0.58 μL, 0.01 mmol, 2 equivalents), *rac*-lactide (144 mg, 1 mmol, 200 equivalents), and CH_2Cl_2 (2 mL).

Table S9, entry 10. By the general procedure with [AD^{Me}HZn$_2$Et$_2$][NTf$_2$] (**6**-NTf$_2$, 4.8 mg, 0.005 mmol, 1 equivalents), *rac*-lactide (144 mg, 1 mmol, 200 equivalents), and CH_2Cl_2 (2 mL), but no ethyl alcohol.

Table S9, entry 11. By the general procedure with [PD^{Me}Zn$_2$Et$_2$][NTf$_2$] (**6**-NTf$_2$, 5.1 mg, 0.005 mmol, 1 equivalents), ethyl alcohol (0.58 μL, 0.01 mmol, 2 equivalents), *rac*-lactide (144 mg, 1 mmol, 200 equivalents), and CH_2Cl_2 (2 mL).

Table S9, entry 12. By the general procedure with [PD^{H}Zn$_2$Et$_2$][NTf$_2$] (**6**-NTf$_2$, 9.1 mg, 0.01 mmol, 1 equivalents), benzyl alcohol (2.0 μL, 0.01 mmol, 2 equivalents), *rac*-lactide (288 mg, 2 mmol, 200 equivalents), and CH_2Cl_2 (2 mL).

Table S9. Catalyst Optimization.

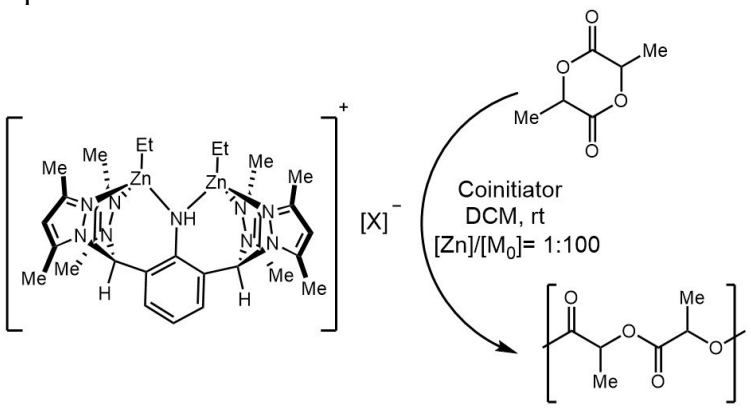

Entry	Catalyst	Alcohol (2 equiv.)	conv. (30 min)[a]	conv. (1 hr)[a]	conv. (24 hr)[a]	M_n [b]	M_n *theo*	M_w/M_n [b]	DP[c]
1	AD^{Me}H$_2$ (**1**) + 2 eq. ZnEt$_2$	none	0 %	0 %	10 %	260	1400	1.36	2
2	ZnEt$_2$	ethyl alcohol (1:1)	0 %	0 %	37 %	--	--	--	--
3	ZnEt$_2$	ethyl alcohol (1:2)	0 %	3 %	96 %	6300	13800	1.09	44
4	AD^{Me}HZnEt (**7**)	ethyl alcohol	0 %	0%	85%	7600	12200	1.08	53
5	[AD^{Me}HZn$_2$Et$_2$][BArF] (**6**-BArF)	ethyl alcohol	0%	0%	2%	--	--	--	--

6	[AD^{Me}HZn$_2$Et$_2$][NTf$_2$] (**6**-NTf$_2$)	ethyl alcohol	13 %	21 %	88 %	7800	12700	1.03	54
7	[AD^{Me}HZn$_2$Et$_2$][BF$_4$] (**6**-NTf$_2$)	ethyl alcohol	0 %	0 %	2 %	--	--	--	
8	[AD^{Me}HZn$_2$Et$_2$][PF$_6$] (**6**-PF$_6$)	ethyl alcohol	0 %	0 %	0 %	--	--	--	--
9	[AD^{Me}HZn$_2$Et$_2$][OTf] (**6**-OTf)	ethyl alcohol	0 %	0 %	3 %	--	--	--	--
10	[AD^{Me}HZn$_2$Et$_2$][NTf$_2$] (**6**-NTf$_2$)	none	0 %	0 %	2 %	--	--	--	--
11	[PD^{Me}Zn$_2$Et$_2$][NTf$_2$] (**11**)	ethyl alcohol	0%	1%	3%	--	--	--	--
12	[PD^{H}Zn$_2$Et$_2$][NTf$_2$] (**12**)	benzyl alcohol	0%	3%	98%	11200	14100	1.12	78

Conditions from Section S7.1. [a]Conversions obtained by ^{1}H-NMR assay via integration of the methine resonances of monomer lactide and PLA. [b]Number-average molecular weight (M_n), polydispersity index (M_w/M_n), and degree of polymerization determined by gel permeation chromatography with styrene standards using the correction factor of 0.58.[10]

S7.3. Stereochemical evaluation of lactide-derived polymers.

P_r and P_m are the probabilities of forming either an *r* or *m* linkage upon monomer addition, respectively, and are calculated based on homodecoupled ^{1}H-NMR from: [*mmm*]=$P_m^2 + P_mP_r/2$, [*mmr*]=[*rmm*]= $P_mP_r/2$, [*rmr*]=$P_r^2/2$, and [*mrm*]=[$P_r^2 + P_mP_r$]/2, and $P_r = 1–P_m$.[11]

Table S10. Stereochemistry of lactide-derived polymers.

Entry	**Catalyst**	**Monomer**	**Table entry**	**Tacticity**
1	ZnEt$_2$/EtOH	*rac*-lactide	Table S9, entry 3	P_r= 0.62
2	AD^{Me}HZnEt (**12**)/ EtOH	*rac*-lactide	Table S9, entry 4	P_r = 0.63
3	[AD^{Me}HZn$_2$Et$_2$][NTf$_2$] (**6**)/EtOH	*rac*-lactide	Table S9, entry 6	P_r= 0.49

[10] Baran, J.; Duda, A.; Kowalski, A.; Szymanski, R.; Penczek, S. Intermolecular Chain Transfer To Polymer With Chain Scission: General Treatment And Determination Of K(P)/K(Tr) In L,LLactide Polymerization. *Macromol. Rapid Commun.* **1997**, *18*, 325− 333.

[11] Chamberlain, B. M.; Cheng, M.; Moore, D. R.; Ovitt, T. M.; Lobkovsky, E. B.; Coates, G. W. Polymerization of Lactide with Zinc and Magnesium β-Diiminate Complexes: Stereocontrol and Mechanism. *J. Am. Chem. Soc.* **2001**, *123*, 3229−3238.

S8. Spectral data for polymers.

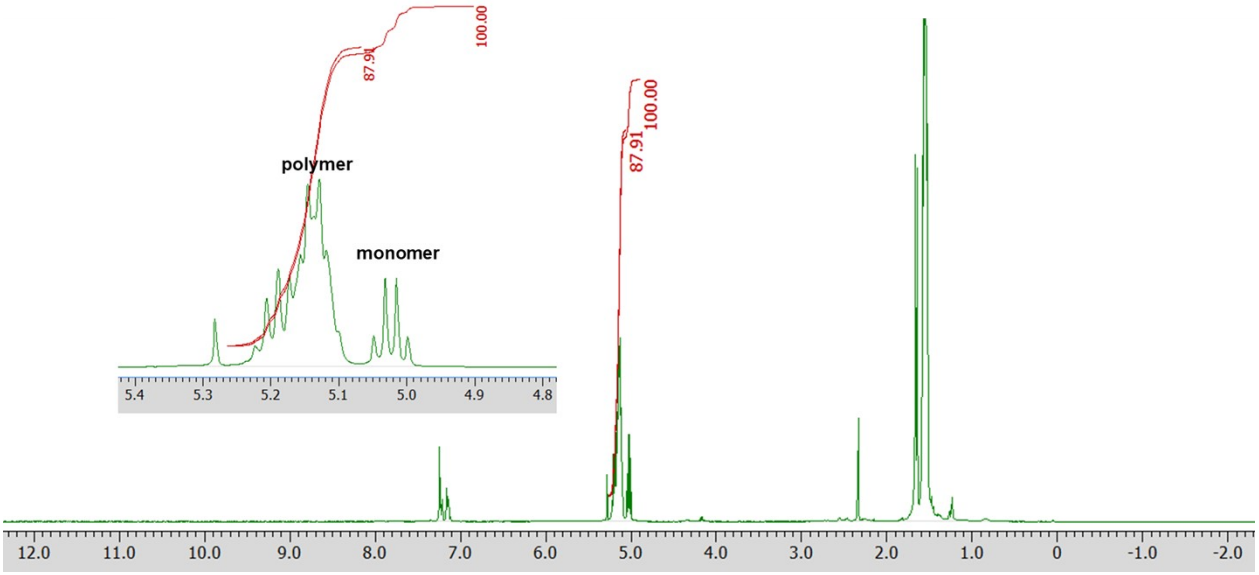

Figure S46. Sample ^{1}H-NMR used for assay yield (Table S9, entry 6).

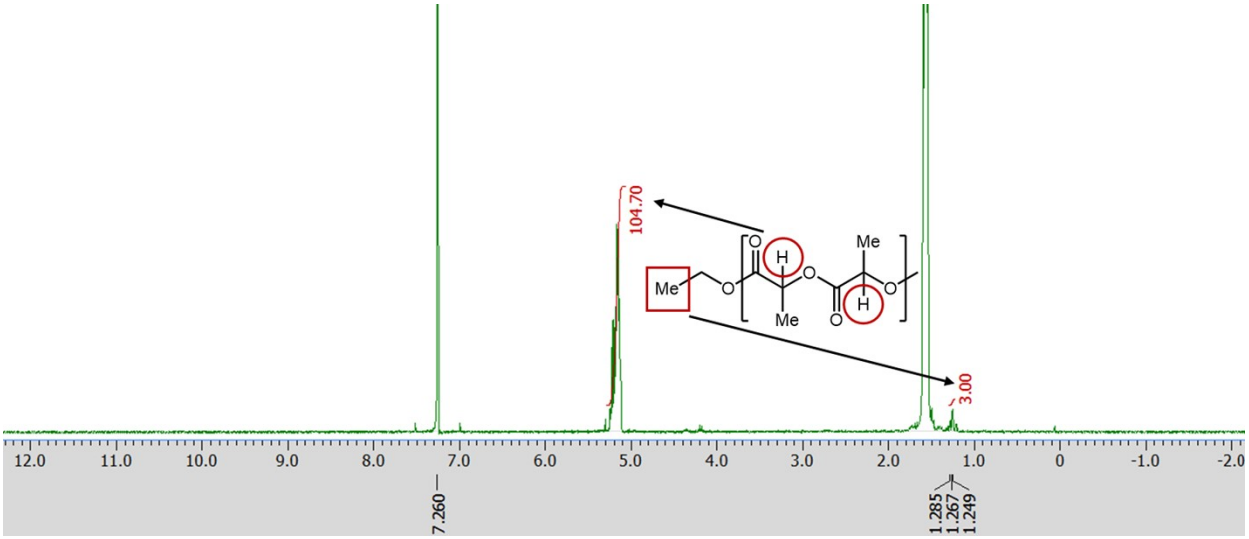

Figure S47. ^{1}H-NMR of isolated poly(*rac*-lactic acid) obtained from $[AD^{Me}HZn_2Et_2][NTf_2]$ (**6**-NTf_2) and EtOH (Table S9, entry 6).

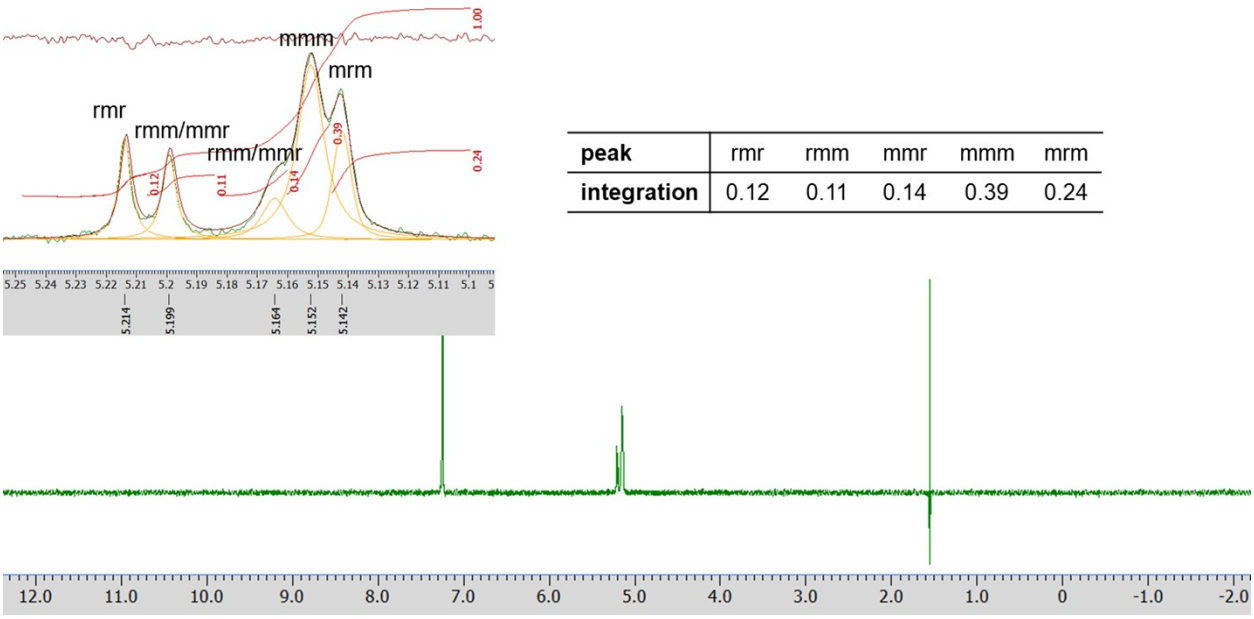

peak	rmr	rmm	mmr	mmm	mrm
integration	0.12	0.11	0.14	0.39	0.24

Figure S48. Homonuclear decoupled ^{1}H-NMR of isolated poly(*rac*-lactic acid) obtained from [AD^{Me}HZn$_2$Et$_2$][NTf$_2$] (**6**-NTf$_2$) and EtOH (Table S9, entry 6). P_r and P_m are the probabilities of forming either an *r* or *m* linkage upon monomer addition, respectively, and are calculated based on ^{1}H-NMR from: [*mmm*]=P_m^2 + P_mP_r/2, [*mmr*]=[*rmm*]= P_mP_r/2, [*rmr*]=P_r^2/2, and [*mrm*]=[P_r^2 + P_mP_r]/2, and P_r = 1–P_m.[12] For the isolated poly(*rac*-lactic acid) obtained from [AD^{Me}HZn$_2$Et$_2$][NTf$_2$] (**6**-NTf$_2$) and EtOH (Table S9, entry 6), P_r was calculated using the integration of [*rmr*], which $P_r = (2*[rmr])^{0.5} = (2*0.12)^{0.5} = 0.49$.

[12] Chamberlain, B. M.; Cheng, M.; Moore, D. R.; Ovitt, T. M.; Lobkovsky, E. B.; Coates, G. W. Polymerization of Lactide with Zinc and Magnesium β-Diiminate Complexes: Stereocontrol and Mechanism. *J. Am. Chem. Soc.* **2001**, *123*, 3229−3238.

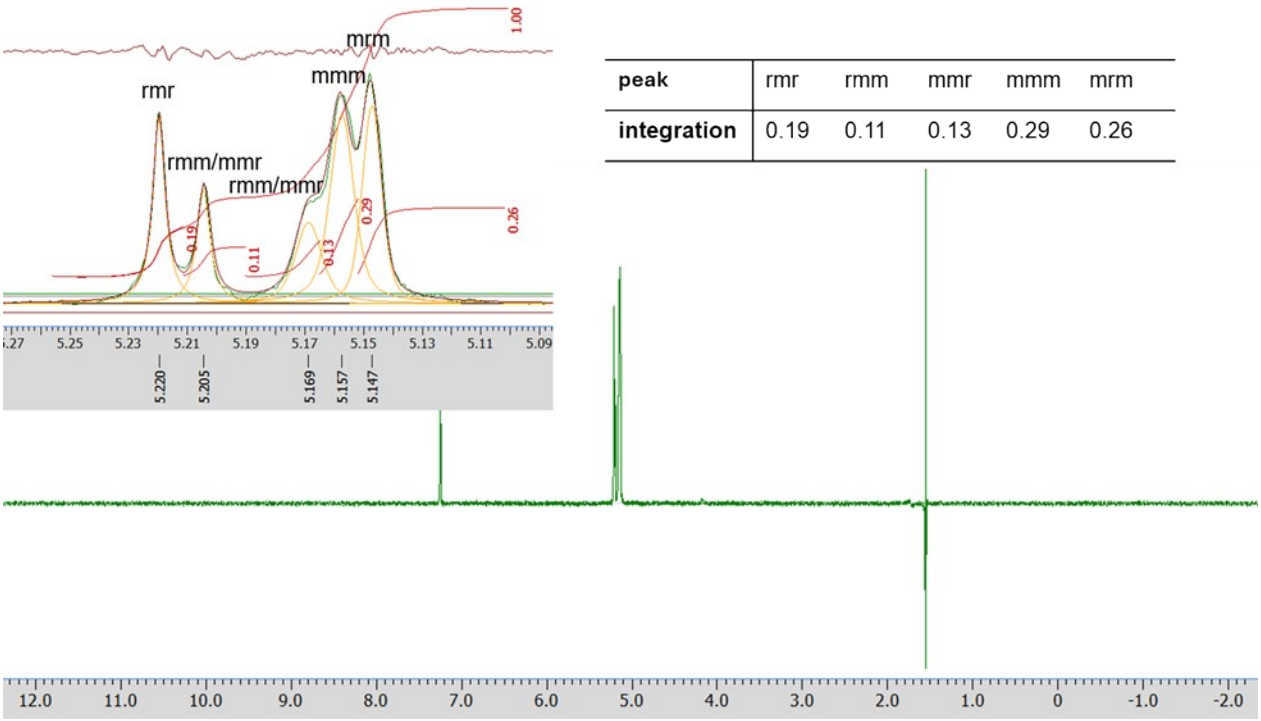

peak	rmr	rmm	mmr	mmm	mrm
integration	0.19	0.11	0.13	0.29	0.26

Figure S49. Homonuclear decoupled ^{1}H-NMR of isolated poly(*rac*-lactic acid) obtained from $ZnEt_2$ and EtOH (Table S9, entry 3). P_r and P_m are the probabilities of forming either an *r* or *m* linkage upon monomer addition, respectively, and are calculated based on ^{1}H-NMR from: $[mmm]=P_m^2+P_mP_r/2$, $[mmr]=[rmm]=P_mP_r/2$, $[rmr]=P_r^2/2$, and $[mrm]=[P_r^2+P_mP_r]/2$, and $P_r = 1-P_m$.[12] For the isolated poly(*rac*-lactic acid) obtained from $ZnEt_2$ and EtOH (Table S9, entry 3), P_r was calculated using the integration of [*rmr*], which $P_r = (2*[rmr])^{0.5} = (2*0.19)^{0.5} = 0.62$.

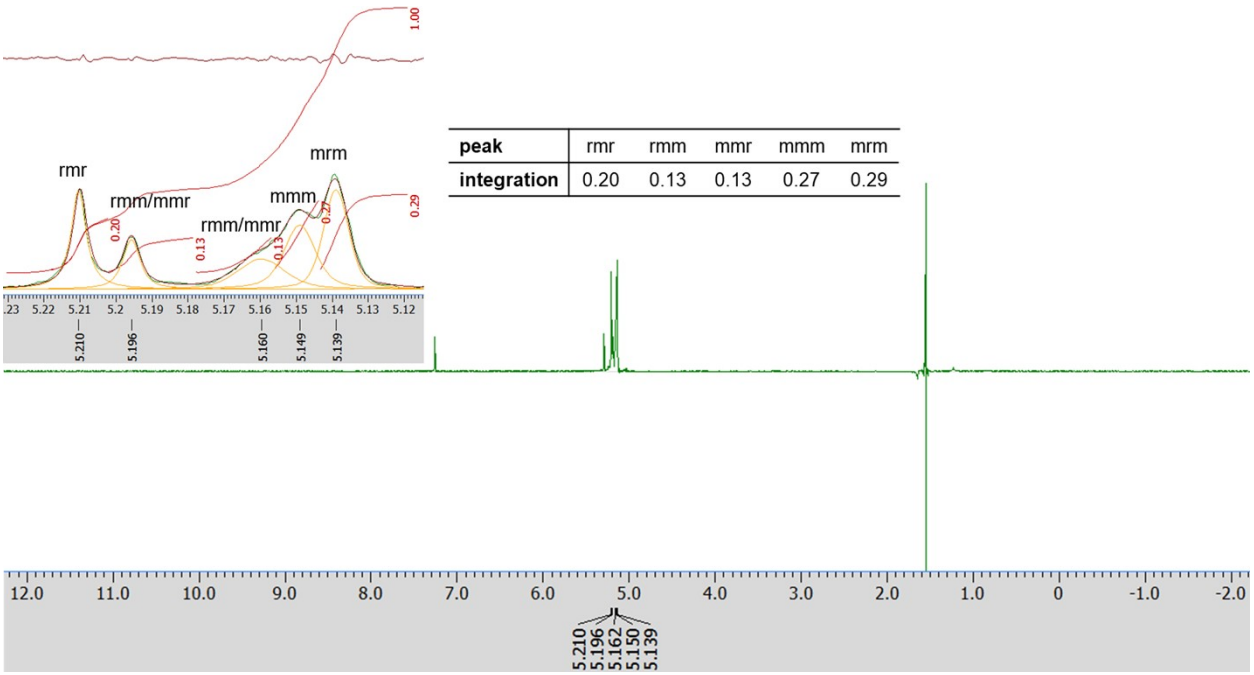

Figure S50. Homonuclear decoupled ^{1}H-NMR of isolated poly(*rac*-lactic acid) obtained from AD^{Me}HZnEt (**7**) and EtOH (Table S9, entry 4). P_r and P_m are the probabilities of forming either an *r* or *m* linkage upon monomer addition, respectively, and are calculated based on ^{1}H-NMR from: [*mmm*]=P_m^2 + P_mP_r/2, [*mmr*]=[*rmm*]= P_mP_r/2, [*rmr*]=P_r^2/2, and [*mrm*]=[P_r^2 + P_mP_r]/2, and P_r = 1–P_m.[12] For the isolated poly(*rac*-lactic acid) obtained from AD^{Me}HZnEt (**7**) and EtOH (Table S9, entry 4), P_r was calculated using the integration of [*rmr*], which P_r = (2*[*rmr*])$^{0.5}$ = (2*0.20)$^{0.5}$ = 0.63.

S8.1. MALDI analysis.

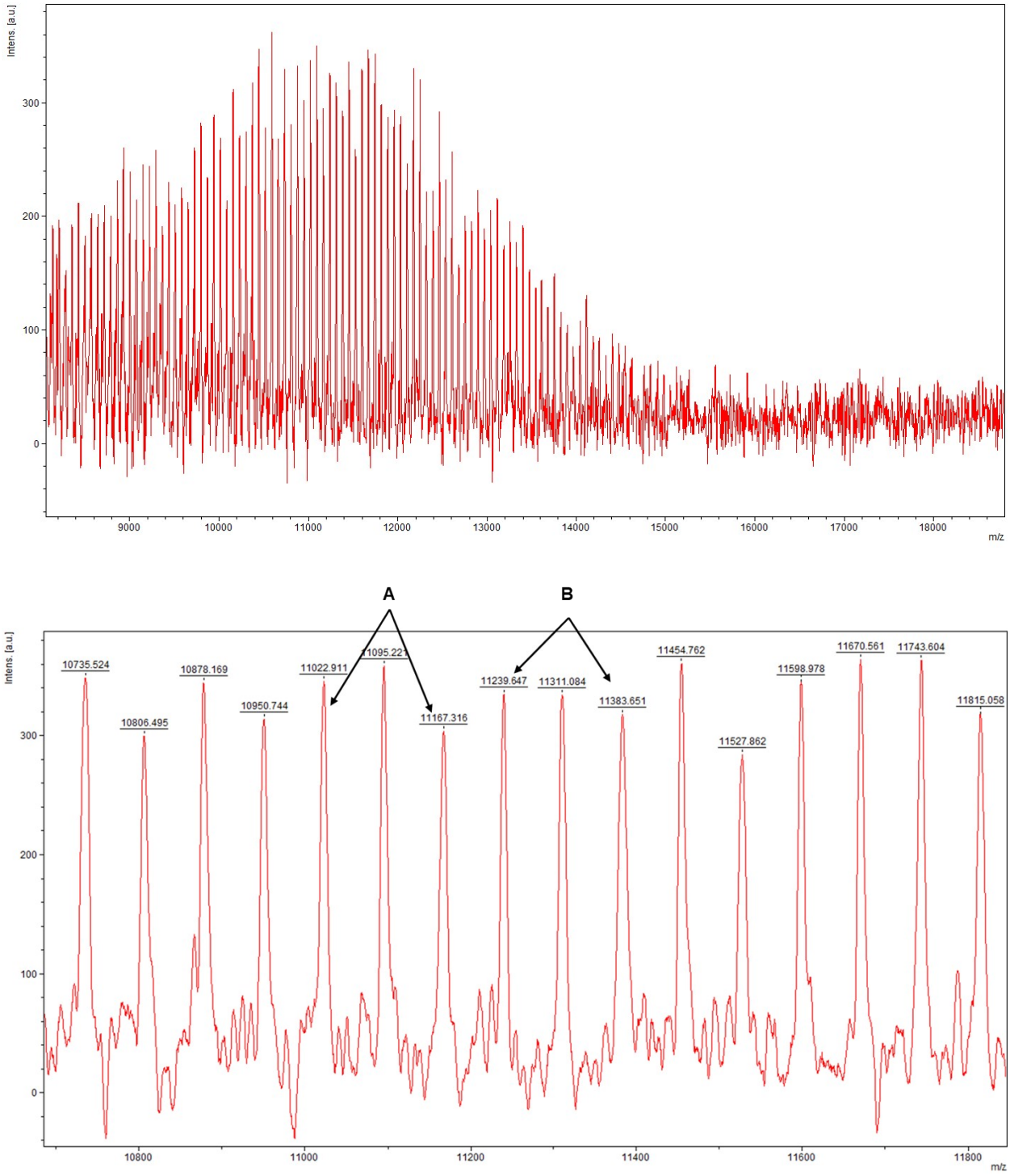

Figure S51. MALDI-TOF spectrum isolated poly(*rac*-lactic acid) obtained from $[AD^{Me}HZn_2Et_2][NTf_2]$ (**6**-NTf_2) and EtOH (Table S9, entry 6).

A. Calculated mass (n = 76 or 77, n is the number of lactide units)

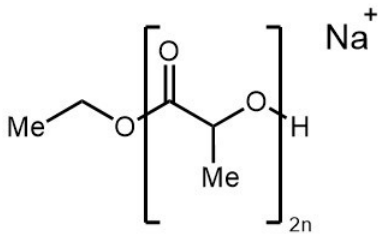

Mw = 11021.93 (n = 76), Mw = 11166.06 (n = 77)

B. Calculated mass (n= 77 or 78, n is the number of lactide units)

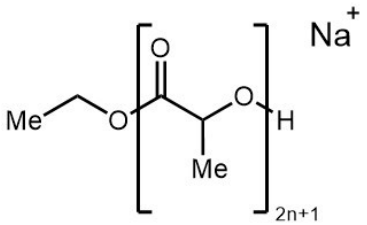

Mw = 11238.13 (n = 77), Mw = 11382.26 (n = 78)

MALDI analysis: Only one type of polymer chains with ethyloxy group chain end were identified by MALDI analysis. The masses of polymers were calculated based on n*144.13+ 22.99+ 45.06 and (n + ½)*144.13+ 22.99+ 45.06, where n is the number of lactide units, 144.13 is the molecular weight of lactide ($C_6H_8O_4$), 22.99 is the exact mass of sodium ion (Na^+), and 45.06 is the molecular weight of ethyloxy group from ethanol. For n= 77, that gives 11166.06 and 11238.13. The fact that nearly equivalent intensity signals are separated by half the mass of a lactide unit indicates rapid transesterification. Chain transfer by transesterification could be a possible explanation why the measured M_n is lower than theoretical.

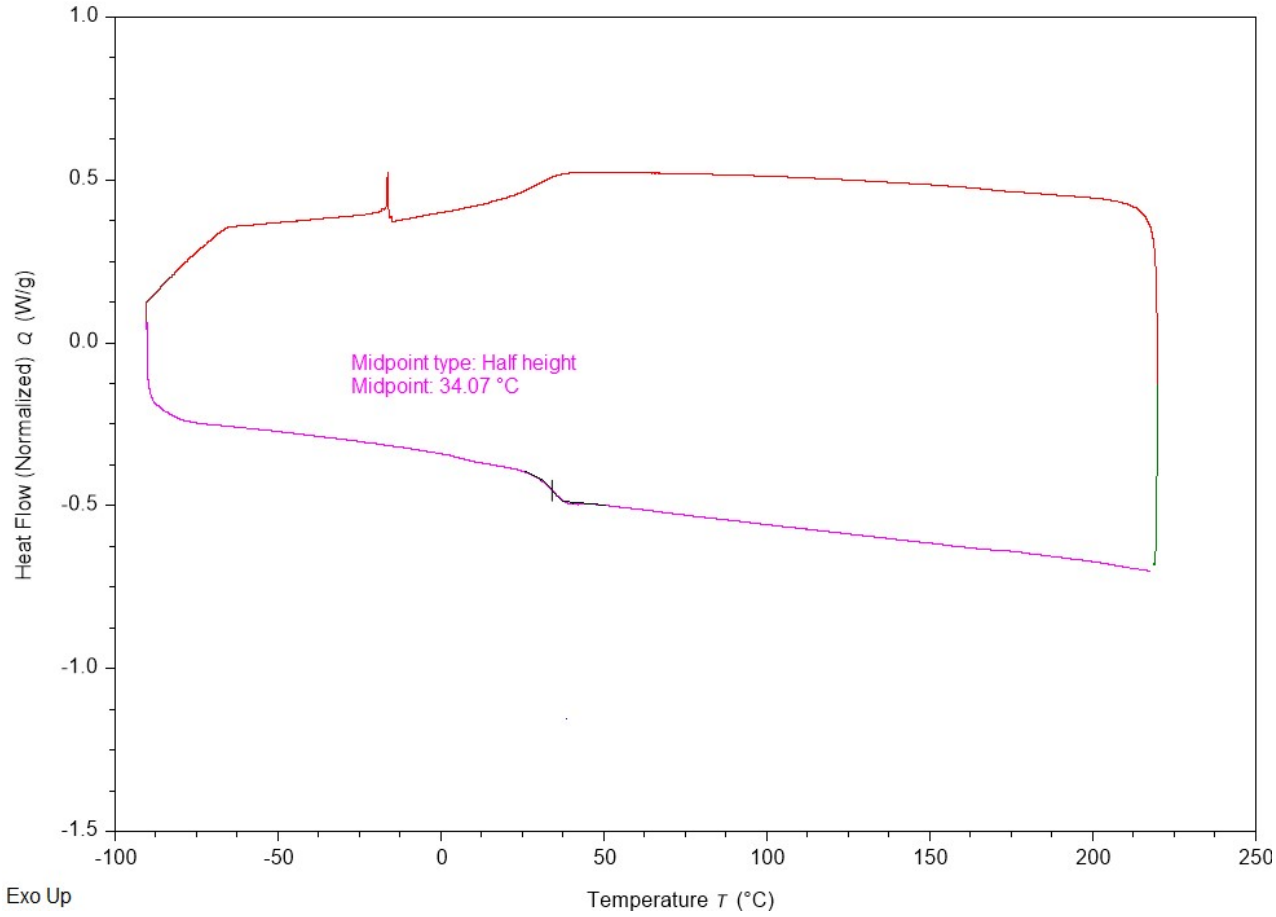

Figure S52. DSC of isolated poly(*rac*-lactic acid) obtained from $[AD^{Me}HZn_2Et_2][NTf_2]$ (**6**-NTf_2) and EtOH (Table S9, entry 6).

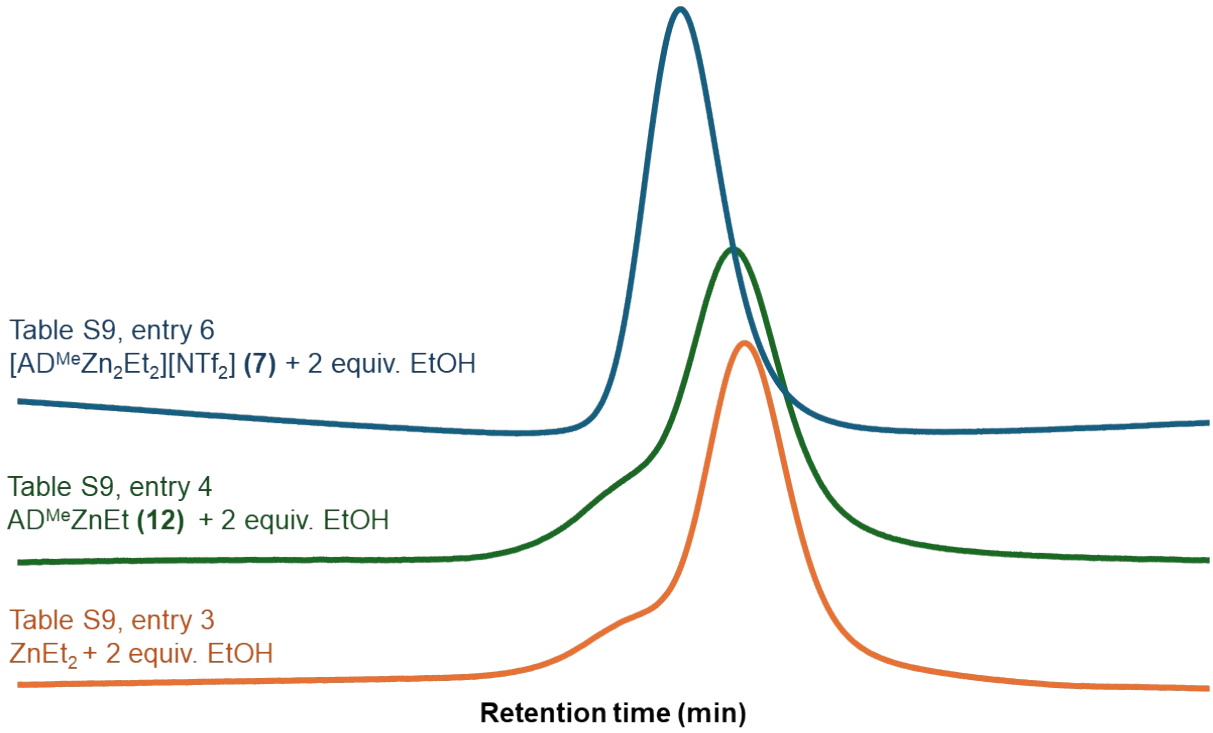

Figure S53. GPC analyses from ligand and counterion screen (From Section S7.1).

S9. Computational models.

S9.1 General. All computations were performed using the Gaussian 16 Software package on the Sabine Cluster at the University of Houston.

S9.2 Energetic analysis for the binding of two zinc atoms in a neutral complex (Scheme S1). All calculations were performed in the gas phase, using temperature = 298.15 K, pressure = 1 atm. A multiplicity of 1 and charge of 0 was assigned for all structures in this section. To simplify the calculation, truncated models were generated by removing the methyl and tert-butyl substituents on the ligand and by substituting dimethylzinc for diethylzinc. Geometries for the three alkylzinc complexes (**S9-1** and **S9-2**) and for dimethylzinc were all optimized at the level of B3LYP/6-311G(2d,p). Free energies of formation were then obtained by a single frequency calculation at this same level and are reported below. The geometry optimization and frequency steps were performed together in a single calculation using the Gaussian keyword combination "Opt Freq". All of the calculations presented here resulted in no negative harmonic frequencies, confirming that the optimized structures were stable local minima on the energy surface. These energies are reported below in hartrees, but were converted to kcal/mol using 1 hartree = 627.50 kcal/mol for discussion in the manuscript.

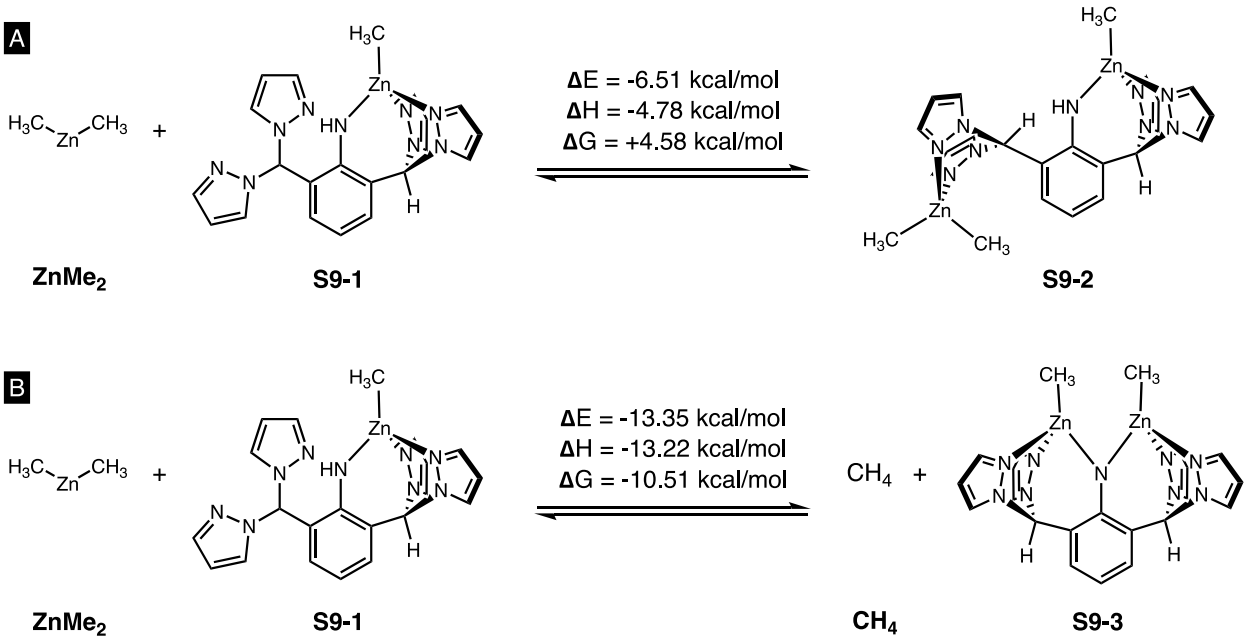

Scheme S1. Equilibrium energies for the binding of $ZnMe_2$ to $AD^{Me}HZnMe$ (A) without protonolysis, and (B) with protonolysis to generate CH_4.

$ZnMe_2$

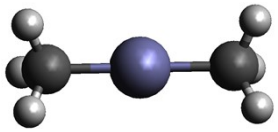

Figure S54. Optimized structure of $ZnMe_2$.

XYZ Coordinates for $ZnMe_2$

C	-1.94114	-0.00010	0.00031
Zn	-0.00000	0.00007	-0.00021
H	-2.33890	0.30458	-0.97062
H	-2.33852	0.68844	0.74982
H	-2.33850	-0.99344	0.22203
C	1.94114	-0.00011	0.00032
H	2.33887	0.30534	-0.97039
H	2.33852	-0.99360	0.22126
H	2.33853	0.68787	0.75034

Sum of electronic and thermal Free Energies = -1859.130024 e.u.
Sum of electronic and thermal Enthalpies = -1859.096709 e.u.
E(RB3LYP) = -1859.17342339 e.u.

S9-1.

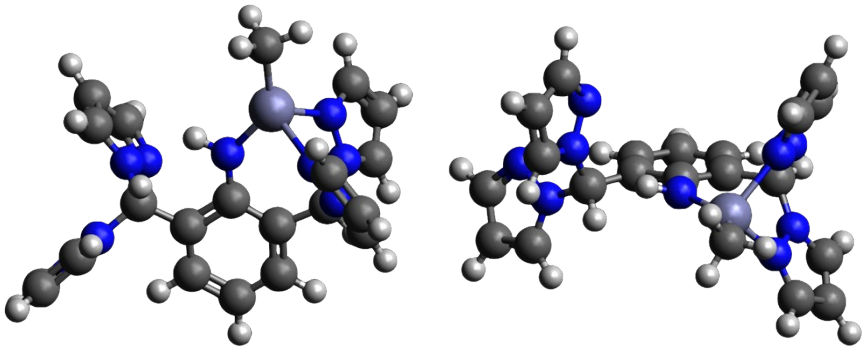

Figure S55. Optimized geometry for **S9-1**.

XYZ Coordinates for **S9-1**:

C	-0.22297	-2.21367	1.99428
C	-0.69872	-1.25021	1.10106
C	1.12467	-2.44768	2.18937
C	2.03377	-1.70400	1.44343
C	1.61004	-0.74961	0.53978
C	0.21801	-0.45152	0.34418
H	-0.94271	-2.79426	2.56535
H	1.46386	-3.19119	2.89823
H	3.09538	-1.87068	1.56807
C	2.60018	-0.04422	-0.36199
C	-2.20595	-1.13083	1.06525
N	-2.86434	-1.58886	-0.16769
Zn	-1.88078	1.05366	-1.29840
N	-2.78316	-0.91001	-1.33052
C	-3.56058	-2.73940	-0.32344
C	-3.44263	-1.63912	-2.22492
C	-3.95057	-2.80913	-1.64242
H	-4.52170	-3.59081	-2.11280
H	-3.71559	-3.41619	0.50030
H	-3.52864	-1.28771	-3.24076
N	2.83928	1.34698	0.01168
N	2.70822	1.76961	1.28706
C	3.07882	3.04055	1.26063
C	3.29881	2.33154	-0.80957
C	3.46216	3.45200	-0.03404
H	3.05284	3.62061	2.17045
H	3.47590	2.15478	-1.85811
H	3.80118	4.42328	-0.35385
N	-2.77630	0.16359	1.47566
N	-2.87119	1.22014	0.64213

C	-3.23149	0.47451	2.71251
C	-3.64107	1.78849	2.68054
C	-3.39571	2.20487	1.36366
H	-3.57313	3.16506	0.90618
H	-3.22018	-0.24771	3.51191
H	-4.05837	2.36069	3.49105
H	-2.57538	-1.82259	1.81863
N	3.87332	-0.74342	-0.53891
N	4.85866	-0.68014	0.37953
C	4.20070	-1.54236	-1.58731
C	5.82387	-1.45203	-0.10691
C	5.46518	-2.02492	-1.34281
H	6.74388	-1.56315	0.44642
H	6.04538	-2.68168	-1.96899
H	3.51922	-1.70451	-2.40660
H	2.16217	-0.01583	-1.36472
C	-2.45002	2.30647	-2.69522
H	-2.05343	2.04271	-3.68005
H	-2.12057	3.32927	-2.49087
H	-3.53997	2.33252	-2.78516
N	-0.17994	0.51082	-0.51654
H	0.58237	1.12816	-0.75592

Sum of electronic and thermal Free Energies= -3084.899962 e.u.
Sum of electronic and thermal Enthalpies= -3084.810605 e.u.
E(RB3LYP) = -3085.242520 e.u.

S9-2.

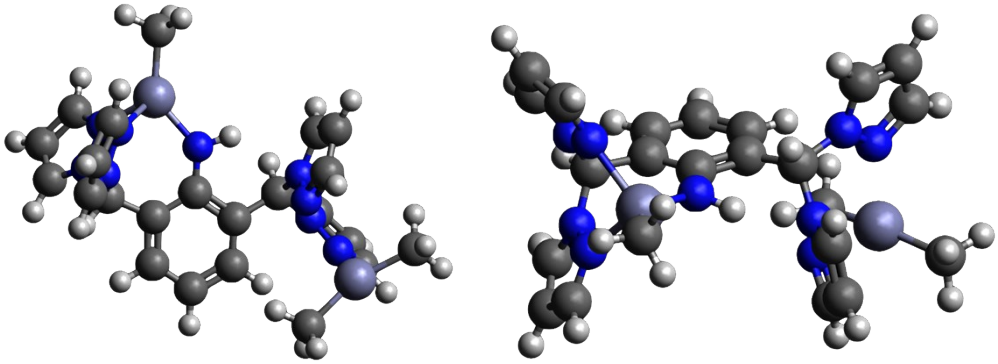

Figure S56. Optimized structure for **S9-2**. Note that the heteroscorpionate zinc atom has much shorter Zn–N bonds (pyrazole: 2.155 Å, 2.182 Å; anilide: 1.953 Å) than the dimethylzinc atom (pyrazole: 2.528 Å, 2.743 Å)

XYZ Coordinates for **S9-2**:

C	-0.91343	-2.24335	1.80730
C	-1.48637	-1.25392	1.00546

C	0.42167	-2.58841	1.72425
C	1.21296	-1.92541	0.79291
C	0.69187	-0.94075	-0.02507
C	-0.68881	-0.54464	0.05015
H	-1.54107	-2.75447	2.53234
H	0.84400	-3.34692	2.36891
H	2.25854	-2.18495	0.70790
C	1.52918	-0.32433	-1.12736
C	-2.95388	-1.00787	1.28088
N	-3.89270	-1.44809	0.23821
Zn	4.66365	0.31824	1.18664
Zn	-2.98339	1.06060	-1.19866
N	-4.00393	-0.82129	-0.95131
C	-4.69711	-2.53570	0.29190
C	-4.89423	-1.51908	-1.64921
C	-5.36075	-2.61676	-0.91207
H	-6.07971	-3.35973	-1.21126
H	-4.72972	-3.16585	1.16511
H	-5.16449	-1.19752	-2.64238
N	1.88751	1.07454	-0.90431
N	2.36322	1.50752	0.28355
C	2.56280	2.80821	0.11617
C	1.80097	2.08372	-1.81351
C	2.22449	3.22858	-1.18404
H	2.95833	3.39470	0.93064
H	1.44670	1.90945	-2.81680
H	2.28066	4.22014	-1.60022
N	-3.32227	0.34233	1.73809
N	-3.52646	1.37278	0.89107
C	-3.46649	0.73299	3.02670
C	-3.77896	2.07364	3.01620
C	-3.80554	2.42169	1.65761
H	-4.01260	3.37620	1.20071
H	-3.32795	0.04146	3.84120
H	-3.96324	2.70608	3.86738
H	-3.20503	-1.64177	2.12799
N	2.71652	-1.09710	-1.49301
N	3.85560	-1.06216	-0.77039
C	2.81113	-1.95765	-2.53686
C	4.67862	-1.90965	-1.37911
C	4.07137	-2.50749	-2.49649
H	5.67721	-2.04924	-0.99548
H	4.49359	-3.22310	-3.18121

H	1.98581	-2.11161	-3.21272
H	0.91545	-0.31255	-2.03269
C	-3.71805	2.31076	-2.51821
H	-3.56375	1.97175	-3.54682
H	-3.26286	3.30267	-2.44530
H	-4.79555	2.44221	-2.38317
C	5.86066	1.48819	0.15601
H	6.09863	2.41067	0.69549
H	5.41703	1.77305	-0.80102
H	6.81660	0.99940	-0.06049
C	4.01200	-0.72723	2.71287
H	2.93687	-0.59538	2.85047
H	4.50288	-0.43505	3.64637
H	4.19830	-1.79781	2.57840
N	-1.19370	0.41862	-0.75164
H	-0.46385	0.97981	-1.16359

Sum of electronic and thermal Free Energies = -4944.022683 e.u.
Sum of electronic and thermal Enthalpies = -4943.914927 e.u.
E(RB3LYP) = -4944.426320 e.u.

Table S10. Change in energy for the reaction in Scheme S1A, the reaction of $ZnMe_2$ with **S9-1** to give **S9-2**.

Units	Difference in E	Difference in H	Difference in G
Hartrees	-0.01037661	-0.007613	+0.007303
Kcal/mol	-6.51	-4.78	+4.58

CH_4.

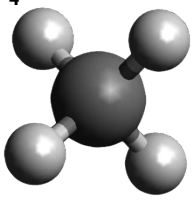

Figure S57. Optimized structure for **CH_4**.

XYZ Coordinates for **CH_4**:

C	0.00000	0.00000	0.00000
H	0.62900	0.62900	0.62900
H	-0.62900	-0.62900	0.62900
H	-0.62900	0.62900	-0.62900
H	0.62900	-0.62900	-0.62900

Sum of electronic and thermal Free Energies = -40.507363 e.u.
Sum of electronic and thermal Enthalpies = -40.486236 e.u.
E(RB3LYP) = -40.534634 e.u.

S9-3.

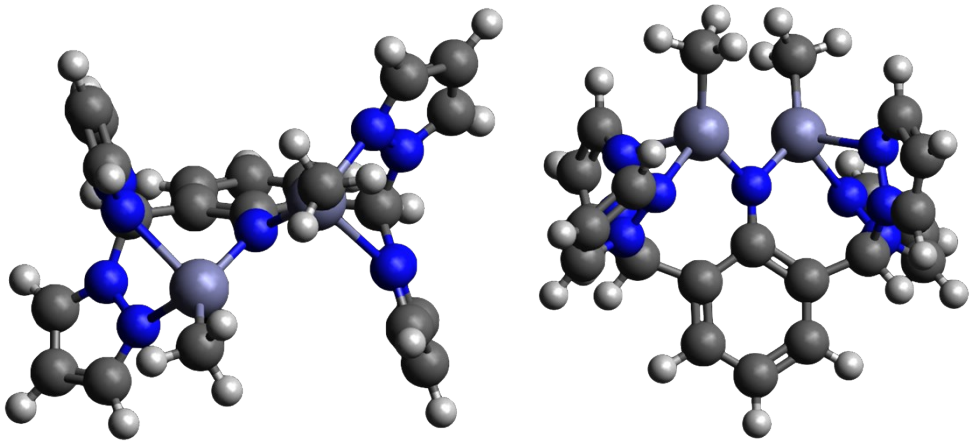

Figure S58. Optimized structure for **S9-3**.

XYZ Coordinates for **S9-3**:

C	-1.14514	3.34330	0.28878
C	-1.18066	1.95450	0.28725
C	-0.00038	4.06929	-0.00273
C	1.14457	3.34311	-0.29307
C	1.18040	1.95432	-0.28960
C	-0.00012	1.14125	-0.00084
H	-2.05466	3.88748	0.53345
H	-0.00047	5.15072	-0.00352
H	2.05402	3.88715	-0.53833
N	-0.00014	-0.18283	-0.00029
C	2.53436	1.39038	-0.66400
C	-2.53431	1.39075	0.66305
N	-2.56364	0.34932	1.70532
Zn	1.43996	-1.35070	0.55565
Zn	-1.44034	-1.35105	-0.55524
N	-2.52101	-0.96539	1.41288
C	-2.61217	0.55963	3.04107
C	-2.54749	-1.59230	2.58419
C	-2.60472	-0.67697	3.64781
H	-2.64014	-0.88528	4.70349
H	-2.64277	1.55539	3.45190
H	-2.51580	-2.66980	2.61206
N	3.36179	0.96772	0.47058

N	2.94361	0.02208	1.33329
C	3.89259	-0.07140	2.25864
C	4.55778	1.47860	0.84491
C	4.93421	0.83273	2.00238
H	3.78981	-0.78881	3.05705
H	5.03874	2.25614	0.27495
H	5.83085	0.99270	2.57621
N	-3.36249	0.96692	-0.47058
N	-2.94486	0.02047	-1.33267
C	-4.55872	1.47744	-0.84464
C	-4.93587	0.83051	-2.00128
C	-3.89442	-0.07388	-2.25734
H	-3.79216	-0.79205	-3.05513
H	-5.03932	2.25551	-0.27510
H	-5.83287	0.98993	-2.57470
H	-3.09824	2.21419	1.09672
N	2.56456	0.34800	-1.70531
N	2.52158	-0.96647	-1.41171
C	2.61464	0.55705	-3.04119
C	2.54937	-1.59447	-2.58240
C	2.60790	-0.68013	-3.64679
H	2.51770	-2.67199	-2.60931
H	2.64451	-0.88943	-4.70224
H	2.64569	1.55242	-3.45291
H	3.09845	2.21350	-1.09808
C	-1.70144	-3.15000	-1.29830
H	-1.10694	-3.90497	-0.77717
H	-1.42428	-3.20709	-2.35585
H	-2.74966	-3.45530	-1.22437
C	1.70153	-3.14908	1.29995
H	1.41453	-3.20832	2.35473
H	2.75167	-3.44996	1.23570
H	1.11519	-3.90609	0.77253

Sum of electronic and thermal Free Energies = -4903.539376 e.u.
Sum of electronic and thermal Enthalpies = -4903.442153 e.u.
E(RB3LYP) = -4903.902589 e.u.

Table S11. Change in energy for the reaction in Scheme S1B, the reaction of $ZnMe_2$ with **S9-1** to give CH_4 and **S9-3**.

Units	Difference in E	Difference in H	Difference in G
Hartrees	-0.02127961	-0.021075	-0.016753
Kcal/mol	-13.35	-13.22	-10.51

S9.3 Conformational interconversion of the cationic dizinc complexes (Scheme S2). All calculations were performed in the gas phase, using temperature = 298.15 K, pressure = 1 atm. A multiplicity of 0 and charge of +1 was assigned for all structures in this section. To simplify the calculation, truncated models were generated by removing the methyl and tert-butyl substituents on the ligand and by substituting methylzinc units for ethylzinc units. Geometries for the two stable conformations (**S9-4** and **S9-6**) were all optimized at the level of B3LYP/6-31G(d). The geometry optimization and frequency steps were performed together in a single calculation using the Gaussian keyword combination "Opt Freq". For both **S9-4** and **S9-6**, no negative harmonic frequencies were obtained, confirming that these are stable ground state structures. Then, transition state **S9-5** was obtained by a single quadratic synchronous transit calculation using **S9-4** and **S9-6**, along with a transition state guess, as input structures with the Gaussian keyword combination "Opt=qst3 Freq". For **S9-5**, only one negative harmonic frequency was observed, consistent with an energy surface saddle point. Free energies of formation were obtained for **S9-4**, **S9-5**, and **S9-6** at this same level and are reported below. More accurate energies were then obtained for these structures at the level of B3LYP/6-311G++(2d,p) by performing single point calculations on the optimized structures. These energies are reported alongside those obtained at B3LYP/6-31G(d). All energies are reported below in hartrees, but were converted to kcal/mol using 1 hartree = 627.50 kcal/mol for discussion in the manuscript. The two conformations **S9-4** and **S9-6** had no difference in free energy (ΔG = 0 kcal/mol), and the barrier to their interconversion was small ($\Delta G^{\ddagger}$ = 0 kcal/mol).

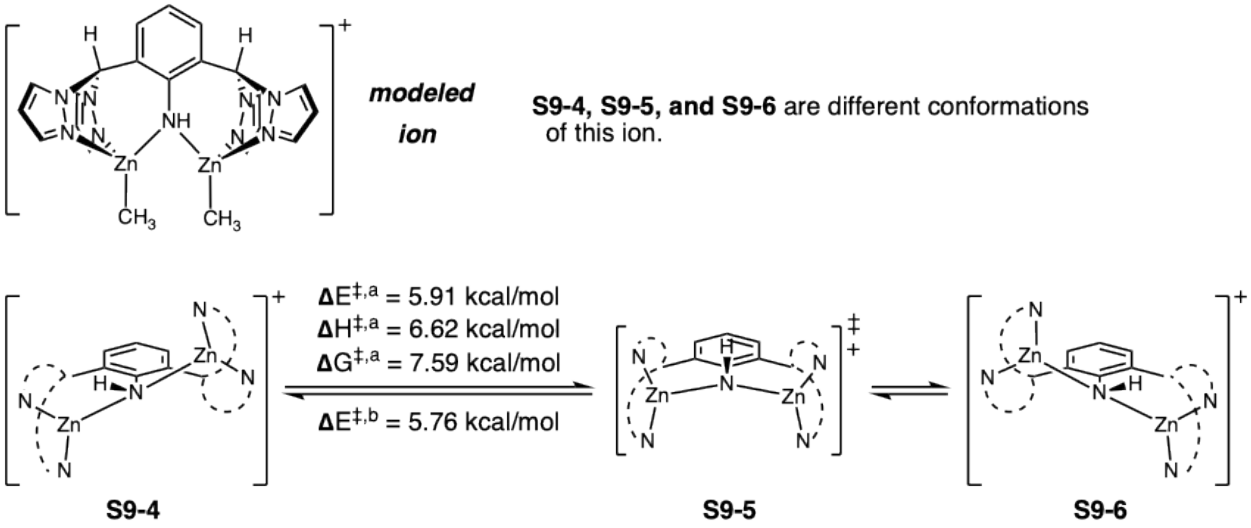

Scheme S2. Interconversion of C_2-symmetric isomers modeled in this section. [a]Energies obtained from a single Opt Freq calculation at the level of B3LYP/6-31G(d). [a]Energy obtained by performing a subsequent single point calculation at the level of B3LYP/6-311++G(2d,p).

S9-4.

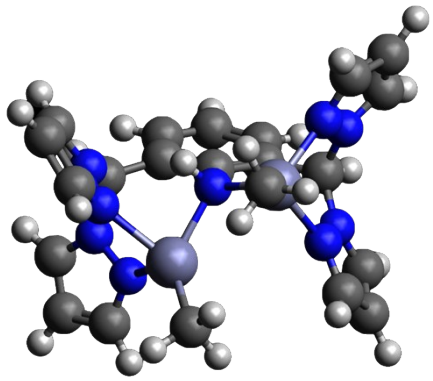

Figure S59. Optimized structure for **S9-4**.

XYZ Coordinates for **S9-4**:

C	-0.96729	3.36221	-0.15973
C	-1.05727	1.97074	-0.06270
C	0.16312	3.99765	-0.63678
C	1.25977	3.21889	-0.96067
C	1.23002	1.83298	-0.83141
C	0.04054	1.15891	-0.44081
H	-1.82183	3.96646	0.12507
H	0.19697	5.07444	-0.73206

H	2.17251	3.70452	-1.28963
N	-0.00884	-0.24977	-0.44189
C	2.61316	1.18368	-0.95979
C	-2.42897	1.48888	0.41566
N	-2.46066	0.58109	1.56415
Zn	1.34438	-1.19089	0.84004
Zn	-1.64951	-1.49574	-0.44454
N	-2.24675	-0.74966	1.44799
C	-2.75725	0.91341	2.84535
C	-2.40372	-1.25244	2.66853
C	-2.72306	-0.24336	3.58855
H	-2.91072	-0.34583	4.64333
H	-2.96662	1.93217	3.12787
H	-2.27885	-2.31095	2.83122
N	3.24891	1.09731	0.35102
N	2.66134	0.39753	1.34920
C	3.44422	0.56154	2.41272
C	4.37960	1.70634	0.78004
C	4.53745	1.38451	2.10921
H	3.19646	0.07264	3.34141
H	4.97491	2.31758	0.12171
H	5.33171	1.69683	2.76485
N	-3.29738	1.00191	-0.65156
N	-3.03162	-0.14614	-1.31431
C	-4.39265	1.61666	-1.16269
C	-4.85736	0.83372	-2.19401
C	-3.97724	-0.25669	-2.24272
H	-3.99002	-1.11557	-2.89472
H	-4.75153	2.55144	-0.76438
H	-5.71432	1.02003	-2.81782
H	-2.93511	2.37884	0.78087
N	2.76859	-0.09940	-1.65790
N	2.58984	-1.28547	-1.02088
C	3.23766	-0.28838	-2.91754
C	2.93228	-2.21886	-1.90288
C	3.34631	-1.64469	-3.11557
H	2.86401	-3.26064	-1.63179
H	3.68303	-2.14838	-4.00518
H	3.45681	0.54347	-3.56725
H	3.22723	1.87674	-1.53034
C	-1.63924	-3.36965	-1.00048
H	-0.86378	-3.94771	-0.49309
H	-1.46645	-3.47586	-2.07496

H	-2.59342	-3.85584	-0.78326
C	1.16952	-2.68676	2.08133
H	0.78773	-2.36637	3.05407
H	2.13780	-3.16138	2.25630
H	0.49316	-3.45522	1.70262
H	0.46269	-0.54006	-1.29229

Sum of electronic and thermal Free Energies= -4904.357907 e.u.[a]
Sum of electronic and thermal Enthalpies= -4903.882544 e.u.[a]
E(RB3LYP) = -4903.978491 e.u.[a]
E(RB3LYP) = -4903.40869171 e.u.[b]
[a]Energies obtained from a single Opt Freq calculation at the level of B3LYP/6-31G(d). [a]Energy obtained by performing a subsequent single point calculation at the level of B3LYP/6-311++G(2d,p).

S9-5.

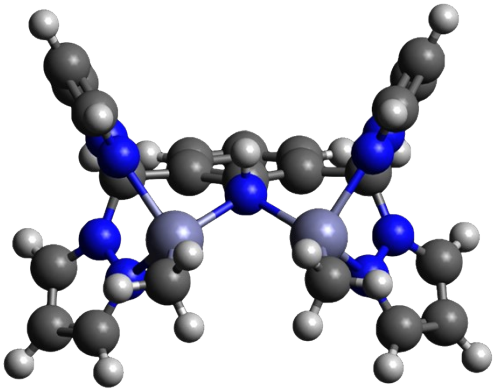

Figure S60. Optimized structure for **S9-5**.

XYZ Coordinates for **S9-5**:

C	-1.17911	3.35332	-0.04110
C	-1.20415	1.96329	-0.18640
C	-0.00006	4.06118	0.05117
C	1.17898	3.35334	-0.04138
C	1.20402	1.96330	-0.18671
C	-0.00006	1.20477	-0.22686
H	-2.11547	3.89865	-0.00458
H	-0.00007	5.13671	0.16713
H	2.11533	3.89869	-0.00505
N	0.00001	-0.22994	-0.32730
C	2.64567	1.44546	-0.28076
C	-2.64580	1.44548	-0.28001
N	-3.15704	0.91672	0.97676
Zn	1.55210	-1.48261	0.28306

Zn	-1.55183	-1.48305	0.28215
N	-2.60294	-0.17180	1.55292
C	-4.14715	1.42805	1.74957
C	-3.26142	-0.35368	2.69390
C	-4.24068	0.63442	2.86949
H	-4.92291	0.74947	3.69390
H	-4.69900	2.30467	1.45239
H	-3.01339	-1.18914	3.32891
N	3.15731	0.91709	0.97600
N	2.60268	-0.17065	1.55320
C	3.26196	-0.35263	2.69372
C	4.14844	1.42790	1.74782
C	4.24223	0.63467	2.86802
H	3.01368	-1.18754	3.32936
H	4.70074	2.30398	1.44985
H	4.92518	0.74955	3.69186
N	-2.98227	0.57012	-1.40090
N	-2.73464	-0.75621	-1.37287
C	-3.64374	0.92015	-2.53362
C	-3.81748	-0.22541	-3.27427
C	-3.23725	-1.24413	-2.50228
H	-3.16637	-2.30056	-2.70752
H	-3.93593	1.93995	-2.72415
H	-4.30342	-0.31497	-4.23047
H	-3.25387	2.32719	-0.46090
N	2.98173	0.56954	-1.40138
N	2.73498	-0.75692	-1.37205
C	3.64300	0.91882	-2.53444
C	3.23772	-1.24568	-2.50105
C	3.81738	-0.22737	-3.27400
H	3.16736	-2.30233	-2.70531
H	4.30328	-0.31755	-4.23016
H	3.93452	1.93862	-2.72601
H	3.25365	2.32709	-0.46224
C	-1.73419	-3.39123	0.66022
H	-1.27946	-3.68300	1.60838
H	-1.27986	-4.01677	-0.10996
H	-2.79475	-3.65290	0.71214
C	1.73159	-3.39094	0.66156
H	1.27582	-3.68192	1.60946
H	2.79170	-3.65430	0.71420
H	1.27675	-4.01582	-0.10885
H	0.00015	-0.44229	-1.32495

Sum of electronic and thermal Free Energies= -4904.348486 e.u.[a]
Sum of electronic and thermal Enthalpies= -4903.874199 e.u.[a]
E(RB3LYP) = -4903.966399 e.u.[a]
E(RB3LYP) = -4904.39950925 e.u.[b]
[a]Energies obtained from a single Opt Freq calculation at the level of B3LYP/6-31G(d). [a]Energy obtained by performing a subsequent single point calculation at the level of B3LYP/6-311++G(2d,p).

S9-6.

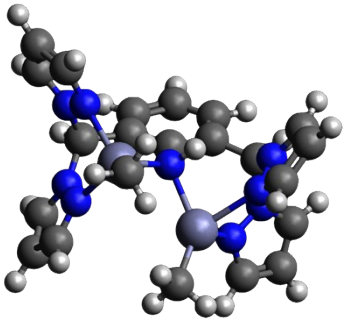

Figure S61. Optimized structure for **S9-6**.

XYZ Coordinates for **S9-6**:

C	-1.26000	3.21852	-0.96203
C	-1.23021	1.83267	-0.83218
C	-0.16331	3.99743	-0.63870
C	0.96720	3.36221	-0.16156
C	1.05720	1.97079	-0.06384
C	-0.04069	1.15877	-0.44142
H	-2.17282	3.70399	-1.29102
H	-0.19719	5.07418	-0.73444
H	1.82182	3.96659	0.12275
N	0.00868	-0.24985	-0.44174
C	2.42889	1.48915	0.41466
C	-2.61329	1.18322	-0.96017
N	-3.24891	1.09719	0.35076
Zn	1.64923	-1.49590	-0.44345
Zn	-1.34476	-1.19093	0.84038
N	-2.66115	0.39778	1.34909
C	-4.37893	1.70724	0.78005
C	-3.44333	0.56293	2.41295
C	-4.53625	1.38634	2.10953
H	-5.33003	1.69944	2.76537
H	-4.97432	2.31832	0.12164
H	-3.19536	0.07446	3.34180
N	2.46055	0.58207	1.56377

N	2.24624	-0.74869	1.44857
C	2.40353	-1.25070	2.66938
C	2.75760	0.91518	2.84465
C	2.72336	-0.24108	3.58864
H	2.27846	-2.30908	2.83280
H	2.96728	1.93408	3.12643
H	2.91130	-0.34291	4.64343
N	-2.76863	-0.10012	-1.65786
N	-2.59006	-1.28599	-1.02037
C	-3.23756	-0.28954	-2.91749
C	-3.34629	-1.64590	-3.11503
C	-2.93246	-2.21966	-1.90207
H	-2.86431	-3.26135	-1.63061
H	-3.45651	0.54209	-3.56754
H	-3.68292	-2.14991	-4.00450
H	-3.22753	1.87602	-1.53086
N	3.29730	1.00147	-0.65223
N	3.03193	-0.14725	-1.31402
C	4.39232	1.61620	-1.16395
C	3.97748	-0.25817	-2.24243
C	4.85725	0.83257	-2.19464
H	3.99049	-1.11755	-2.89376
H	5.71414	1.01864	-2.81862
H	4.75093	2.55141	-0.76642
H	2.93512	2.37928	0.77933
C	-1.16892	-2.68710	2.08115
H	-0.78739	-2.36679	3.05403
H	-0.49212	-3.45502	1.70219
H	-2.13693	-3.16231	2.25601
C	1.63966	-3.37003	-0.99884
H	0.86322	-3.94790	-0.49274
H	2.59344	-3.85608	-0.77950
H	1.46904	-3.47670	-2.07362
H	-0.46299	-0.54061	-1.29191

Sum of electronic and thermal Free Energies= -4904.357907 e.u.[a]
Sum of electronic and thermal Enthalpies= -4903.882543 e.u.[a]
E(RB3LYP) = -4903.978491 e.u.[a]
E(RB3LYP) = -4903. 40869298 e.u.[b]
[a]Energies obtained from a single Opt Freq calculation at the level of B3LYP/6-31G(d). [a]Energy obtained by performing a subsequent single point calculation at the level of B3LYP/6-311++G(2d,p).